Gut-brain Axis Regulation of Food Intake and Visceral Illness

by

Anita Patel

A dissertation submitted in partial fulfillment
of the requirements for the degree of
Doctor of Philosophy
(Neuroscience)
in the University of Michigan
2021

Doctoral Committee:

Professor Randy J. Seeley, Chair
Professor Malcolm Low
Professor Martin G. Myers, Jr.
Professor Darleen Sandoval, University of Colorado

Anita Patel

anitarp@umich.edu

ORCID: 0000-0003-0359-1929

Dedication

To my parents Pushpa and Ramesh Patel, whose warmth and resilience will always inspire me.

Acknowledgements

There are many who have substantially contributed to my journey while completing this dissertation. I would like to acknowledge my committee which has challenged me and provided thoughtful scientific feedback through dissertation pivots. I will always be especially thankful to and inspired by Drs. Louise McCullough and Lauren Sansing, who sparked my interest for scientific research. I am only here because of your unwavering encouragement.

I have been exceptionally lucky to have a large support system. Ann Arbor became a home away from home, and only so with the help of friends both near and far, old and new. Those who celebrated and remembered the highs and grounded me during the lows. Kate Weskamp, Anwesha Banerjee, Elika Ridelman, Carlos Puentes, Bailey Peck and Chelsea Hutch, with whom I've shared countless laughs and tears- you are all my most cherished gifts from Michigan. I am also thankful to colleagues Simon Evers, Mouhamadoul Toure and Henriette Frikke-Schmidt who have donated much time and energy brainstorming with me. I am humbled to have met this group of uplifting and brilliant folks at UM. To Sonam Patel, Suan Lue and Lexi Essa - my rocks. Your love and support has sustained me through the most challenging and tumultuous years. I would be nowhere without the lifelong sacrifices and unconditional love of my family, particularly my brother who unceasingly amazes me. Finally, I must express my deepest gratitude to my husband Patrick, who has lifted me back up time and time again.

For all of you, I am profoundly grateful.

Table of Contents

List of Figures

Abstract

Body weight and feeding regulation are carefully governed by complex homeostatic neural networks that respond to a myriad of peripheral signals that reflect both short- and long-term energy status. A critical component of that regulation involves communication between the gut and the brain. This "gut-brain" axis delicately coordinates ingestive behaviors with physiological systems that must process and absorb what gets ingested. The gastrointestinal tract maintains two predominant but contrasting functions. One is nutrient absorption and the other is to act as a barrier to protect against toxic compounds and bacteria.

The gut-brain axis plays a crucial role in an organism's ability to regulate energy balance and maintain an appropriate body weight. A negative energy balance will stimulate hunger and food seeking and vice-versa to maintain a set-point of body weight and adiposity. In doing so, energy input and expenditure are carefully matched to maintain fuel availability and prevent shifts in long-term body weight. Under various conditions, this set-point can become too high and the resultant increase in body mass can have a myriad of detrimental effects. Similarly, under particular stress conditions, intestinal and neural signaling are altered to maintain a pathologically low set-point, resulting in maladaptive feeding and illness responses. Central networks that regulate illness symptoms of anorexia in pathophysiological states are still yet to be completely identified and understood.

Deciphering the key gut-brain signals that regulate feeding related disorders will open opportunities for critically needed therapeutics. For example, obesity has become one of the world's largest health threats. Obesity and the associated comorbidities can decrease the quality of life and substantially increase susceptibility to pathologies such as cancer and infection. This dissertation examines the role of various peripheral signals in regulating feeding networks, weight patterns and illness in pathophysiological states of infection and obesity.

Studies in Chapter 2 examined growth differentiation factor 15 (GDF15) and GDNF family receptor alpha-like neuronal signaling in a model of bacterial sepsis. We demonstrated that GDF15 secretion was highly induced with exposure to lipopolysaccharide (LPS) in mice, rats, and humans. Because infection responses are influenced by housing temperatures, we examined mice at several temperatures to increase the translational relevance of rodent to human thermoregulatory responses. We then tested the necessity of GDF15 in body weight regulation, feeding behavior, and illness outcomes in response to LPS. As physiological responses vary for differing microorganisms, we investigated a model of trichothecene infection in Chapter 3. Using genetically altered mouse models of GDF15 and glucagon-like peptide 1 (GLP-1) ligand and receptor, we determined that these gut-brain signals are not necessary for the illness and feeding responses to deoxynivalenol and LPS.

Chapter 4 focuses on gut signals that are highly altered in gastro-intestinal restructuring surgeries. Bariatric surgeries result in long-term weight loss demonstrating the importance of the gastro-intestinal tract in regulating overall energy balance. One important goal is identifying the signals that are altered that account for the potent effects of bariatric surgeries. After surgery, there is a prominent increase of the hormone glucagon-like-peptide 2 (GLP-2). We used a loss-of-function mouse model to test the role of GLP-2 in the effects of surgery to reduce weight,

improve glucose regulation and alter levels and composition of bile acids. We demonstrated that while GLP-2 is required for changes in bile acids, it is not necessary for the benefits of bariatric surgery.

Chapter 1: Introduction

1.1 Body weight set-point

Homeostatic neural mechanisms delicately balance nutritional and feeding states on a minute-to-minute basis. In response to nutrients entering the gastrointestinal tract, satiety signals influence the motivational and motor pattern generating aspects of brain signaling to generate decisions about which foods and the caloric content to ingest. In doing so, energy input and expenditure are carefully maximized to maintain metabolic needs and prevent shifts in long-term body weight. A negative energy balance will stimulate hunger and food seeking and vice versa to maintain a set-point of body weight.

However, under certain environmental, social and genetic conditions, an organism's body weight set-point can be altered. As such, obesity has become one of the world's largest health threats. Two-thirds of the nation's population suffer from comorbidities that decrease the quality of life and increase economic health burden. In mice, this increase in set point can be modeled by feeding rodents a palatable high-fat diet to induce diet induced obesity (DIO). While fasting can result in an acute reduction of body weight, obese rodents and individuals are able to maintain and defend elevated levels of fat mass when given free access to food. Thus, obesity represents a pathological state in which the energy homeostasis system is dysregulated.

When challenged with infections, shifts in metabolic demands to mount immune responses are required. These mechanisms necessitate changes in metabolism and energy usage,

thus a change in energy balance. During illness, a negative energy balance is not accompanied by counterregulatory food seeking. Instead, food refusal/avoidance and negative energy balance are favored. Although acute shifts in energy balance are occasionally beneficial in recovery from acute challenges, chronic decrease can result in the lowering of the body weight set point that is pathological and can contribute to mortality. Illness associated weight loss is often present along with symptoms such as nausea and emesis, a response that is beneficial in the event of ingested toxins, but can be deleterious in the absence of the acute need to rid the body of toxins.

To control both aspects of feeding (satiety vs illness) diverse peripheral signals communicate the state of nutrition, immunity, and energy stores to the brain. A variety of circulating mediators can activate receptors in the enteric nervous system, the vagus, or directly in the brain to signal peripheral health status. As such, central networks create a coordinated response to control ingestive behavior. In doing so, proper nutrient absorption and protection against harmful toxins are maintained. While the satiety response leads to reward and increased nutrient absorption, the infection response leads to aversion and expulsion of ingested substance. This key difference emphasizes that the signals generated by the gut and what the brain does with those signals must be distinct from one another. Neuronal signals and networks that regulate the illness symptoms such as anorexia and nausea in pathophysiological states are still yet to be completely identified. Whether the symptoms and severity of anorexia and nausea are on a continuum, regulated by similar neural networks and reliant on the potency of the stimulus, or whether distinct neural networks signal distinct symptoms is also yet to be determined.

The hindbrain represents a key integration point of gut to brain signaling as it represents a convergence of afferent and efferent projections from and to the intestinal tract as well as hormonal signals from the gut or its absorbed nutrients. Understanding the complex peripheral

and neural signaling, the gut-brain axis, that is necessary to drive behavioral changes creates therapeutic opportunities to regulate pathological conditions in which energy balance is skewed. Here we examine gut to brain signaling using models of obesity, weight loss surgery, and infection while highlighting the roles of peripherally derived mediators in circulation.

1.1.1 GDF-15

Amongst the peripheral mediators that signal to the brain, one protein that has recently gained attention is growth differentiation factor 15 (GDF15). GDF15 was initially characterized by the Breit academic group and initially calling it macrophage inhibitory cytokine 1 (MIC-1) due to its release from activated macrophages [1,2]. Several other groups also cloned the GDF15 gene and named it placental transforming growth factor beta (PTGF-β), prostate derived factor (PDF), non-steroidal anti-inflammatory drug-activated gene 1 (NAG-1), and placental bone morphogenic protein (PLAB) depending on the results and conditions of their experiments. GDF15 is localized to a 2 exon gene on chromosome 19p13.11b [2] and circulates as a 24.5kDA homodimer once it is cleaved from a 62kDa intracellular protein [2]. Although GDF15 does not bind any transforming growth factor (TGF-β) receptors [3], GDF15 is a distant member of the TGF-β superfamily of proteins due to the conserved 9 cysteine region conferring sequency homology. GDF15 has been found in a variety of organs, illustrated by detectable gene expression in the lung, heart, adipose, pancreas, small intestine and placental trophoblasts but most commonly detected in high levels within the liver and kidney [4–11]. The exact origins of GDF15 in various pathophysiological states are still poorly understood. A variety of tumors produce high levels of GDF15 that can enter the circulation which led to hypotheses about its potential role in various sequalae associated with specific tumors including weight loss [12] .

1.1.2 GFRAL

2017 was a groundbreaking year for the field of GDF15 signaling. Four pharmaceutical companies simultaneously published the identification of GDNF family receptor α-like (GFRAL), all of which showed the ability of GFRAL signaling to decease food intake and body weight in various species, including rodents and non-human primates [3,13–15]. Intriguingly, GFRAL expression is exceptionally narrow in the CNS. The companies discovered that GFRAL expression is restricted to a small hindbrain region near the fourth ventricle, the area postrema (AP), but is also present in a second hindbrain region of the NTS in lesser amounts. The AP is heavily interconnected to the lateral parabrachial nucleus (PBN) and the NTS. Both the AP and NTS play a crucial role in mediating satiety signals and appetite through a network including the lateral PBN and central amygdala (CeA). The AP is part of the circumventricular organs (CVO), an area that is outside of the blood brain barrier, and adjacent to the nucleus tractus solitarius (NTS). The CVOs are one of the only areas of the brain that have fenestrated vasculature along with slowed blood flow. These properties have resulted in the AP acquiring the nickname "chemoreceptor trigger zone" as many circulating factors can penetrate and signal onto receptors to regulate appetite and metabolism [16,17]. Thus, the AP/NTS is particularly situated as a hub of gut to brain signaling.

GFRAL has been characterized as a distant member of glial cell line derived neurotrophic factor (GDNF) receptors. GFRAL is a transmembrane protein receptor that, unlike other GDNF family receptors GFRa1-4 which are anchored to the plasma membrane by GPI, is attached by a short cytoplasmic domain of 23aa [3,18]. Competitive binding assays testing BMP-1, TGFβ, and other GDNF family ligands found that GFRAL binds exclusively to GDF-15. Upon binding GDF-15, GFRAL forms a heterodimer with the coreceptor tyrosine kinase RET to induce

downstream Akt signaling pathway. Additionally, *in vitro* studies have shown phosphorylation of Erk1/2 and PLCγ [3,15]. Due to contamination of commercial GDF15, SMAD signaling was an initial mischaracterization of GDF15 action, primarily in cardiomyocyte *in vitro* experiments, often resulting in anti-inflammatory and anti-apoptotic action [19,20]. Unlike TGF-βR1/2s, GFRAL does not activate serine/threonine kinase to downstream activate the SMAD family of transcription factors [3,14,15,21].

1.1.3 GDF15 in health and feeding

Homeostatic feeding mechanisms coordinate peripheral hormonal signaling to hypothalamic neuronal circuits to maintain proper body weight and feeding behaviors. This circuitry is tightly controlled in normal states. Under stress or pathophysiological conditions, classically non-homeostatic neuronal mechanisms outside of the hypothalamus can be activated to reduce feeding. In the case of GDF15-GFRAL circuit, there is little evidence thus far for endogenous GDF15 to control feeding in lean, normal states. For example, healthy, lean mice fed chow diet seldom vary circulating GDF15 levels. Unlike many satiety factors, GDF15 is not released into circulation postprandially [22]. In fact, there is limited evidence to suggest that it is regulated by acute feeding states at all. As a testament to this, humans that ate 40% greater calories for 1 week had no change in circulating GDF15. Further, 24 hours of fasting in mice did not alter serum GDF15 [8]. Although a human study monitoring serum GDF15 every 30 minutes initially seemed to be associated with postprandial states, the authors found that the modest increases were explained by diurnal variation [22], an effect that likely also explains the postprandial fluctuation observed in a recent human blood sampling study [4]. In this study, the minor shifts in GDF15 are still within the range of normal circulating basal levels in healthy individuals (200-1200pg/ml). The effects of modest shifts in GDF15 within this normal range are

unknown, but unlikely to impact energy intake. Further, although some hindbrain cells such as calcitonin receptor neurons activate after an overnight fast and refeeding event, GFRAL neurons do not [23]. In contrast to gut satiety factors, GDF15 is therefore not influenced by nutritional status.

The function of GDF15 signaling under nonpathological states remains elusive. Genetic deletion of GDF15 and GFRAL in lean animals fed chow diets alters body weight slightly in some studies and not at all in others. Both male and female GDF15 KO mice had 6-10% more body weight than WT controls at 5 weeks and increased fat mass by 14 weeks [24]. Two other reports of GDF15 KO mice show no differences in body mass, body composition, or feeding behaviors [3,14]. GFRAL KO mice have no difference in food intake and body weight up to 6 months of age [15]. In contrast, genetic overexpression of GDF15 in mice decreases food intake, body weight and fat mass in mice fed chow or low-fat diet [25–28]. Under normal physiologic conditions and chow diets, loss of GDF15 or GFRAL in mice has little to no effect on energy balance.

However, when challenged with chronic high-fat diet (HFD) or obesity, serum GDF15 levels rise in mice, rats, and humans compared to lean controls [6]. Germline deletion of GFRAL or GDF15 in mice with overnutrition leads to a modest increase in weight gain and fat mass due to increased food intake. GFRAL KO mice were predisposed to HFD diet-induced obesity (DIO) in 2 studies [3,15]. In one study, after 12 weeks of HFD DIO, GFRAL KO mice accumulated 32% greater fat mass and 9% greater lean mass compared to WT mice [3]. Mullican *et al.* showed that HFD for 9 weeks led to a small increase in food intake and at 18 weeks an increased body weight and adipose mass gain [15]. In other studies, lack of GFRAL after 16 weeks of HFD was not associated with alterations of body weight, food intake, or fat mass compared to

WT mice [14]. To circumvent the impact of developmental adaptations in GFRAL and GDF15 KO mice, Tsai *et al.* used shRNA to knock down GFRAL in the AP and NTS and showed increase weight gain and fat mass of bilaterally injected AP/NTS with AAV-shRNA vs AAV-shControl. They also tested the impact of a weekly injection of a monoclonal human GDF15 neutralizing antibody in mice engineered to express human GDF15 and challenged with HFD. 14 weeks of antibody use showed reduced body weight gain and food intake compared to vehicle treated mice [29]. Tran *et al.* also found that loss of GDF15 in DIO male mice leads to significant increase in body weight and food intake when fed HFD [30]. Consistently, GDF15 signaling has been shown to induce weight loss and reduced energy intake under the challenge of diet induced obesity (DIO) in rodents.

A correlational example in humans comes from the mostly prominent glucose lowering treatment used for type 2 diabetes (T2D) used since the 1950s, metformin . Interestingly, metformin is associated with a small but reliable reduction in body weight. The dose of metformin in humans correlates with GDF15 levels in a trial of >8,000 participants [31]. Metformin treatment in humans for 2 weeks induced elevated serum GDF15 which was sustained for the duration of intervention and up to 18 months. This elevation of GDF15 is also correlated with the modest reduction of body weight accompanying metformin treatment. Further, metformin induced weight loss and anorexia under HFD conditions for 11 days were only present in WT mice and not in GDF15 KO and GFRAL KO mice, suggesting that metformin relies on GDF15 signaling for these effects [7].

Not surprisingly, subcutaneous administration of recombinant GDF15 in mice, rats and non-human primates induces reductions of caloric intake and body weight [15]. Similar results are seen with i.c.v administration of recombinant GDF15 into obese rats and chow-fed mice

[14,32]. Rats that are pair-fed to those administered subcutaneous GDF15 lose just as much body weight and fat mass as those treated with GDF15, indicating that weight loss is a result of reduced food intake as opposed to alterations in energy expenditure [14]. Moreover, artificial activation of GFRAL neurons slows gastric emptying and pharmacological administration of GDF15 alters food choice preference in which fat intake is reduced in mice [23,33], both representing other potential ways of limiting calorie absorption and intake.

While the ability of pharmacological GDF15 to elicit anorexia has been well investigated in both lean and obese animals, the current body of literature largely supports a role for endogenous GDF15 signaling to be of significance primarily during challenges of overnutrition, rather than during normal, healthy states. In contrast to peripheral satiety signals that are released in response to meal ingestion to control meal size and frequency, GDF15 is largely independent of nutrient intake. GDF15 thus represents a gut to brain alarm signal of threatening conditions. It is a peripheral signal that mediates a reduction of feeding behaviors when there is potent physiological stress, potentially to increase chances of survival, rather than a reaction to nutrient intake and long-term energy homeostasis.

1.1.4 GFRAL neuronal circuitry

Energy homeostasis is coordinated through a plethora of protein signaling mediators originating from peripheral organs such as the intestine, stomach, pancreas, and adipose tissue in response to a variety of factors including the feeding, circadian rhythms, adipose tissue mass, and metabolic states. In addition to direct hormone to receptor signaling in the brain, paracrine signals from the intestinal mucosa are released in response to nutrient intake and signal through vagal afferents to the NTS to relay information about nutrient content, density, volume of ingested food [34]. As such, the hindbrain regions of the AP and NTS are a central hub for

integrating diverse peripheral signals. A myriad of peripherally derived hormones such as CCK, ghrelin, leptin, PYY, and GLP-1 are well known to communicate nutrient and adiposity signals and impact food consumption via the NTS. Some of the downstream projections go to the hypothalamus and play a role in day to day energy balance, and others to the PBM to signal meal size in physiological and stress states. While it is established that many gut-brain signals reduce food intake, there is differential abilities of neural networks to transduce satiety compared to illness responses that still need resolution.

Both the AP and NTS are included in the dorsal vagal complex (DVC), a region that is involved in gut-brain signaling. The AP receives modest vagal input but has the advantage of receiving peripheral signals via circulating factors. On the other hand, the NTS receives heavy input from both the AP and visceral structures via the vagus nerve in response to the ingestion of both meals and toxins. The largest neuronal output from the NTS is the PBN which integrates visceral signals of taste, sickness, pain, and importantly appetite suppression [35].

The discovery of GFRAL and its narrow distribution in the CNS presented an important opportunity to identify the circuit that mediates the potent effects of GDF15 to reduce food intake and body weight. Prior to the discovery of GFRAL, early ablation studies showed the AP and NTS to be necessary for GDF15 induced anorexia. i.p. and i.c.v. injection of hGDF15 induced cFOS immunoreactivity in the AP, NTS [12,32] and CGRP neurons in the PBN and CeA [23]. Although a 5 day infusion using an osmotic minipump of recombinant (human) hGDF15 induced significant weight loss in sham mice, mice with an ablated AP or AP/NTS had stunted or no difference in weight gain, respectively [32]. Furthermore, subdiaphragmatic vagal deafferentation studies consistently show no impact on GDF15 mediated anorexia, confirming

that GDF15 likely signals directly onto the AP and NTS rather than through peripheral afferents. In fact, removal of the vagus nerve slightly heightened anorexia [14,36].

Though some of the projections of GFRAL neurons are beginning to be mapped, there is less clarity on their composition and protein expression patterns that can distinguish differing neural populations. For example, since GLP-1 produces anorexia via GLP-1R and is highly expressed in the AP and NTS, it was hypothesized that GFRAL and GLP-1Rs are present on the same neuronal population, or at least work through similar neural pathways. Though GLP-1R expression is largely similar to GFRAL expression in the hindbrain, only a small portion of GLP-1R neurons express GFRAL. GDF15 and GLP-1 agonists activate separate neuronal circuits in which the anorexic effects are additive if administered together [33]. In contrast, Worth *et al*. found that a subset of CCK neurons, which project from the NTS to the PBN, are GFRAL positive and that blocking CCK or GFRAL signaling can disrupt GDF15 induced anorexia [37]. Additionally, 27%-45% of GFRAL neurons immunostain for tyrosine hydroxylase, suggesting that they are catecholaminergic dopamine β-hydroxylase (DBH) cells [14,37], although one study investigating immunostaining following GDF15 administration recently opposes this finding [32]. Both CCK and DBH neurons from the NTS to the PBN have been known to induce anorexia [38]. Over half of the GFRAL neurons within the AP colocalized with the glutamate transporter Slc17a6 fluorescent tag in mice, which is consistent with the understanding that ~80% of NTS to PBN neuronal transmission is glutamatergic [37–39]. The exact composition of GFRAL neurons and downstream neuronal projections and circuitry is still under investigation.

To further investigate the neuronal network downstream of GFRAL AP and NTS, our group recently used designer drug receptor DREADD and GFRAL^{cre} mice to artificially activate GFRAL neurons using clozapine N-oxide (CNO). CNO administration leads to subsequent cfos,

an early activation gene, expression in the PBN, central nucleus of the amygdala (CeA), and paraventricular nucleus (PVN). Furthermore, GFRAL neurons project from the AP to the lateral PBN in close proximity to calcitonin gene-related peptide (CGRP) expressing neurons. When stimulated, CGRP neurons cause a rapid and a profound reduction of food intake [35,38] and when silenced with TetTox, the anorectic (and aversive) response to GDF15 was dampened [23], suggesting that GFRAL neurons signal through CGRP PBN neurons. The PBN, however, also integrates satiety signals. Gastric distention and intestinal meal termination hormones such as CCK and GLP-1 can signal meal termination via the vagus to CGRP PBN pathway [38]. GFRAL neurons thus may signal through a pleiotropic neuronal population.

The NTS to CGRP neuronal circuit is an interesting one, as it combines signals of meal termination as well as aversive, fear conditioning, pain and temperature stress responses [40]. Additionally, part of the hypothalamic feeding neurocircuitry to induce meal termination comes from orexigenic AgRP inhibition of $CGRP^{PBN}$ [41–43]. As such, the PBN represents a "hub" integrating diverse signals. Importantly, $CGRP^{PBN}$ neurons do not play a role in normal energy homeostasis, as the inhibition of neuron activity increases meal size but leads to a compensatory increase in meal frequency as well [43]. Instead, activation of CGRP ^{PBN} circuit represents an "emergency" response to noxious stimuli, as exemplified by induction by tumor bearing and cisplatin therapy, both of which produce malaise, lethargy, and sickness symptoms in both humans and mice [44,45]. If CGRP neurons in the PBN are inactivated by using cre dependent TetTox in mice, anorexia and malaise are reduced in the presence of cancer [46] and blocks pain and memory responses to foot shock [47]. Inhibition of $CGRP^{PBN}$ neurons using hM4Di/CNO or with tetanus toxin attenuates CTA formation [35]. This circuit is therefore an example of a network that signals anorexia in part due to illness, transducing cautionary signals to forebrain

regions. It is possible that GDF15 signaling on GFRAL neurons may contribute to the illness associated $CGRP^{PBN}$ circuit, resulting in the induction of both anorexia and aversion (Fig. 1).

The hindbrain houses a heterogenous population of neurons that integrates continuous signals from the gut. Ingested compounds trigger vagal and hormonal signals that ultimately drive anorexia, both in the case of ingested nutrients as well as toxins. The NTS to PBN pathway is utilized by a variety of gut and adipose stimuli, including CCK, leptin, and GLP-1. Although some of this neurocircuitry is shared, there are many differences in the induction and impacts of gut signals that communicate satiety compared to illness from GDF15 (Table 1). For example, although CCK, leptin, and GLP-1 are triggered in response to the presence or absence of nutrients, GDF15 is not. Differences in NTS and PBN populations of neurons that drive the anorexia induction by satiety in contrast to illness are still being mapped and will be discussed further in this dissertation

1.1.5 Biomarker of illness and mortality

Normal circulating levels of GDF15 range from 200pg/ml- 1200pg/ml [48] with diurnal variations, but can become elevated in stress, injury, and pathophysiological conditions and infections. This elevation has made it a popular candidate as a biomarker or prognostic marker in a variety of diseases. In addition to cancers, GDF15 elevation specifically in cardiovascular disease has become one of the more popular pathologies for researchers. GDF15 circulating levels predict progression of cardiovascular disease (amongst many other disease states) [49,50]. For example, circulating GDF15 is correlated with both hospitalization and death due to heart failure [51]. It is upregulated in infarcted myocardium in humans but the source of GDF15 is debated [52–54]. Similarly, ischemic kidney tissue has upregulated GDF15 mRNA and there is an association with GDF15 and chronic kidney disease [55]. Currently, there are ongoing clinical

trials worldwide in progress to test the effectiveness of GDF15 as a plasma biomarker for a variety conditions, including polycystic ovarian syndrome, diabetes, and acute kidney disease.

Interestingly, though not surprisingly, GDF15 has been associated with severe disease states and all-cause mortality in several studies [56] In a study done of 219 critically ill ICU patients, GDF15 levels predicted organ failure, severe illness, and ultimately mortality [57]. The Rancha Bernardo Study examined 1391 older patients and found serum GDF15 to be a predictor of all-cause mortality, including both cardiovascular and non-cardiovascular mortality [49]. Additionally, the Framingham study found GDF15 to be a marker for all-cause mortality, incident heart failure, and significant cardiovascular insults [50]. GDF15 can be thought of as a stress protein, due to its release in diverse pathologies and its strong prediction of death.

1.1.6 Cancer anorexia and chemotherapy

In a variety of cancers, patients often experience a reduction of appetite and food intake, leading to drastic and adverse weight loss which is termed cancer anorexia. A disease state that represents a chronic state of stress is cancer, as well as its popular treatment, chemotherapy. In fact, the very first account of the ability of GDF15 to induce anorexia came from a landmark study that discovered nude mice implanted with a human prostate cancer cell line overexpressing GDF15 lost weight compared to control groups, with mice with greater circulatory GDF15 levels associating with higher weight loss, along with a reduced fat mass and food intake. This weight loss was reversed with an injection of an anti-GDF15 monoclonal antibody with no impact on tumor size [12]. This discovery opened the door to test a variety of tumors that induce cancer anorexia. GDF15 is found elevated in circulation in colorectal [48], esophageal [58,59], pancreatic [60], ovarian [61], and prostate cancers [62], and often correlates with progression of disease [36]. Levels as high as 10,000-100,000 pg/ml have been reported in advanced cancers

[12,63,64]. A cross-sectional study of male cancer patients found that patients with body weight loss had greater GDF15 than patients without weight loss and control subjects without cancer. GDF15 was further associated with decreased fat mass and poor survival with higher circulating GDF15 levels [65].

Cancer cachexia is a devastating wasting syndrome of several advanced cancers in which there is an involuntary degradation of skeletal muscle, adipose, and overall body weight, a part of which is due to a reduction in appetite and energy intake [66,67]. Cachexia occurs in about 80% of advanced cancers [65]. Just a 5% loss in body weight is associated with an increase in poor clinical outcome and the risk increases with greater weight loss. Cancer cachexia accounts for approximately 25% of cancer mortality, rendering GDF15 a potential candidate for pharmacological therapies to control the anorexia associated with cancer and cachexia. Recently, a GFRAL monoclonal antibody antagonist (3P10) reduced cancer cachexia in mice [68]. Blocking GDF15 using a monoclonal antibody prevents anorexia, but not muscle atrophy in a model of GDF11 induced cachexia [69]. The discovery that blocking GDF15 using a monoclonal antibody prevents disease in seven additional models of rodent cachexia and increases survival [70] has led to ongoing clinical trials for potential treatments that target GDF15/GFRAL. One current phase 1a study involves an antagonistic antibody to GFRAL signaling to treat cancer anorexia and cachexia in metastatic pancreatic cancer and a variety of 10 advanced metastatic tumors (NCT04068896; NGM; NGM120). Another current clinical trial is a monoclonal antibody against GDF15 for cachexia in patients with non-small cell lung carcinoma (NCT04299048; Pfizer; PF-0646860).

A commonly used treatment for many cancers is a platinum-based chemotherapeutic agent called Cisplatin. There is a growing body of research around the role of GDF15/GFRAL

network in mediating cisplatin therapy. Mice with cisplatin treatment at 6 weeks exhibit increased circulating GDF15 along with a reduction of energy intake and body weight of 15%. GFRAL knockout and monoclonal antibody against GFRAL pretreated mice both exhibit resistance to the effects of cisplatin [3,71]. Because of GFRAL's implication in both cancer anorexia and the mechanism of action of cisplatin treatment, its therapeutic potential in cancer patients is two-fold. Patients suffering from cachexia and/or those that are being treated with cisplatin may benefit from cotreatments that reduce GDF15/GFRAL signaling.

1.1.7 Nausea and emesis/aversion

Several groups, including ours, have identified that pharmacological administration of GDF15 as a principal agent to trigger nausea and emesis. GDF15 induces a potent CTA [4,8,23,72] in addition to PICA behavior [72] and a conditioned place aversion [37] in rodents. A strong CTA is also induced when GFRAL neurons within the AP are activated using DREADDs [73]. Although we do not have clinical trial data from human studies, we can rely on data from patients with conditions or treatments that significantly elevate nausea to shed light into GDF15's role in nausea and emesis. While short term activation of the GDF15 network via artificial GFRAL neuron activation or GDF15 administration certainly induces aversion and avoidance, the effects of long-term activation is not as conclusive.

Along with anorexia, metformin side effects also include nausea and gastrointestinal malaise. However, patients using metformin long-term do not report a persistent symptom of nausea. A second clinical example comes from women with severe nausea and vomiting in pregnancy (NVP), called hyperemesis gravidarum (HG). Modestly elevated circulating GDF15 has been associated in one study of women in their second trimester who experience vomiting within, but not in those who experience nausea without vomiting [74]. 50-90% of women

experience nausea during their pregnancy and the vast majority of those women (<95%) do so beginning in the first trimester [75–77]. While GDF15 levels are highest in the first trimester when rates of nausea are highest in pregnant females, the elevations persist for the second and third trimesters, when many cases of nausea are significantly decreased [10]. Additionally, many females that do not experience nausea and vomiting in pregnancy also exhibit heightened GDF15 at levels from 10,066-10,147 pg/ml. There is no question that GDF15 administration leads to an aversive response in rodents and may induce initial illness symptoms in humans. However, the cases in which endogenous GDF15 is elevated to high levels do not always present with persistent nausea. As pregnancy represents a large stressor on multiple organ system, elevations in GDF15 could be a secondary effect representing other factors. Unfortunately, current testing of this condition is limited to correlational human studies. Further testing of this hypothesis is difficult and requires clinical studies, as there are no adequate preclinical models for NVP and HG.

1.2 Infection induced anorexia

In response to infectious challenges, humans have evolved a number of host defense systems. Release of immune mediators, fever thermoregulatory responses, lethargic behavior, altered energy expenditure, metabolic changes, and of particular relevance for this thesis, altered feeding. An infection is often accompanied by anorexia and reduced energy intake. These mechanisms can be acutely advantageous and protective to the host. A response that may be initially adaptive, can become chronic and adverse, such as in the case of cancer cachexia.

Anorexia in acute and chronic illness unsurprisingly often results in the catabolism of energy stores and reduction of body weight [78]. Fluctuations in body weight (under normal

circumstances) triggers a counter homeostatic responses. However, during infection, a reduction of food intake and weight with negative valence are favored. As early as the 1970s, we learned that anorexia is often adaptive and critical for the survival in the face of acute infection. Force feeding mice infected with some bacteria [79–82] results in increased mortality, illustrating the often protective effects of reducing food intake. Evolutionarily, illness induced anorexia is well conserved from flies to rodents and mammals, including humans [83,84]. Some researchers hypothesize that reduction of food seeking was developed to protect humans from infection particularly during bouts of famine [80]. Moreover, anorexia may serve to starve the invading microbe of necessary nutrients in the host to inhibit microbe replication, a resistant mechanism known as nutritional immunity [85,86] and lower the demands for humans to search for food in illness [87]. In contrast, mice infected with influenza and viral sepsis improve survival with caloric supplementation, regardless of the behavioral anorexic response [79] and worse outcomes with restriction [88]. Further, counterregulatory responses from particular microbes can adapt to host fasting [87], leading to unnecessary and potentially detrimental anorexia. Thus, whether the illness induced anorexia is beneficial or detrimental depends on the balance of host tolerance and resistance mechanisms.

Sepsis is defined as organ dysfunctions from dysregulated host responses to infection [89]. Viral, fungal, and most commonly bacterial infections can result in sepsis, accompanied by high risks of severe tissue damage, organ failure and lethality. The signaling pathways and neural mechanisms that mediate anorexia during illness still largely remain elusive, though some gut to brain signals have been proposed [87]. Dissecting the driving mechanisms remain crucial to our understanding of feeding networks and understanding of illness induces metabolic dysregulation.

Altering gut-brain signals mediating anorexic responses that are detrimental is a profoundly impactful therapeutic opportunity for critically ill patients.

1.2.1 Bacterial infection

One of the most commonly used model systems to study the impact of bacterial infection is lipopolysaccharide (LPS), a component of gram-negative bacterial cell wall. Depending on the dose of infection, LPS in humans is capable of stimulating anorexia, lethargy and fever, all of which are well replicated in mouse models. Various brain regions activated by LPS injection have been long identified. However, the specific neural circuits responsible for signaling anorexia and nausea of LPS still remain undefined. Amongst the populations that are activated are PBN CGRP neurons [35]. Additionally, hypothalamic inhibitory AgRP signaling modulates CGRP PBN anorexic circuits. Optogenetic activation of AgRP terminals reduces PBN CGRP activation [43] and results in a blunting of the anorectic response to meal related signals, such as CCK and amylin [41]. Therefore, it was hypothesized that hypothalamic regulation of PBN CgRP neurons may directly control infection related signals from the PBN CGRP neurons as well. However, this is not the case for administration of LPS, which resulted in similar anorexia despite increased AgRP to PBN CGRP terminal stimulation [41]. These results show that neural networks regulating bacterial infection are to some capacity distinct from satiety in the hindbrain.

LPS injection has been shown to activate rodent AP and NTS [90–92] and increase levels of glutamate in the NTS [93]. Further, peripheral LPS administration specifically induces cFos immunoreactivity in GFRAL cells within the hindbrain [73], suggesting a potential role of GFRAL neuronal signaling in mediating illness effects of bacterial infection. While cecal ligation puncture (CLP) in which a needle is passed through the cecum to create a perforation is a common model for bacterial sepsis. Though the needle gauge size is usually defined, the length

is poorly reported in research studies which contributes to the high variability of disease and mortality [94]. Endotoxin infection by administration of LPS represents a second model of sepsis. The role of GDF15 in LPS and CLP mediated sepsis has been debated, specifically whether GDF15 is protective or detrimental to the host. To date, two studies suggest that GDF15 plays a protective role in LPS induced infection [5,95]. Li *et al.* shows increased survival with administration of recombinant GDF15 in a LPS and B-Galactosamine induced model of liver injury. Luan shows that blocking GDF15 with a monoclonal antibody increases mortality in sublethal LPS infection in mice. GDF15 activation is proposed to be necessary for to mediate immune tolerance mechanisms for improved survival. Taken together, these findings suggest that GDF15 may play a protective role in bacterial infections. It should be noted that the purity of the recombinant GDF15 is unknown and the antibody against human GDF15 has not been validated in these studies. In contrast, a separate group illustrated a positive correlation between survival and GDF15 levels in human patients with severe sepsis. GDF15 KO mice infected with a polymicrobial CLP model of sepsis exhibit longer survival compared to WT mice, suggesting a detrimental correlation of circulating GDF15 [96], which supports a number of studies linking GDF-15 to all-cause mortality [49,56]. The role that GDF15 plays in the pathology of bacterial infections and whether GFRAL signaling is necessary to alter physiological illness parameters such as food intake is still unknown. Chapter 2 tests the necessity of GFRAL signaling using a model of LPS in mice.

The original name of macrophage inhibitory cytokine-1 (MIC-1) was earned due to the observation of GDF15/MIC-1 to inhibit macrophage TNF secretion in response to a LPS, prior to the discovery of GFRAL [2]. Further, many proinflammatory cytokines when administered ICV can induce anorexia [97]. LPS induces a dramatic inflammatory cytokine response and elicits

inflammation, both peripherally and centrally. IL-1b, TNF, IL-6, and IFN-y are elevated in LPS infection. One hypothesis for LPS anorexia is cytokine signaling [98]. Thus a combination of LPS induced cytokines and peptides may in concert contribute to physiological illness. While there are several proposed mechanisms, the neural network and signaling mediators responsible for the illness and food reduction have yet to be defined [99,100].

1.2.2 Fungal infection

A wide variety of fungal infections elicit illness symptoms that alter gut-brain signaling. Mycotoxins, secondary metabolites produced by several fungi, are potent chemical signals that are capable of inducing a wide variety of effects, ranging from antibiotic to mycotoxicosis [101]. Fungal contamination of food has made humans and animals particularly vulnerable for centuries. Trichothecenes, a family of mycotoxins, are common contaminants of grains such as corn, barley and wheat. For example, deoxynivalenol (DON) is a highly stable type-B mycotoxin produced by the *Fusarium* fungi and is found at highest concentrations of all trichothecenes in foods.

The anorectic effect of DON toxicity was commonly observed in swine exhibiting chronic feed refusal and a reduction of body weight in the early 1900s. DON was later isolated during a human epidemic in Japan in the 1970s and its discovery explained many previous worldwide cases of human and animal gastroenteritis outbreaks [102]. Mice given DON, drastically reduce energy intake in a dose dependent manner, primarily within the first 4 hours after toxin administration. By 24 hours, mice rebound with increased total food consumption [103]. Thus, mild, acute doses of DON do not lead to a change in body weight, as the initially reduced energy intake is followed by a compensatory increase in food intake. DON exemplifies

an illness anorectic response and it received the nickname “vomitoxin” due to its ability to rapidly elicit gastrointestinal malaise symptoms such as diarrhea, nausea, and emesis.

The mechanisms by which DON induces anorexia and nausea are not known but there are several hypotheses. DON can bind and activate calcium sensing receptor (CaSR) which is expressed in a variety of organs including the intestine and the brain. In the intestines, CaSR can be found on enteroendocrine cells, potentially explaining the mechanism by which gut hormones are increased into circulation after DON exposure. Exposing STC-1 cells to DON exhibits a dose dependent increase of GLP-1 and CCK release [104] which is reduced when a CaSR antagonist NPS2143 is present [105]. Within 15 minutes of DON exposure, intestinally derived peptides PYY, GLP-1, and CCK are highly elevated into circulation [106] and stay elevated for several hours. PYY, CCK and GLP-1 are all well-known anorectic hormones that signal to central networks via either vagal or direct brain activation.

It is plausible to hypothesize that intestinal hormones may contribute to the anorectic response. For example, pharmacological PYY administration can acutely reduce feeding with accompanied nausea, however *in vivo* pharmacological antagonist studies have failed to alter DON induced anorexia [106]. Similarly, GLP-1 activates GLP-1Rs found in both the vagus and various brain regions, including the AP and NTS. In addition to a reduction of food intake, currently used GLP-1R agonists exhibit dose-dependent nausea, vomiting, and diarrhea as side effects [107–109]. This similarity between exogenous GLP-1 administration and DON suggests that GLP-1 and DON signaling may activate similar neurocircuitry. This hypothesis is tested Chapter 3. Whether changes in a combination or individual gut hormones lead to functional DON symptoms is debated, as differing animal models and time points show conflicting results.

A wide range of evidence points to the role that the brain plays in the response to DON. Low dose exposure of DON directly administered to the brain via i.c.v. injection leads to potent anorexia. Moreover both i.c.v and peripheral administration of DON leads to the activation of the NTS and AP neurons [110]. Whether these regions are activated directly by circulating DON or indirectly by peripheral mediators or vagal activation is currently unknown. Unilateral vagotomy has no impact on neuronal activation in the NTS after oral DON exposure [104,111,112]. Further, DON has been shown to cross the blood brain barrier in several species [104]. In mice, DON protein is detectable within 5 minutes in the brain after a single oral gavage of DON [113,114]. Thus, DON can directly reach the brain rapidly after exposure and may directly contribute to neural food intake and nausea signaling pathways. Some of these neurons that are activated within the AP may be GFRAL neurons. We directly test the necessity of GFRAL signaling in DON illness utilizing several genetic mouse models in Chapter 3.

1.3 Metabolic disease

1.3.1 Obesity

Within the last 3 decades, obesity has become one of our country's largest public health challenges. Though defined as excess body fat mass, obesity is most commonly assessed as an elevated body mass index (BMI). BMI is limited by accuracy, as it cannot differentiate between fat and lean mass, but excels in convenience and ease of measurement. BMI measures body weight as a function of height in which normal and obese BMI is defined as <25 kg/m^2 and >30kg/m^{2,} respectively. While average BMI in the US remained stable within the 1960s, since 1975, worldwide obesity has tripled [115–117]. In 2017-2018, over 40% of the US population

was deemed obese. Thus, the US is currently in the midst of a severe obesity epidemic which is rapidly spreading to developing countries around the world.

The burden of obesity on the individual spans far and wide. In 2006 alone, the estimated national medical cost for obesity was $147 billion dollars [118], amounting to an additional cost of $2,741 for each person with obesity. The reason for this grave economic cost to the healthcare system can be attributed to the wide variety of comorbidities associated, including higher risks of cardiovascular diseases, diabetes, and cancers. The result is not only a heavy economic burden, but reduction on the quality of life and lifespan for individuals with obesity. The demand for creating new treatments becomes increasingly high, as our rates nationally (and worldwide) soar.

The steep incidence of obesity can be attributed to a combination of factors, changing environments and adaptive biology, much of which still remains only partially understood. In contrast to the common popular belief, obesity has proven to not be simply a matter of exercise and caloric intake, as defense of a higher energy set point in obese individuals suggests otherwise. The changing global food system with increasingly cheap, fast, and high-density food availability in combination with the impacts of our genetics, epigenetics, decreased physical activity contributes to the proliferation of obesity. This multifactorial nature makes obesity a complex area of study, therefore a complex disease to treat.

1.3.2 Bariatric surgery

In an attempt to alter the energy equation, diet and exercise are often the first line treatment for overweight patients. While this strategy can often lead to successful initial weight loss, this result is often short lived, as exemplified by the “yo-yo” dieting effect and more famously from the participants of the US television program “The Biggest Loser”. Although

participants were able to shed a dramatic amount of weight quickly, they regained most of the weight after the end of the show [119,120].

This leaves us with more invasive approaches including permanent alterations to the anatomy of the GI tract termed bariatric surgery. Bariatric surgery comes in a variety of forms, the most common in the US being vertical sleeve gastrectomy (VSG) and roux-en-y gastric bypass (RYGB). In VSG, ~80% of the stomach along the greater curvature is removed, leaving a tube-shaped pouch (a sleeve). In RYGB, a small gastric pouch of the stomach and duodenum (the size of a walnut) is created and reattached to the middle of the jejunum. Nutrients thus flow through bypassing ~95% of the upper GI tract. While both VSG and RYGB involve a physical restructure and reduced capacity of the stomach, RYGB alters nutrient flow.

Despite the differences in mechanical restructuring between the two surgeries, VSG and RYGB both lead to a sustained ~40% reduction of food intake and body weight in VSG and RYGB in addition to about a 38% remission of T2D [121–123]. Since glucose regulation is heavily tied to weight, this positive change may not seem surprising at first glance. However, for some patients, changes in glucose metabolism occur prior to weight loss, often while the patient is still in the hospital or within several days after the procedure [121]. For those whose diabetes isn't completely resolved, necessity of diabetes medication usage decreased by 65% compared to 0% in the lifestyle intervention alone group [121–123]. Further a first large case controlled clinical study called the Swedish Obesity Subjects study showed that bariatric surgery results in a reduction in mortality by 40% within 18 years, which includes a 92% reduction of mortality from diabetes specifically [124].

The mechanism underlying the potent effects of VSG and RYGB remain elusive. Diverse hypotheses have been postulated and tested. The most prevalent theory revolves around

the mechanical changes imposed on the GI tract. It has long been hypothesized that a reduction in both stomach volume and intestinal nutrient absorption represents the driving factors behind weight loss. However, there is much data that challenges this hypothesis.

To this point, the alterations in the pattern of food intake following VSG and RYGB is remarkable in both humans and rodents. The major point of appetite changes following bariatric surgery is that after an initial reduction of food intake, over several weeks, rodents return to eating the same daily caloric load as they had prior to surgery, without regaining the fat mass and weight [122,125,126]. In other words, rodents exhibit sustained weight loss despite a return to normal food intake. They defend a lower body weight. VSG rats that are food restricted, expectedly lose additional weight. When later given access back to food, they increase their food intake to gain weight. Further, rodents are able to increase energy intake and weight during pregnancy [127]. This illustrates that VSG does not eliminate homeostatic mechanisms, rather, changes them to maintain a lower body weight [128]. While the malabsorptive and mechanical restriction hypothesis are still widely cited, they simply do not explain the complex changes in eating behavior observed in both humans and rodents after bariatric surgery. The viability of surgery reminds us that it is possible to alter energy homeostasis sufficiently to battle obesity.

Annual bariatric surgery procedure numbers jumped from 16,000 to 228,000 within the last 3 decades [129,130]. Understanding the mechanisms by which weight loss is attained and importantly, sustained, could drastically improve the accessibility of therapy for obese patients and allow us to treat a wider swath of the population. The last several decades have opened up a variety of hypotheses that have centered around altered communication between the GI tract and other organs including the brain. A key research goal is to identify the basis for this altered communication so that it may be more directly manipulated to mimic the potent effects of

surgery in a manner that does not require permanent rearrangement of GI anatomy. Further, bariatric surgery is a good model to study altered gut brain signaling that results in altered body weight and feeding behavior through changes in neural and hormonal signaling.

1.3.3 Glucagon-like peptides

Some of the gut signals that are clearly altered after bariatric surgery are glucagon-like peptides. These peptides that are made in both the gut and in the brain are thought to be a key component of the gut-brain axis as they coordinate food digestion and nutrient absorption. Specifically, glucagon like peptide 1 (GLP-1) has become on the most popular targets of gut secreted peptides. GLP-1 is a pleiotropic incretin involved in nutrient absorption, appetite regulation, intestinal motility, and glucose regulation. It is cleaved by proglucagon prohormone convertase 1/3 from the preproglucagon (*Gcg*) gene. Peripherally it is produced in enteroendocrine L cells primarily in the distal ileum and pancreatic islet cells. Centrally, it is cleaved in preproglucagon neurons largely residing in the NTS. While basal levels of GLP-1 are low, they are greatly elevated in response to a meal. Post-prandially, GLP-1 is well-known for its incretin effect which stimulates insulin secretion and inhibits glucagon to promote glucose clearance, but it also reduces appetite, gastric emptying and intestinal motility to increase nutrient absorption [131].

Peripherally, GLP-1 receptors (GLP-1R) are expressed in pancreatic β cells, intestinal vagal afferents and throughout the brain, including in key feeding regions such as the hypothalamus and hindbrain. Interesting, postprandial circulating GLP-1 levels dramatically and rapidly increase in circulation following both RYGB and VSG, nearly 10-fold, potentially due to intestinal adaptation and the resulting increase of L cells in the intestines [132]. Moreover, circulating levels are elevated in humans following surgery when compared to patients who have

lost weight via diet, confirming that the elevation in GLP-1 is specific to surgery and not weight loss [133]. Vagal GLP-1R transmission is not necessary to induce the weight loss effects, as illustrated by pharmacological agonism with liraglutide in a model of subdiaphragmatic vagal afferent deafferentation [134] . Despite the marked elevation of GLP-1 levels after weight loss surgery, studies using GLP-1R KO mice have shown that GLP-1R signaling after surgery is not critical to the resulting beneficial effects on weight and glucose metabolism [135].

Although it is likely not the critical component of surgery, GLP-1 has therapeutic value to diabetic patients whose endogenous incretin responses are blunted. Because GLP-1 is rapidly cleaved and inactivated by dipeptidyl peptidase 4 (DPP4) within minutes, long acting peptides were created. Several GLP-1R agonists, such as liraglutide, exenatide and semaglutide, and DPP4 inhibitors are approved for clinical use to improve glycemic control and body weight. However, a common side effect of these drugs is nausea and vomiting. To reduce feeding, GLP-1 may work better in conjunction with other gut hormones. For example, newer therapeutics are focusing on dual and triple agonists of GLP-1 in combination with glucagon and GIP to improve therapeutic potential.

Interestingly, GLP-1 is not released in isolation. *Gcg* processing concurrently cleaves GLP-2, which signals onto GLP-2R, from L cells in the ileum. Unlike it's incretin sibling, the main role of GLP-2 is intestinotrophic. It plays a principal role in intestinal cell proliferation, growth and barrier function. GLP-2 increases crypt and villus height in rodents and humans (Jeppesen 2005). Whether this effect is mediated by neural activation of enteric neurons is debated [136,137]. GLP-2 enhances mucosal structure and nutrient absorption in mice and rats with bowel resection, importantly, without causing malignant growth [138,139]. GLP-2 increases energy absorption, lean mass, crypt depth and villus height. These advantageous properties have

led a long-acting GLP-2 analog, Teduglutide, to become an approved treatment for short bowel syndrome, which presents with nutritional imbalance, diarrhea and weight loss.

Although accurate measurement of GLP-2 has been a challenge, as reliable assays were not produced until recently, GLP-2 is released along with GLP-1. It is not surprising that GLP-2 is increased in circulation along with GLP-1 after bariatric surgery, as the two hormones are processed by the same enzymes [140,141]. This increase has been associated with crypt cell proliferation and could reflect an adaptation to the mechanical structuring in an effort to increase nutrient absorption. Additionally the increase in enteroendocrine hormone secretion could thus be the result of GLP-2 action on intestinal growth. However, the necessity and function of GLP-2R signaling following surgery is not well documented. Although GLP-2R has been mapped in various brain regions such as the medulla, amygdala, hippocampus, pons, and pituitary gland [142] there is little data on their impact to central neural signaling. It is therefore best known for the local paracrine signaling effects within the intestine itself. Like glucagon like peptides, there are a variety of local intestinal changes following obesity and surgery.

1.3.4 Microbiota

Bariatric surgeries are highly successful long-term treatments that help reverse both obesity and the accompanying metabolic pathologies such as T2D. One of the potential mechanisms by which bariatric surgery impacts patients is via the gut microbiota. Both humans and rodents display significant alterations in intestinal microbial colonies following gastric bypass [143,144]. Alterations in composition may have a dramatic impact on obesity promoting parameters as illustrated by studies involving fecal transfers from one animal to another to alter microbial compositions in the receiving animal.

As a testament to this, germ-free mice colonized with bacterial composites isolated from the intestines of donor humans that previously went through a bariatric surgery, exhibit weight loss and reduced levels of body fat [145]. Further type II diabetes patients who are colonized with microbiota from lean donors using a fecal transplant have better metabolic parameters such as increased insulin sensitivity [146]. These effects suggest that the microbiota may be capable of producing changes to metabolic processes and phenotypes.

Although the intestinal microbiota is best known for its role in processing nutrients, gut microbes are capable of generating metabolites and altering production of other intestinal signals, including EEC gut hormone secretion. GABA, serotonin, histamine, short chain fatty acids (SCFA) and secondary bile acids are some microbially derived signaling mediators [147,148]. It is hypothesized that refining the diversity and signaling molecules produced by gut microbiota could impact a variety of pathologies both locally in the GI tract (inflammatory bowel diseases and colorectal cancer), distally within the CNS (autism and Parkinson's disease), and in whole body metabolism by altering gut-brain signaling [147,149]. Thus, therapeutic interventions centering the modulation of gut microbiota and microbial derivatives is a growing area of interest for a range of pathologies.

The role of the microbiota in metabolic diseases is developing, but research has only just grazed the tip of the iceberg. Diverse factors such as diet, genetics, cognitive pathologies and exertion of stress pathways all impact composition and diversity of microbiota, potentially via the gut-brain axis. Thus, it is a complex system to study. Many microbial studies are limited to correlational analysis, as model systems to study microbial alterations are far from perfect. Germ-free mice are the primary model used to test the impacts of microbiota, but they usually present with a vast array of confounding developmental deformations. In many studies, it is

unclear whether microbial changes are a cause or effect of metabolic diseases. Further, the diverse species and strains of microbiota that inhabit the gut can vary from individual to individual, with over a 1000 different species and trillions of bacteria inhabiting the intestinal tract [150,151]. The way the statistical analysis is completed and taxonomic composition is defined and compared is tremendously important, but often greatly variable between studies.

1.3.5 Bile acids

A factor that has been proven to be a critical component for the beneficial impacts of bariatric surgery include farnesoid X receptor (FXR) which are the target of endogenous bile acids. Mice lacking FXR receptor fail to display improved blood glucose and weight loss induced from VSG surgery in mice [152]. Interestingly, wildtype mice receiving VSG exhibit microbial changes that mimic a "lean" phenotype, but mice lacking FXR do not. Taken together, FXR and bile acid signaling may impact microbial and metabolic changes following surgery.

Bile acids are secreted from the liver postprandially into the duodenum via the common bile duct where they aid in the digestion and absorption of dietary fats. Primary bile acids such as cholic acid (CA) and chenodeoxycholic acid (CDCA) are created in the liver via oxidation of cholesterol [153]. Secondary bile acids on the other hand are derived via dehydroxylation by dehydroxylase enzymes of primary bile acids by the intestinal microbiota. Either primary or secondary free bile acids can form bile salts through conjugation to the amino acids glycine or taurine. Thus, a wide range of bile acids/salts are made, making the composition and effects of circulating bile acids diverse. Further, gut microbial composition and prevalence can impact the diversity of bile acids in circulation [154]. When microbial colonization was completely removed or altered using antibiotics in mice, levels of bile acids plummeted [155].

Beyond their role in lipid absorption, bile acids can act as signaling molecules by binding two receptors: an intracellular ligand-activated nuclear receptor (FXR) and a G protein-coupled receptor Gpbar-1 (TGR5). Bile acid binding to FXR can lead to secretion of fibroblast growth factor (FGF15/19), a gut hormone implicated in glucose tolerance and weight loss via signaling in the brain [156,157]. Intriguingly, increased enterohepatic circulation of bile salts and free acids is a major consequence following bariatric surgery, a change that is independent of weight loss. RYGB patients show increased serum bile salts along with increased production of FGF15/19 [158]. Although the function of elevated bile acids after surgery remains elusive, it is hypothesized that bile acids are important for improved metabolic parameters and weight loss [152,153,159,160] following surgery. Thus, bile acids represent yet another mechanism capable of altering gut to brain signaling and impacting metabolic phenotypes.

Bile acids can signal to the CNS indirectly via the release of FGF15/19 or by directly by crossing the blood brain barrier [161]. In various models of neurodegenerative diseases such as Alzheimer's disease [162], Huntington's disease [163] and prion disease [161], bile acids (TUDCA or UDCA) administration exhibited neuroprotective effects. The mechanisms by which bile confers protection within the nervous system remain to be elucidated as central bile acid signaling research is still quite sparse.

For all studies regarding bile acids in rodents, we must take into consideration the variability of bile acid composition between rodents and humans. While mice are primarily composed of hydrophilic acids such as muricholic acids and cholic acids, humans tend to display a hydrophobic profile of acids with increased CDCA, cholic acid and deoxycholic acid [155].

1.4 Summary and aims of dissertation

This body of work is focused on periphery to brain signaling in the context of obesity and illness responses. It tests intestinal and peripheral signaling molecules to influence feeding networks and weight patterns in response to physical stressors such as infection, obesity, and bariatric surgery. Our understanding of gut-brain feeding networks and signaling will provide solutions for diverse diseases that present with dysregulated ingestive behaviors which reflect alterations in satiety (obesity) and illness responses (sepsis, cachexia) but currently have inadequate treatments.

To do so, it is crucial to investigate signaling proteins and differential neural networks that are induced to regulate feeding in illness which can be modeled by bacterial and fungal infection. In Chapter 2 and Chapter 3, the hypothesis that the circulating stress hormone GDF15 contributes to bacterial and viral illness respectively is associated anorexia and nausea is tested.

Further, bariatric surgery in rodents is an exemplary model system in which gut brain signaling is altered and results in potent and sustained feeding and weight changes. The rising rates of obesity and metabolic disorders is a large public health concern, creating a need for developing accessible therapeutics. Bariatric surgery procedures to restructure the stomach and intestinal tract are highly successful treatments. The physiological systems by which the reversal of diabetes and adiposity is conferred with surgery has yet to be elucidated. Identifying mechanistic origins of the metabolic benefits for bariatric surgery are key to developing therapeutics targeting pathways rid of surgical intervention available to a wider population of patients with obesity. For example, both gut and liver derived hormones and bile acids may be crucial to beneficial impacts of surgery. To this end, we tested the contributions of GLP-2 and examined bile acid composition in mice undergoing bariatric surgery in Chapter 3.

	Leptin	GDF15	Citations
Tissue secretion	Adipose	Inducible in most peripheral tissues	[164,165]
Receptor expression	Widely in the CNS	AP, NTS	[15,166]
Loss of function ligand	Hyperphagia Obesity Increase fat mass	Slight hyperphagia or no change Slight increase body mass or no change Slight increase fat mass or no change	[3,14,28,165]
Loss of function receptor	Hyperphagia Obesity Increase fat mass	No difference in food intake No difference in weight No difference in fat mass	[3,15,167]
Circulating levels in lean	Proportional to fat mass	Low (<1200pg/ml)	[8,168]
Circulating levels in obese	Proportional to fat mass	Elevated	[8,168,169]
Pharmacological administration in lean	Reduce body weight Reduce feeding	Reduce body weight Reduce feeding	[14,170]
Pharmacological administration in obese	No change in body weight No change in feeding	Reduce body weight Reduce feeding	[15]
Effect of fasting on circulatory levels	Decrease	No effect	[8,171,172]
CTA induction	No	Yes	[8,173,174]

Table 1: Comparison of Leptin and GDF15 effects

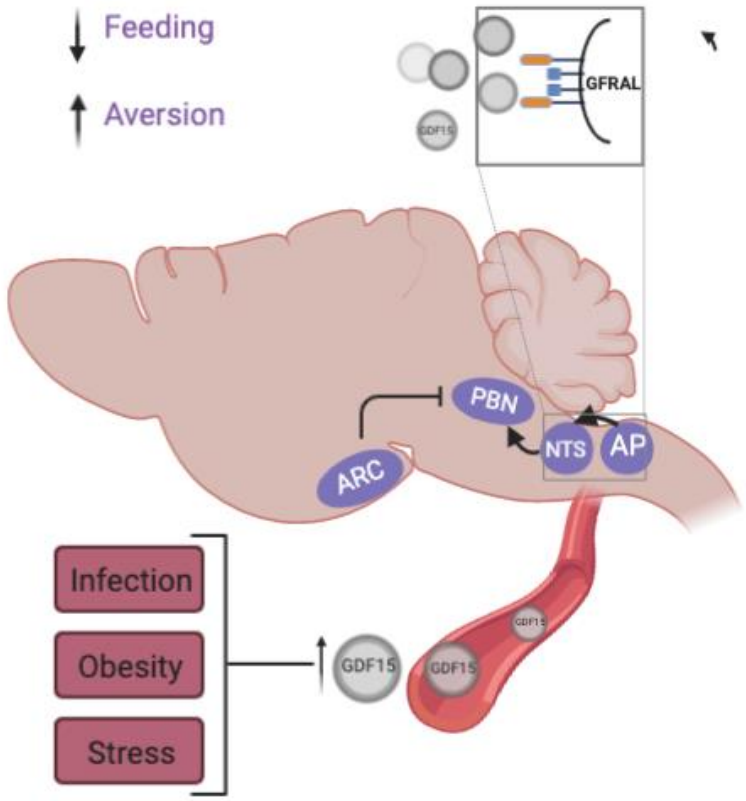

Figure 1: GDF15 signaling in response to pathophysiological stressors

GFRAL is induced into circulation by pathophysiological states of obesity, tissue and organ stress, and sepsis in a myriad of peripheral organs. It signals onto GFRAL located primarily within the area postrema (AP) and secondarily in the nucleus tractus solitarius (NTS). Upon binding GDF15, GFRAL forms a heterodimer with the coreceptor tyrosine kinase RET to induce downstream Akt signaling pathway. The AP has dense projections to the NTS which further signals on the lateral parabrachial nucleus (PBN). The PBN receives GABAergic projections from hypothalamic arcuate nucleus (ARC) AgRP neurons. Figure was created using BioRender.

[1] Chapter 2: LPS Induces Rapid Increase in GDF15 Levels but is Not Required for Anorexia in Mice

2.1 Chapter summary

Growth differentiation factor 15 (GDF15), a TGFβ superfamily cytokine, acts through its receptor, GDNF-family receptor α-like (GFRAL), to suppress food intake and promote nausea. GDF15 is broadly expressed at low levels but increases in states of disease such as cancer, cachexia, and sepsis. Whether GDF15 is necessary for inducing sepsis associated anorexia and body weight loss is currently unclear. We used a model of moderate systemic infection in GDF15KO and GFRALKO mice with lipopolysaccharide (LPS) treatment to define the role of GDF15 signaling in infection-mediated physiologic responses. Since physiologic responses to LPS depend on housing temperature, we tested the effects of subthermoneutral and thermoneutral conditions on eliciting anorexia and inducing GDF15. Although we found a conserved LPS-mediated increase in circulating GDF15 levels in mouse, rat and human, we did not detect differences in LPS induced anorexia between WT and GDF15KO or GFRALKO mice. Further, there were no differences in anorexia or circulating GDF15 levels at either thermoneutral or subthermoneutral housing conditions in LPS treated mice. Our data

[1] This chapter reflects the following manuscript:

Patel AP, Frikke-Schmidt H, Bezy O, Sabatini PV, Rittig N, Jessen N, Myers MG, Seeley RJ. LPS induces rapid increase in GDF15 levels but is not required for anorexia in mice. Submitted to Endocrinology.

demonstrate that GDF15 is not necessary to drive food intake suppression in response to moderate doses of LPS.

2.2 Introduction

Growth differentiation factor-15 (GDF15) is a widely expressed, peripherally derived TGFβ superfamily cytokine. Pharmacological administration of GDF15 potently suppresses food intake via actions on glial cell line-derived neurotrophic factor a-like receptor (GFRAL), which is present primarily on limited sets of neurons that reside in the area postrema (AP) with fewer located in the nucleus solitary tract (NTS) [3,13–15]. Rather than being regulated by nutrient flux, as many peripherally derived anorectic agents, circulating GDF15 levels are associated with a wide array of pathological states including cardiovascular disease, kidney disease, cancer, chemotherapy and infection, sometimes correlating with weight loss and disease severity [48,175,176]. This has led many to hypothesize that GDF15 functions independently of the hypothalamus to act on circuits involved in non-homeostatic regulation of food intake.

Reduction of energy intake is a common response to illness and is initially induced as a protective mechanism but can become chronic and dysregulated. A prime example is cancer anorexia. A wide variety of tumors are associated with reduced appetite and precipitous weight loss that contributes to mortality [66,78,177]. The discovery that blocking GDF15 using a monoclonal antibody prevents disease in seven models of rodent cachexia and increases survival [70] has led to ongoing clinical trials for potential treatments that target reduced GDF15/GFRAL signaling. Similarly, a reduction of energy intake is common in states of visceral infection and sepsis. In a study done of 219 critically ill ICU patients, GDF15 predicted organ failure, severe illness, and ultimately mortality [57]. As one of the leading causes of death in hospitalized

patients with poorly understood mechanisms, new treatment options for sepsis are still needed. Whether GDF15 contributes to the response, either in a protective or pathogenic manner, is currently unclear. The focus of this study is to define the role of GDF15 in mediating the reductions in energy intake that occur during bacterial infection.

LPS, a component of the outer membrane of gram-negative bacteria, is a common and potent stimulator of the bacterial infectious response including loss of appetite and changes in body temperature. In addition to its appetite suppressing property, exogenously administered GDF15 can produce a conditioned taste aversion (CTA), a well-known behavior that accompanies illness including LPS infection in rodents [8,178], in which animals develop an aversion to a novel substance associated with visceral illness. Specific neural circuits involving the parabrachial nucleus (PBN) and central amygdala (CeA) are responsible for transducing visceral illness into behavioral responses [46,179]. Interestingly, the PBN is a hindbrain region well-known to contribute to the development of a CTA and more recently suggested to be involved in regulating appetite in stress. Specifically, calcitonin gene-related peptide (CGRP) neurons within the PBN are critical in acquiring and maintaining a CTA [44,179]. Activation of this neuronal circuitry by both GDF15 administration and LPS has been demonstrated in rodents [8,35,46,178,180]. Our group has recently shown GFRAL -expressing neurons in the AP project to CGRP neurons in the PBN and that silencing these neurons ablates both the anorexic and visceral illness responses to exogenous GDF15 [73]. Thus, CGRP neurons that appear to be critical to the response to both LPS and tumors are downstream of GDF15 responsive neurons in the area postrema.

Given the similarities between the physiologic response to pharmacological administration of GDF15 and LPS and that they appear to depend on CGRP neurons in the PBN, we

hypothesized that GDF15 may mediate some of the critical responses to LPS. To that end, we measured circulating levels of GDF15 in response to LPS in mice, rats and humans. Additionally, we used both GDF15 and GFRAL knockout mice to test the necessity of GDF15 signaling to various responses to LPS.

2.3 Results

LPS is a potent driver of GDF15 secretion, anorexia, and hyperthermia

To understand the dynamics of GDF15 in human subjects in infection, we measured GDF15 levels in humans using a randomized crossover-trial (n=8) in which participants were administered an intravenous bolus infusion of either saline or LPS (1 ng/kg). We detected a ~1.5-fold elevation in plasma GDF15 concentrations 3 hours after LPS exposure when compared with baseline (0 hours) concentrations (Fig. 2 A). We further tested the effect of two doses of LPS in inducing plasma GDF15 in rodents (Fig. 2 B). Hourly blood samples were drawn from rats implanted with carotid artery catheters and dosed with either saline, 500 μg/kg LPS, or 1500 μg/kg LPS. Circulating GDF15 levels rose rapidly, peaking at 2 hours after LPS administration. As the potent GDF15 stimulating effects of LPS were conserved between rats and humans, we lastly tested the response in mice.

In rodent models of LPS infection, it is important to take housing temperature into account. The impact of the housing environment in the rodent response to LPS infection has been previously described [181–184]. When housed at thermoneutral conditions ~(28-30°C), a fever response is common and detectable, often at earlier stages [181,185]. However, when housed at subthermoneutral conditions and challenged with moderate or high doses of LPS, rodents drop their internal temperatures during the early phase of the febrile response [183,186–188]. At low

and high doses, rats increase warm environment seeking behaviors during the later phase of the fever response [186]. Additionally, septic patients displaying hypothermia have increased mortality [189,190]. As our goal was to adequately challenge the mice, without eliminating their food intake response, and ensuring recovery and survival, we performed studies at thermoneutral housing conditions, where hyperthermia would be predicted and detectable.

To choose an appropriate dose for mouse studies, we conducted a dose response curve in WT mice in response to i.p. administration of 100 μg/kg, 250 μg/kg, 500 μg/kg and 600 μg/kg of LPS or saline. LPS injected mice exhibited a dose dependent increase in rectal temperature (Fig. 2D, G) along with a decrease in body weight (Fig. 2C, F) after 24 hours. Food intake was significantly reduced in 250 μg/kg 500 μg/kg and 600 μg/kg doses within 4 hours (Fig. 2E). Administration of the highest dose of 600 μg/kg LPS caused a ~50% reduction of food intake within 4 hours (Fig. 2E). A separate and larger cohort of mice was used to confirm these findings and measure circulatory GDF15 levels (Fig. 2F-H). Within 24 hours, plasma GDF15 levels increased by ~14 fold in mice injected with 600 μg/kg compared to saline injected mice, reminiscent of LPS stimulated plasma levels in rats within 2 hours (Fig. 2H). As the highest dose of 600 μg/kg displayed the greatest measurable hyperthermia, moderate anorexia, along with strongly elevated levels of GDF15 protein in circulation, we continued to use this dose for all further studies.

We then aimed to determine whether housing temperature would alter the behavioral and physical response to LPS. To test this, we administered 600 μg/kg LPS to WT mice housed either at subthermoneutral (STN) or thermoneutral (TN) temperatures, 22°C or 29°C respectively (Fig. 3). LPS reduced body weight (Fig. 3A) and food intake (Fig. 3B-C) within the first 2 hours under both STN and TN housing temperatures. This effect was still present at 48 hours after

injection at both housing temperatures (Fig. 3D-F). Differences in body weight and food intake between LPS treated mice at STN and TN conditions were not significantly different at any timepoint. Within both the STN LPS and TN LPS groups, there are two animals that show unexpectedly elevated food intake for having been given LPS. This opens up the possibility that the few animals that failed to respond to the LPS potentially were not administered the appropriate dose of LPS. The data and analysis that is represented in figure 3 includes the entire data set, with no exclusions. However, when the data were analyzed excluding these outliers, there is still a significant effect of LPS and no effect of room temperature. Importantly, GDF15 levels were significantly elevated at both temperatures with LPS infection (Fig. 3G). At the dose tested, we saw a similar anorexia, body weight loss, and GDF15 response between the TN and STN conditions. As there was no substantial difference observed between the two housing temperatures, we used TN temperatures for all further experiments.

GDF15/GFRAL is not necessary for LPS induced anorexia, weight loss and inflammatory response

To investigate the necessity of GDF15 in mediating pathological and stress associated anorexia, we used mice lacking GFRAL or GDF15 protein. WT and GDF15 KO mice lost 7.4% and 7.8% body weight 24 hours after 600 μg/kg LPS, respectively (Fig. 4A). Food intake was significantly reduced in both WT and GDF15 KO mice with LPS beginning at 2 hours and lasting until 48 hours after infection (Fig. 4B-E). There was no significant difference between the anorexia induced in GDF15KO vs WT mice in response to LPS.

LPS, an activator of toll like receptor 4, is a potent stimulator of prostaglandins and proinflammatory cytokines, including TNF-α and IL-6[191]. The patients studied for our experiment measuring serum GDF15 protein levels in humans (Fig. 2A) additionally exhibited increases in TNF-α by 25 fold and IL-6 by >90-fold 3 hours after receiving LPS as opposed to

placebo, as previously reported [191]. Many of these inflammatory mediators can exacerbate organ damage in severe sepsis [192,193], mediate the thermoregulatory response, and influence food intake [98,194]. Additionally, GDF15 has been hypothesized as a modulator of peripheral inflammation in models of visceral stress and organ damage [5,52,96,195–200]. We therefore asked whether GDF15 is involved in maintaining the peripheral inflammatory response to LPS by comparing WT and GDF15KO mice. Using an ELISA assay, we measured circulating inflammatory cytokines known to be regulated by LPS (Fig. 4F-G). Both LPS injected groups had expectedly elevated levels of circulating TNF-α and IL-6, confirming an acute proinflammatory response to LPS. No differences in cytokines levels were observed between GDF15 KO and WT mice 3 hours after LPS treatment. GFRAL KO mice exhibited a 43% and 44% reduction in food intake 4 and 24 hours after LPS administration, respectively when compared to saline controls. Similar to GDF15KO mice, no differences in either weight loss or food intake were observed between WT and GFRAL KO mice in response to LPS (Fig. 4H-J). Taken together, GDF15 and its receptor GFRAL were not necessary for the behavioral and physiological responses to LPS.

GDF15 is not necessary for progression of disease with sublethal doses of LPS

To understand if long-term deficiency in GDF15 could affect the progression of severe infection, we administered sublethal doses of LPS (i.p. 5mg/kg) to mice lacking GDF15 at subthermal housing temperatures of 22°C. Appearance (Fig. 5A), natural behavior (Fig. 5B), provoked behavior (Fig. 5C), and body condition (Fig. 5D) scores were assessed during the study using a health scoring scale (Fig. 6). Within 6 hours after LPS administration, mice exhibited a 35-40% average reduction of appearance score due to a depreciation of their physical welfare including posture, fur, and facial expression. Indeed, mice displayed decreases in both natural activity within the home cage (Fig. 5B), and when provoked (Fig. 5C), an abnormal movement

response, often including movement delays and lethargy. Interestingly, there was no significant difference between the health of the GDF15 KO mice, when compared to WT mice in neither appearance nor movement behavior at any time point (Fig. 5A-C). Both WT and KO mice that survived the infection began recovery by 72 hours and were indistinguishable from their saline counterparts by 96 hours post injection, suggesting that GDF15 is not a necessary component of behavioral and physical degradation or recovery from infection, as the KO mice looked and behaved similarly as the WT control groups in all of our physiological measurements of illness. Finally, WT and GDF15 KO mice followed a similar survival trajectory with most deaths occurring at 72- and 96-hours post LPS administration. 58% and 75% of WT and KO mice survived by the 72-hour time point, respectively, with a total of 50% and 77% by 96 hours (Fig 5D).

An effect on body weight was observed at 48hr with LPS leading to 12-14% reduction when compared to saline controls (WT $p<.036$, KO $p<.014$) (Fig 6A). There was no significant difference of LPS induced anorexia or body weight loss between WT and GDF15 KO mice at any time point. Similarly, LPS challenged mice significantly reduced food intake within 24 hours for up to 72 hours when compared to saline injected mice with no significant differences between WT and GDF15 KO mice (Fig. 6B). These data further demonstrate that chronic inhibition of GDF15 does not affect the impact of severe sepsis on body weight, food intake, health condition and survival induced by sublethal dose of LPS.

2.4 Discussion

Our study demonstrates that peripheral LPS infection rapidly induces circulating GDF15 in humans, rats, and mice. Within 2 hours of infection, rat serum GDF15 levels peak at a 30-fold

increase from baseline levels in both a high and moderate LPS dose in rats. By 3 hours, GDF15 levels are elevated by 7-fold from baseline, remaining steady for the next several hours. Our data show that circulating GDF15 in mice are comparable to those of rats at 2 hours. Administering LPS to humans significantly elevated GDF15 levels as well, though to a lesser degree compared with our rodent studies. One reason for this difference may be the 3-hour timepoint at which we collected human blood, potentially missing the peak values. Needless to say, some of these intra-species comparisons are also limited by the smaller dose that was used in humans as compared to rats and mice.

The physiological and behavioral response to LPS varies depending on the concentration of LPS, timepoint after administrations and housing environment conditions. Specifically, thermoregulatory responses can fluctuate greatly and often predict the severity of disease in response to infection[187,189,190]. Both hyperthermia and hypothermia have been observed with LPS, depending on the ambient housing temperature and dose administered. Elevated body temperature, i.e. fever, is the predominant thermoregulatory response in thermoneutral environments to lower doses of LPS in rodents. Subthermoneutral environments and greater LPS doses often lead to hypothermia, which is predictive of increased mortality with severe bacterial infection or septic shock [187,201]. In order to model moderate illness, we used a dose response curve of LPS and found a dose-dependent increase in temperature and decrease in food intake. Furthermore, our studies show that in response to the same dose of LPS (600 μg/kg), GDF15 is similarly and significantly elevated in the circulation of mice under both thermoneutrality and subthermoneutral environments. However, GDF15 does not contribute to the food intake effects in either environment. While the housing temperature makes an important difference in the

physiological responses to LPS, it does not appear to be critical to the anorexic response. This finding implies that the key anorexic circuits engaged by LPS are not temperature dependent.

Given the potent ability of LPS to increase circulating GDF15, regardless of housing temperature, it made sense to further test whether GDF15 and its receptor, GFRAL, are required for the anorexic response. We did careful dose-effect curves to evaluate the appropriate dose of LPS to use that would elicit moderate illness including reducing food intake, without eliminating all food intake, and elevate body temperature. A dose of 600 μg/kg LPS moderately and acutely impairs the mice within hours of infection, reducing food intake of both WT and GDF15KO mice, while ensuring survival of all mice.

This dose of 600 μg/kg was subsequently tested in mice with targeted genetic disruption of either GDF15 or GFRAL. Surprisingly, the anorexic response to LPS was similar in both knockout models as compared to their respective littermate controls. These data make a strong case that the GDF15 system is not necessary to the anorexic responses to LPS. Studies of whether GDF15 is a critical component of disease recovery and risk has had conflicting results, particularly in models of LPS infection [5,197]. A previous study evaluating the contribution of GDF15 to the LPS illness response utilized lethal and sublethal doses of LPS in rodents [5], both of which elicit a drastic infection response to severe sepsis that makes behavioral assays difficult to assess. The food intake test represents one such assay. When the infectious response renders the rodent sick enough to stop eating, it becomes difficult to resolve the contribution of GDF15 with granularity. Additionally, in order to remove GDF15 signaling, Luan *et al* blocked GDF15 using a monoclonal antibody designed for humans and its effects in mouse are unclear. In contrast, we use a moderate dose of LPS which did not result in lethality. Using GDF15 and

GFRAL KO mice, we found that GDF15 and GFRAL are not necessary components driving the energy intake and body weight responses in LPS infection.

While a large amount of data pointed towards GDF15 as a mediator of LPS responses, including anorexia, our results do not support this role. Both infections and LPS administration are complex stimuli that activate a host of systemic inflammatory responses, including the release of inflammatory cytokines and cellular immune activation. Many of these factors are also capable of inducing anorexia, at least under some inflammatory conditions [98,202]. Our data show proinflammatory mediators, TNF-α and IL-6, as robustly elevated in both WT and GDF15KO mice when given LPS. In addition to TNF-α and IL-6, IL-1β has been shown to further inflammatory mediator production and induce anorexic responses [98,203]. Furthermore, distinct peripheral (hepatic and pulmonary macrophages) and central cell types (perivascular, glial, endothelial cells) can produce prostaglandins, including PGE2 to drive anorexia by signaling onto neurons [194,202]. Prostaglandin production, including PGE2 which is synthesized by COX2, is involved in mediating other sickness responses. It is a critical factor to the thermoregulatory fever response [181,184,204] and has been implicated in illness-associated aversion learning [205]. Studies of which distinct cell types produce the various mediators and where they signal is still evolving. It is likely that this complex milieu of factors drives the anorexic response to LPS and any single factor is not required. Key questions remain around the role that the pronounced increase in circulating GDF15 plays in directing the physiological responses to systemic infections.

2.5 Materials and methods

Animals and housing

All rodent experiments were approved by the University of Michigan Institutional Animal Care & Use Committee at (Animal Use Protocol # PRO00007908). Animals were single housed (at minimum for 1 week prior to experimentation) in temperature controlled rooms containing a 12hr:12hr light:dark cycle and given *ad libitum* access to chow diet (PicoLab 5L0D). Subthermoneutral and thermoneutral housing conditions were maintained as 22°C +/- 2°C and 29°C +/-2°C, respectively.

Rats**:** Male Long Evans rats (Envigo; Indianapolis, IN) weighing between 415-490 g were used for vascular catheterization surgeries and housed at 22°C.

Mice**:** 21 week and 9 week old C57blk6/c mice (no: 000664, Jackson Laboratories; Bar Harbor, ME) were used to generate both the LPS dosing curve and housing temperature comparison studies, respectively. $GDF15^{-/-}$ and $GFRAL^{-/-}$ mice were generated as previously described [33]. 28 week-old male $GDF15^{-/-}$ mice and 15 week-old male (n=9) and female (n=11) $GFRAL^{-/-}$ mice were used for food intake experiments. For $GFRAL^{-/-}$ experiments, we did not include a WT LPS group due to a shortage of WT littermate mice.

LPS stock

For all rodent studies, lyophilized lipopolysaccharides from Escherichia coli O111:B4 (Sigma Aldrich; St Louis, MO; L4391-1MG; mouse studies lot 088M4067V) was diluted in saline and stored as 100ul of 1mg/ml aliquots at -80°C. On the day of the experiment, saline was used to further dilute the aliquots to appropriate concentrations for use. For human subject experiments,

E. coli endotoxin (The United States Pharmacopeial Convention, Inc.;10,000 USP Endotoxin, lot H0K354; Rockville, MD) was used.

Human blood collection

A randomized crossover design was used over several experimental days in 8 human subjects as described previously (NCT01705782) [191]. The study and design was approved by The Central Denmark Region Ethics Committee in accordance with the Declaration of Helsinki (1-10-71-410-12). Male subjects between the ages of 25-40 with a BMI of 20-30 kg/m^2 were included. Blood was drawn from inserted catheters at baseline (0 hours) and 3 hours following an intravenous bolus infusion of either saline or LPS (1ng/kg). Plasma was separated and used to measure GDF15 levels.

Rodent blood collection

In rats, a catheter was surgically implanted into the left common carotid artery to allow *in vivo* blood sampling from an externalized sampling port as previously described [206]. Saline, 500 μg/kg LPS or 1500 μg/kg LPS was i.p. injected into rats 1 hour prior to hourly blood sampling for 6 hours. In mice, tail vein blood from the tips of clipped tails was collected, kept on ice, and centrifuged at 2000g for 15 min in EDTA coated microvette blood collection tube (Sarstedt Inc.; CB300; Nümbrecht, Germany) to separate plasma.

ELISA assays

In all studies measuring GDF15 levels, a sandwich ELISA (R&D Systems, Inc.; MGD150; Minneapolis, MN) was used according to manufacturer's directions. In rodent and human

studies, samples were diluted 1:1 and 1:10 respectively . To detect mouse plasma cytokines, a custom V-PLEX plus cytokine panel kit (Mesoscale Discovery, K152AOH-1, Rockville, MD) was used to detect IL-1ß and TNF-α cytokines according to manufacturer's directions. Plasma samples from mice were diluted 1:200 and run in duplicates.

Food intake test

Food was removed from cages and mice were fasted for 17-18 hours with full access to water. Animals were randomized for treatment and administered LPS or saline i.p. 1 hour prior to dark onset and return of pre-weighed chow diet. Remaining food in cage was measured at 2, 4, 24, and 48 hours after food return to determine food intake.

Body temperature

Mice were habituated to handling and rectal probe insertions prior to experimentation. Body temperatures were measured by inserting a microprobe thermometer probe (Physitemp Instruments; BAT-12; Clifton, NJ), lightly coated in petroleum jelly, 2 cm into the rectum of scuffed mice prior to any other measurements or injections on days of experimentation.

Statistical analysis

All statistical analysis was performed in either GraphPad Prism v8.4.2 or v9.0.0 and is represented as mean +/- SEM. Student's t-test, one-way, two-way or three-way ANOVA with Tukey's or Dunnett's post-hoc tests were utilized to determine significance. Significance was defined as $p<0.05$.

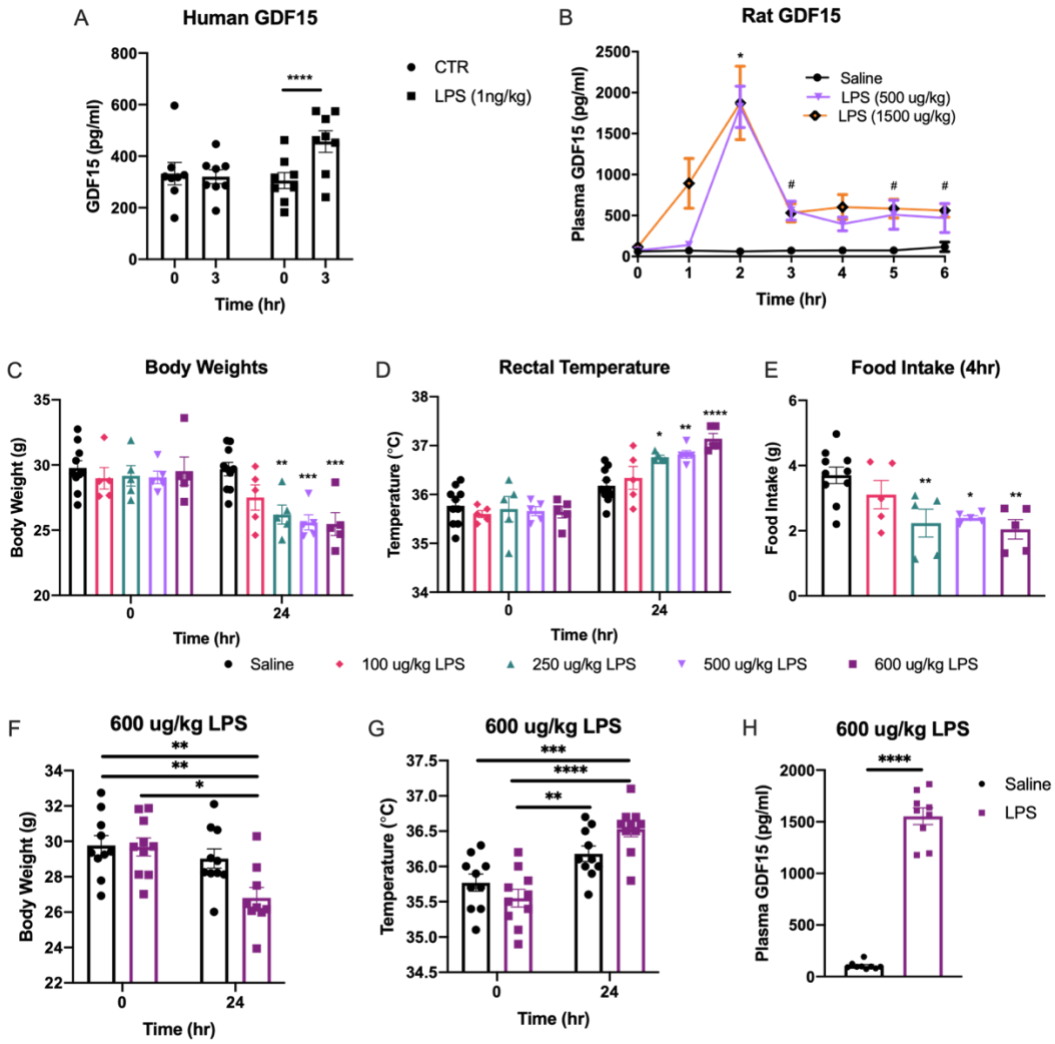

Figure 2: GDF15 in rats, mice, humans, and LPS dosing curve

Plasma GDF15 levels in humans 3 hours after receiving a bolus of LPS or saline (A)(n=8). 2-way ANOVA with Tukey's multiple comparison test; ****p<0.0001 compared to 0hr (baseline) LPS treated subjects. Hourly plasma GDF15 levels from carotid cannulated rats administered i.p. saline, 500 µg/kg LPS, or 1500 µg/kg LPS from 0hr (baseline) to 6hrs post-injection (B) (n=2-4 per group). 2-way ANOVA with Tukey's multiple comparison test, *p<0.05 500 µg/kg compared to saline; #1500 µg/kg compared to saline. LPS dose effect measurements of WT mice administered 100 µg/kg, 250 µg/kg, 500 µg/kg, or 600 µg/kg LPS or saline at 0hr (baseline) and after 24 hours post injection (C-E). Body weights (C), rectal temperatures (D) and 4-hour post-LPS injection food intake test (E)(n=5-10 per group). 2-way ANOVA with Tukey's multiple comparison test (C,D) and Dunnett's multiple comparison test (E); *p<0.05; **p<0.01; ***p<0.001, ****p<0.0001 compared to 24 hr (C-D) or 4hr (E) saline. Body weights (F), rectal temperatures and (G) plasma GDF15 levels (H) at 0 and 24 hours (n=9-10 per group). 2-way ANOVA with Tukey's multiple comparison test (F-G) or two-tailed students t-test (H); *p<0.05; **p<0.01; ****p<0.0001. All data are represented as mean ± SEM.

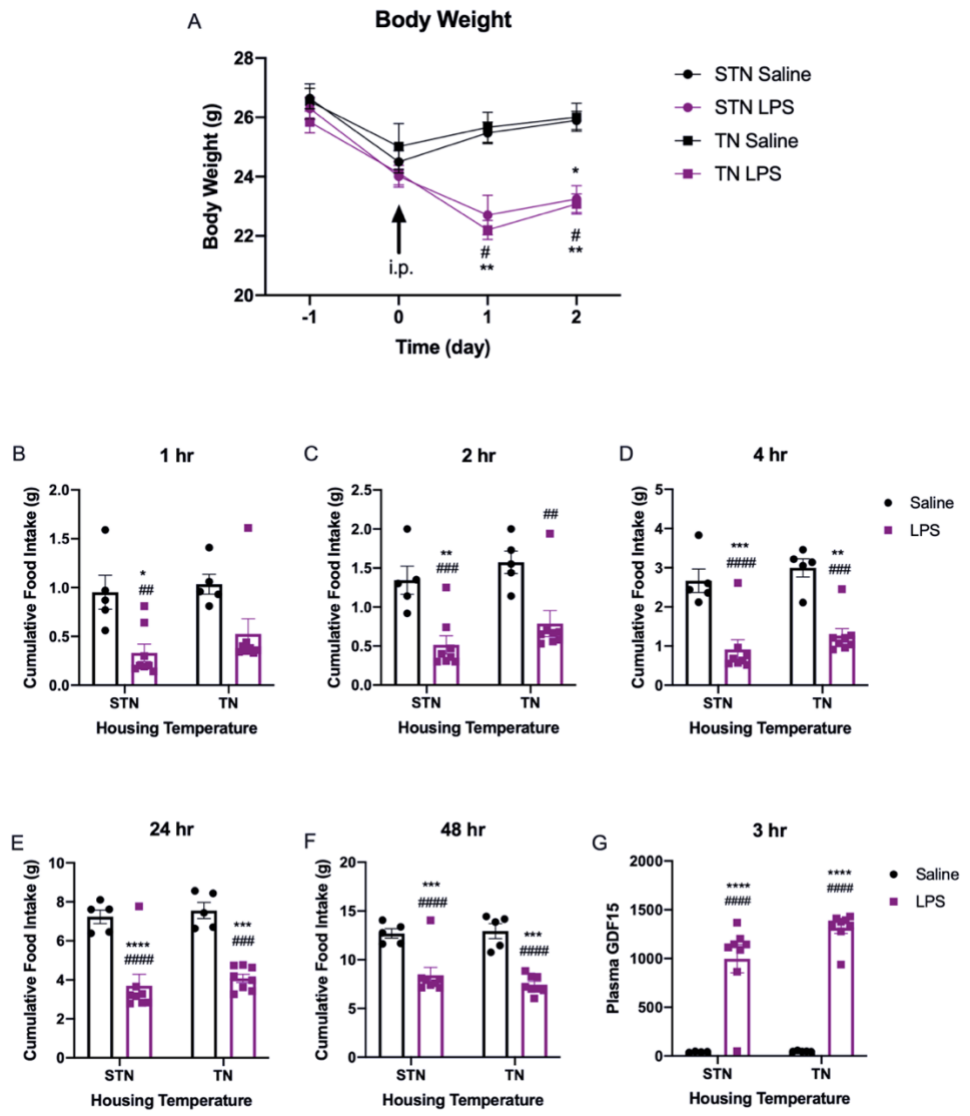

Figure 3: Effects of housing temperature on body weight, food intake, and circulating GDF15

WT mice housed at ambient temperatures of 22°C (subthermoneutral; STN) or 29°C (thermoneutral; TN) i.p. injected with saline or 600 µg/kg LPS. Body weight measurements one day prior, on the day of, and up to two days after treatment (A) (n=5-8 per group). Cumulative food intake test of overnight fasted mice at 1hr (B), 2hr (C) , 4hr (D), 24hr (E), and 48hr (F) post treatment (n=5-8 per group).Concentration of plasma GDF15 3hrs after treatment (G) (n=5-8 per group). All data are represented as mean ± SEM. */#p<0.05; **/##p<0.01; ***/###p<0.001; ****/####p<0.0001 with */ **/ ***/ **** compared to STN saline and #/ ##/ ###/ #### compared to TN saline by 3-way ANOVA (A) and 2-way ANOVA (B-G) with Tukey's multiple comparison tests.

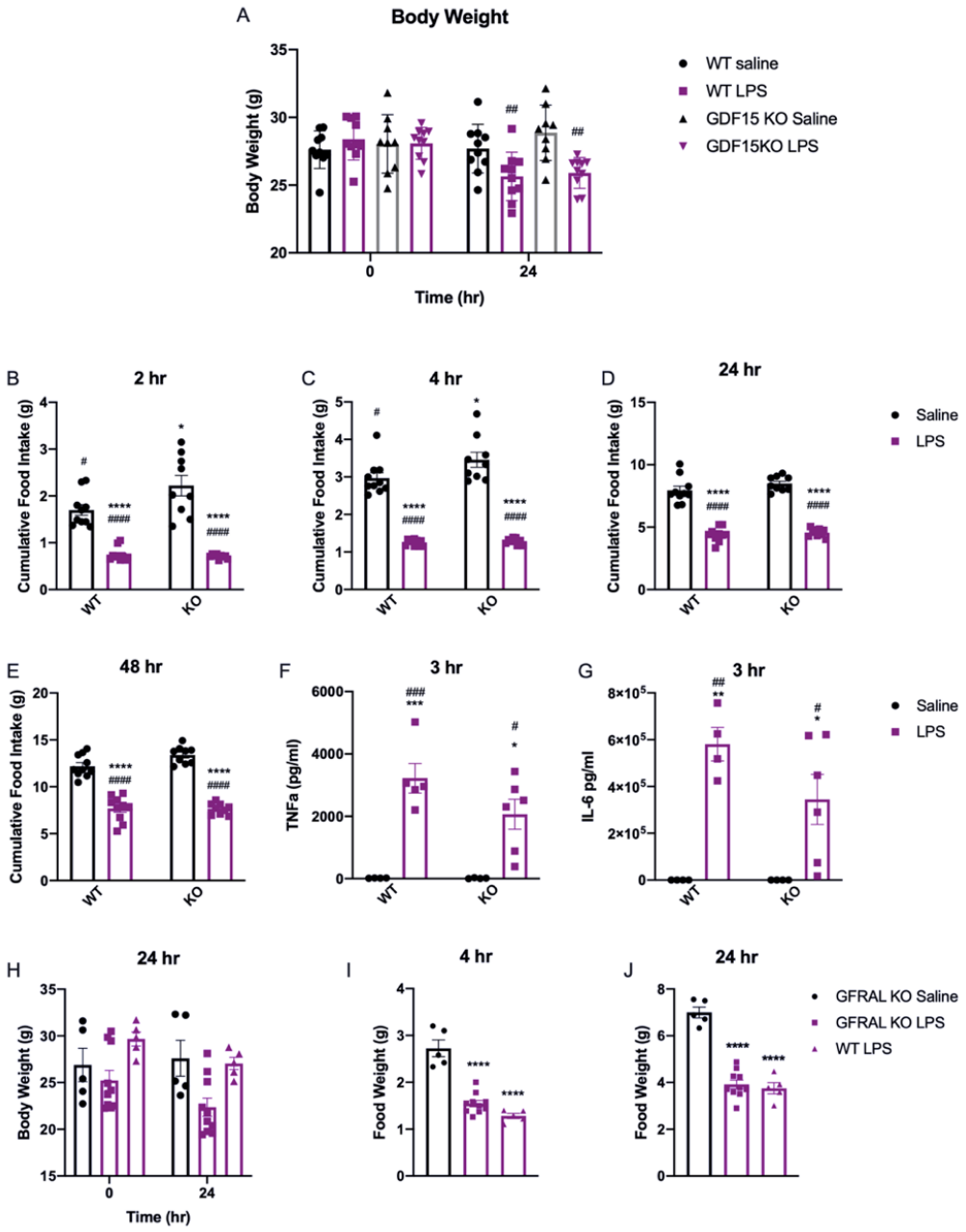

Figure 4: GDF15 and GFRAL KO mice response to LPS

Body weights of WT and GDF15KO mice before (0hr, baseline) and 24 hr after LPS (600 µg/kg) or saline i.p. injection (A) (n=10 per group). Cumulative food intake measurements from 2hr (B), 4hr (C), 24 hr (D), and 48 hr (E) after LPS (600 µg/kg) or saline i.p. injection of overnight fasted WT and GDF15KO mice (n=10 per group). Plasma levels of TNFa (F) and IL-6 (G) 3 hours after treatment (saline or 600 µg/kg LPS) (n=4-6 per group). */ **/ ***/ **** compared to WT saline and #/ ##/ ###/ #### compared to KO saline by 2-way ANOVA with Tukey's multiple comparison tests. Body weights before (0hr, baseline) and after 24 hr from saline or LPS (600 µg/kg) i.p. injection of WT and GFRAL KO mice (H) (n=5-10 per group). Cumulative food intake measurements at 4 hr (I) and 24hr (J) of WT and GFRAL KO mice i.p. injected with LPS

(600 μg/kg) or saline (n=5-10 per group). **** compared to GFRAL KO saline by 2-way ANOVA (H) and ANOVA (I,J) with Tukey's multiple comparison tests. All data are represented as mean ± SEM. */# $p<0.05$; **/## $p<0.01$; ***/### $p<0.001$; ****/#### $p<0.0001$.

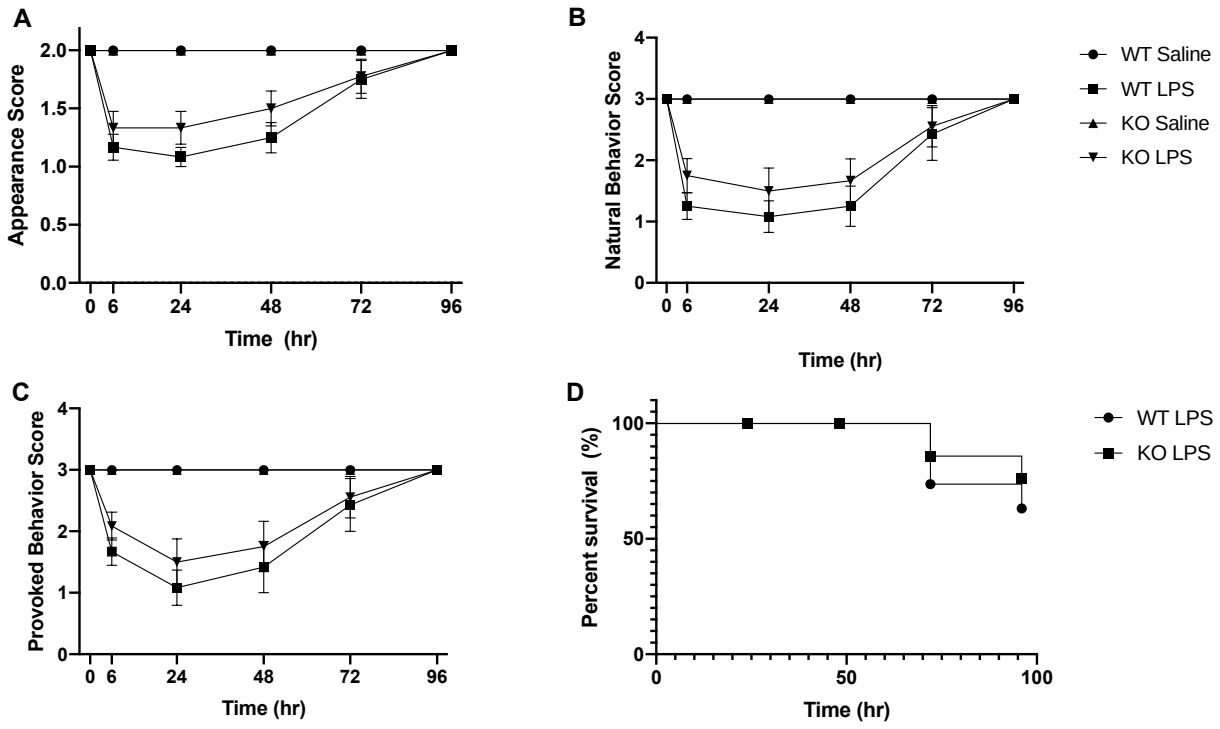

Figure 5: GDF15 deficiency does not modulate body condition or survival with sublethal dose of LPS.

LPS induced body condition score of WT and GDF15 KO mice following a i.p. 5 mg/kg LPS dose when housed at ambient temperatures of 22°C. Appearance (A), natural behavior (B), and provoked behavior (C) scores for 4 days following LPS injection. Kaplan-Meier survival curve indicating % survival in WT and GDF15 KO mice following LPS injection (Fig D); (n=6-12 per group); two-way ANOVA. Data were represented as mean ± SEM.

Observation Criteria	Appearance	Natural behavior (in home cage undisturbed)	Provoked behavior (out of cage, nudge at back)	Body condition score
Possible Score range (1-13):	0 - 2	0 - 3	0 - 3	0 - 5
Description	2 = Normal	3 = Normal, active	3 = Quickly moves away	5 = Obese
	1 = Slight hunching, unkempt, dull fur, slight paleness, ears back, squinty eyes	2 = Slight decrease in activity	2 = Slow to move away or exaggerated response, gait appears slightly off	4 = Overweight
	0 = Hunched, piloerection, vocalizing, very pale	1 = Pronounced decrease in activity, isolated	1 = Very slow to move away, abnormal gait, slight lethargy	3 = Normal
		0 = immobile, self-mutilation, extreme hyperactivity	0 = Does not move away, reacts with excessively exaggerated response, complete lethargy	2 = Thin (Vertebral column prominent)
				1 = Emaciated (can see hip bones, individual vertebrae)

Figure 6: Health score chart for monitoring animal's health condition.

Animals were observed and scored on appearance, natural behavior, provoked behavior, and body condition score. Scores from these four criteria were summed into a final cumulative score.

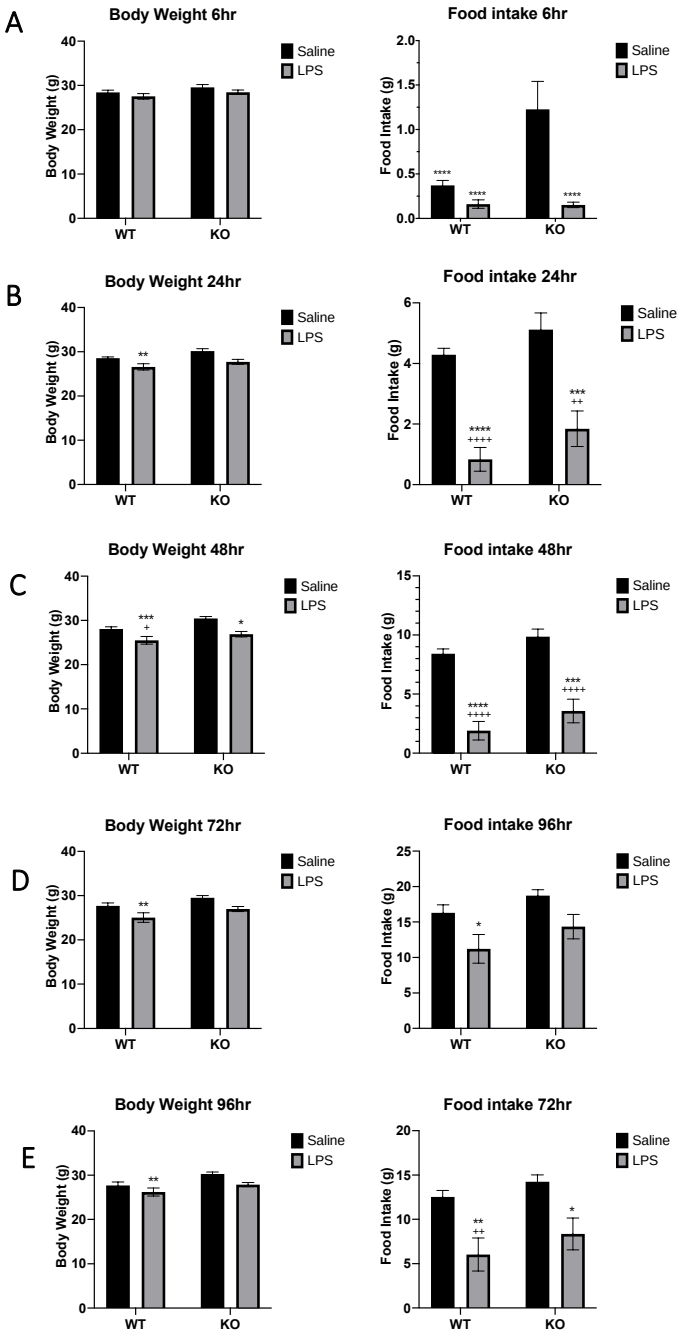

Figure 7: GDF15 deficiency does not modulate weight loss or anorexia induced with a sublethal dose of LPS.

LPS induced body condition score of WT and GDF15 KO mice following i.p. 5 mg/kg LPS dose when housed at ambient temperatures of 22°C. Body weight and cumulative food intake at 6 (A), 24 (B), 48 (C), 72 (D) and 96 (E) hours following LPS in WT and GDF15 KO mice. #/ ##/ ###/ #### compared to WT and */ **/ ***/ **** compared to KO saline by two-way ANOVA with Tukey's post hoc. */# $p<0.05$; **/## $p<0.01$; ***/### $p<0.001$; ****/#### $p<0.0001$.Data were represented as mean ± SEM. N=6-12 per group.

[2]Chapter 3: GFRAL Neurons Do Not Contribute to the Aversive or Anorectic Response to Deoxynivalenol

3.1 Chapter summary

Deoxynivalenol (DON), a type B trichothecene mycotoxin contaminating grains, promotes nausea, emesis and anorexia. In DON infection, circulating levels of intestinally derived satiety hormones, including GLP-1 are elevated. To directly test the role for GLP-1 signaling in mediating the effects of DON, we examined the response of GLP-1 or GLP-1R-deficient mice to dose of DON. We found comparable anorexic and conditioned taste aversion learning responses in GLP-1/GLP-1R deficient mice compared to control littermates which suggests that DON induces the effects via other mechanisms. We then used translating ribosome affinity purification with RNA sequencing (TRAP-seq) analysis of area postrema neurons that express the receptor for the circulating cytokine growth differentiation factor (GDF-15), growth differentiation factor α-like (GFRAL). Interestingly, this analysis showed that a receptor for DON, calcium sensing receptor (CaSR), is heavily enriched in GFRAL neurons. Given that GDF15 potently reduces food intake and can cause visceral illness via activating GFRAL neurons, we hypothesized that DON may also act via activating CaSR on GFRAL neurons. When administered DON, GFRAL neuron-ablated mice exhibited similar aversion learning

[2] This chapter reflects the following manuscript:

Patel AP, Frikke-Schmidt H, Bezy O, Sabatini PV, Rupp A, Myers MG, Seeley RJ. GFRAL neurons do not contribute to the aversive or anorectic response to deoxynivalenol. In preparation.

compared to the WT littermates and intact anorexia. Thus, GLP-1 signaling and GFRAL neurons are not required for DON-induced visceral illness or anorexia.

3.2 Introduction

Growth differentiation factor 15 (GDF15) is a peripherally derived cytokine that signals onto its receptor within the brain, GDNF family receptor α-like (GFRAL). GFRAL has a very narrow distribution in the CNS that is limited to neurons within the area postrema (AP) and to a lesser extent the nucleus of the solitary tract (NTS) [3,13–15]. GDF15 and analogues of GDF15 potently suppress food intake and cause weight loss via action on GFRAL neurons. Despite these profound effects on food intake and weight, there is little evidence for GDF15 or GFRAL to regulate body weight under normal circumstances. Rather, it would appear more likely that this system contributes to anorexic responses to a variety of pathophysiological states such as cancer, cachexia, sepsis, and cardiovascular disease in which circulating levels of GDF15 have been shown to be elevated [62,175,176].

Given this small population of GFRAL neurons in the AP/NTS, we hypothesized that these neurons may input other signals that are related to pathophysiological states. To identify other receptors on these neurons, we used Translating Ribosome Affinity Purification (TRAP-seq) with RNA-seq (TRAP-seq) [207] to identify mRNA that are enriched in GFRAL neurons. We found that one of the highest enriched mRNAs on GFRAL neurons was the *casr*. Calcium sensing receptor (CaSR), is a g-protein coupled-receptor that responds to extracellular calcium. In addition to calcium, CaSR is activated by deoxynivalenol (DON), a type-B trichothecene mycotoxin produced primarily from *Fusarium* fungi. DON is a contaminate of grains and cereals including corn, wheat, oats, and barley and is frequently ingested by animals and humans. The

visceral illness effects of DON earned it the colloquial name of “vomitoxin” when it was discovered in the 1970s [208]. As summarized in a 1973 study, and later confirmed by dozens of additional studies, oral intake of DON contaminated grains by swine decreased body weight gain, induced food refusal and emesis [209–211]. Short-term exposure can cause gastroenteritis symptoms of acute nausea, vomiting, diarrhea, and pain [212] and long term exposure can induce a reduction of body weight gain [213–216]. These adverse symptoms have since additionally been described in humans, rodents, and mink [212,217].

The emetic response is a protective mechanism against potentially hazardous ingested compounds. In swine, the most sensitive species to DON [217], and mink animals exhibit emesis as quickly as 30 minutes after i.p. and 15 min after i.p. or oral DON administration, respectively [210,218]. Because rodents lack the vomiting reflex, assessing nausea typically uses a conditioned taste aversion (CTA) assay. A CTA is when a novel tastant is paired with the administration of a toxic compound that subsequently elicits malaise and nausea leading the animal to avoid that tastant when tested later. Consistent with the documented nausea associated with DON in other species, DON induces a potent CTA in rodents [219,220].

Like many emetic agents, administration of DON also activates neurons in the AP. This could be the result direct neuronal activation in the AP since DON appears in the brain within 5 minutes of administration. Given that CaSR is highly expressed in GFRAL neurons, it is possible that some of these AP neurons also express GFRAL. Activation of GFRAL neurons (either via GDF15 administration or via activation of DREADD receptor) results in a profound CTA [8,23]. Consequently, we hypothesized that the potent and rapid effects of DON are the result of direct activation of CaSR/GFRAL neurons in the AP. To test this hypothesis, we used a variety of novel mouse models to test the role of GDF15 and GFRAL neurons to mediate effects of DON.

In addition to CaSR and GFRAL, receptors for the glucagon like peptide-1 (GLP-1) are also found in the AP. GLP-1 agonists also cause potent reductions in food intake and induce an aversion response that are the result of GLP-1R activation [221]. DON increases circulating GLP-1 levels presumably by increasing secretion of GLP-1 from the intestine [105,107,108]. Thus it is possible that rather than acting directly upon AP neurons, DON activates circuits in the AP via increasing levels of GLP-1 that in turn activates emetic circuits in the AP. To test this hypothesis, we used mice that lacked the ability to produce GLP-1 or to respond to GLP-1 via the GLP-1 receptor.

3.3 Results

As GLP-1, an anorectic intestinal hormone, has been shown to increase in circulation with DON infection, we hypothesized that GLP-1 signaling contributes to the food refusal and aversive effects. To test the necessity of GLP-1, we used mice lacking either GLP-1R or the preproglucagon gene (Gcg). We chose to use a dose (2.5mg/kg) of DON that has previously been shown to increase GLP-1 into circulation by 2-fold within 30 min in mice [107]. Male and female GLP-1R^{KO} and GLP-1R^{WT} mice do not show any differences in body weight due to genotype, however the female mice weigh significantly less than male mice (Fig. 8A). To assess the necessity of GLP-1R in inducing the nausea effects of DON, we performed a two-bottle choice CTA assay using 0.15% saccharine solution. DON induces a strong CTA in both GLP-1R$^{f/f}$ and WT littermate mice, reducing intake from 65-70% to merely 10-17% saccharine solution intake with no statistical impact of genotype (Fig. 8B). In a food intake test, DON induced a potent anorexia as early as 1-2 hours after food presentation in both GLP-1R^{WT} and GLP-1R^{KO} male (Fig. 8C) and female (Fig. 8D) mice. At 4 hours, DON reduced food intake in GLP-1R^{KO} and WT mice by 33-35% in males and 29-30% in females. By 24 hours, there is no

statistical difference between DON and saline treated groups in males. Female GLP-1R^{ff} mice continue to show a statistically significant slight decrease in feeding. However, we predict that this response would be eliminated within several hours. Although the data shown is separated by the sex of mice, when male and female data is combined there is still a similar trend, with DON inducing anorexia at 2 and 4 hours and no differences in the responses between genotypes.

Next we tested the necessity of GLP-1 using Gcg ^{KO} mice. Gcg ^{KO} mice do not exhibit differences in body weight compared to Gcg ^{WT} littermates (Fig. 8E). DON induces a CTA in both Gcg ^{KO} and Gcg ^{WT} littermates, illustrated by reduction of saccharine intake beginning at 1 hr and lasting for 25 hours (Fig. 8F). There was no significant difference between WT and Gcg KO DTA response. Further, food intake is reduced within 1 hour and up to 24 hours after DON injection (Fig. 8G). Gcg ^{WT} and Gcg ^{KO} mice reduce feeding by 35% and 32% within 1hr of DON exposure. Although data is represented with male and female mice combined, similar to GLP-1R^{KO} mice, there is no difference between male and female food intake response when data are separated. This data demonstrates that neither GLP-1 nor GLP-1R are necessary for the anorexia and aversion effects of DON.

We then investigated central neuronal activation within the AP using DON injected GFRAL$^{eGFP-L10}$ mice. 2 hours after DON injection, we found a high colocalization of eGFP positive GFRAL cells and immunofluorescence for cfos within the AP (Fig. 9A). Since DON clearly induces activation of GFRAL neurons, we then asked whether GFRAL signaling was necessary to the acquisition of a CTA and anorexia in response to DON. To test this, we used female GFRAL^{KO} and GFRAL^{WT} littermate mice. DON treated GFRAL^{KO} and GFRAL^{WT} mice both reduced saccharine intake and increased water intake within 2 hours and lasting for 24hours following two-bottle choice presentation (Fig. 9B-D). GFRAL^{KO} saline treated mice consumed

the saccharine solution 66-80% of total volume compared to only 10-13% in DON treated mice at 2 (Fig. 9B) and 4 hours (Fig. 9D). Although DON induced a potent CTA response, there were no differences observed between $GFRAL^{KO}$ and $GFRAL^{WT}$ mice. We then did a food intake test, in a separate cohort of male and female $GFRAL^{KO}$ and $GFRAL^{WT}$ mice. Within 1 hr, $GFRAL^{KO}$ mice and WT littermates exhibit a strong reduction in food intake with DON compared to $GFRAL^{KO}$ saline controls (Fig. 9E). DON induced anorexia was detectable at 2 and 4 hours (Fig. 9E-G), and reduced by 24 hours (Fig. 9H) with no difference between the $GFRAL^{KO}$ and $GFRAL^{WT}$ DON responses at any timepoint. Taken together, this data determines that GFRAL signaling is not a necessary component regulating aversive or anorexic responses to DON.

Although GFRAL is not necessary, other cell surface receptors on AP GFRAL neurons may be responsible for activation of the neuronal population. Thus, we next isolated the brains of $GFRAL^{eGFP\text{-}L10}$ mice for TRAP analysis on harvested AP extracts to separate the GFRAL (GFP-L10+) containing cell mRNA from the non-GFRAL expressing supernatant (eGFP-L10-) mRNAs. Mice contain eGFP tagged ribosomal subunits in GFRAL cells. Key genes were measuired and analyzed for enrichment and expression levels. We observed a high enrichment of CaSR mRNA in AP GFRAL cells (Fig. 9I). This led us to hypothesize that GFRAL neuronal activation is the primary signaling network for the anorectic and aversive effects of DON. To functionally test the necessity of GFRAL neurons in mediating DON induced physiological illness, we used mice with GFRAL neuron ablation. We crossed $GFRAL^{cre}$ mice onto the cre-inducible diphtheria toxin receptor background, permitting the specific ablation of GFRAL neurons by i.p. diphtheria toxin (DT) administration in $GFRAL^{DTR}$ mice while leaving GFRAL neurons intact in the $GFRAL^{WT}$ mice. We administered 200ug/kg diphtheria toxin (DT) to all mice. To understand the impact of DT on the phenotypes of mice with and without GFRAL

neuron ablation, we measured body weight (Fig. 10A), fat and lean mass (Fig. 10B-C) before and after DT in a cohort of male and female mice. Weekly body weights, fat and lean mass did not differ between $GFRAL^{WT}$ and $GFRAL^{DTR}$ mice before or after DT administration (Fig. 10A-C).

7 weeks after DT administration, we conducted a two bottle choice CTA test in which we paired the flavor of 0.15% saccharine solution with DON. $GFRAL^{WT}$ and $GFRAL^{DTR}$ saline paired mice both drank saccharine 67% saccharine solution. $GFRAL^{WT}$ and $GFRAL^{DTR}$ mice paired with vomitoxin, consumed only 8% and 16% of saccharine solution at 4hrs, respectively, illustrating that DON induced a potent CTA in both genotypes (Fig. 10D). There was no significant difference between the amount of saccharine solution consumed by $GFRAL^{WT}$ vs $GFRAL^{DTR}$ mice at either 4 or 24 hours (Fig. 10E), suggesting that GFRAL neurons are not responsible for triggering a CTA. There is greater variability in saccharine intake for $GFRAL^{DTR}$ mice at 24 hours, potentially reflecting differential ablation of GFRAL neurons in each subject. To test whether GFRAL neurons play a role in the strong anorexia induced by DON, we subjected mice to a food intake test after i.p. injection of either saline or 2.5mg/kg DON. While DON induced anorexia within 2 hrs of administration in both $GFRAL^{WT}$ and $GFRAL^{DTR}$ mice, we did not observe a difference in food intake between the $GFRAL^{WT}$ and $GFRAL^{DTR}$ mice (Fig. 10F) 4 (Fig. 10G) or 24 hours (Fig. 10H). Thus, we conclude that GFRAL neurons are not necessary for DON induced food refusal.

To functionally confirm the ablation of GFRAL neurons, we next challenged $GFRAL^{WT}$ and $GFRAL^{WT}$ mice with 60% high fat diet (HFD) feeding for 5 weeks and performed a food intake test following GDF15 administration. Pharmacological GDF15 is a potent anorectic agent, the effects of which are clearer in obese mice. Daily administration of GDF15 for 3 days does

not change body weight (Fig. 11A). GFRAL^{WT} mice exhibit a decrease in cumulative food intake in response to GDF15 by day 3 (Fig. 11B) and day 4 (Fig. 11C) compared to GFRAL^{DTR} mice. Next, we perfused and harvested mouse brains 4 hours after s.c. administration of GDF15. The AP/NTS of GFRAL^{WT} mice contained elevated eGFP fluorescence staining GFRAL neurons expressing eGFP compared to GFRAL^{DTR} mice (Fig. 11D). Further cfos in reponse to GDF15 is significantly reduced in GFRAL^{DTR} mice compared to GFRAL^{WT} (Fig. 11D).Taken together, the reduced anorexia in response to GDF15 and of eGFP signal in GFRAL^{DTR} mice confirm that GFRAL neurons are sufficiently depleted by DT in GFRAL^{DTR}

3.4 Discussion

A wide range of hypotheses have been offered to explain the potent effects of DON to induce anorexia. We tested the necessity of peripheral signaling molecules using GLP-1R^{KO}, Gcg^{KO}, GFRAL^{KO}, and GFRAL^{DTR} ablation of GFRAL. Enteroendocrine cells are important in detecting luminal content and influencing appetite and satiety through the release of hormones. CaSR is found in enteroendocrine cells and downstream signaling leads to the exocytosis of GLP-1 [105,222,223] as quickly as 15 minutes after DON exposure [109,218,224,225]. Our results demonstrate that DON is a potent visceral illness inducing agent that does not require the production of GLP-1 or GLP-1R signaling to cause aversion or anorexia. GLP-1R KO and Gcg KO mice exhibited a similar anorexia and aversion response as the WT littermate controls when peripherally administered DON. Our results are in contrast to Jia et al, in which GLP-1 antagonist Exendin$_{9-39}$ pharmacologically increases food intake in orally infected mice. This is likely due to the differences in the genetic vs pharmacological manipulation of GLP-1 model systems used. Feeding responses to a anorectic agent of GLP-1 and administering an anorectic of DON can vary depending on the dosage of each. The effect of Exendin$_{9-39}$ to elicit increased

feeding may be overriding the anorectic capabilities of DON, but does not imply that the two mechanisms are inherently shared. Thus, manipulating well-known food reducing agents such as GLP-1 and DON signaling may be highly variable depending on the doses administered [226].

Although we found that GLP-1 is not a necessary component, other intestinal hormone signals may be contributing to the response. Many peripheral agents are capable of signaling to the hindbrain to elicit behavioral responses. The AP and NTS have been identified as important regions for DON induced illness. An early lesion study showed that the development of a CTA in rats in response to DON is dependent on the AP [219] which is consistent with our current understanding of the AP's role in illness. A population of neurons in the brain containing GFRAL receptor elicit similar illness behaviors of anorexia and aversion formation when activated [8,23]. We hypothesized that DON elicits GFRAL to produce nausea and food refusal and directly tested this hypothesis using $GFRAL^{KO}$ mice. $GFRAL^{KO}$ mice exhibit the same anorexia and aversion response as $GFRAL^{WT}$ littermates. Thus, we concluded that GFRAL is not required for the physiological symptoms of DON.

After peripheral DON administration, levels of DON detectable in the brain increase rapidly [114]. Instead of peripheral signaling, DON may induce CaSR directly in the brain. Using TRAP-seq to measure mRNA in the AP, we found a high enrichment of CaSR on GFRAL neurons. We then hypothesized that although GFRAL is not necessary, the neurons may play a critical role by direct activation of CaSR by DON. To test this, we developed $GFRAL^{DTR}$ mice that specifically express diphtheria toxin receptor on GFRAL neurons. DT administration ablates GFRAL cre expressing neurons. To control for DT, we administered DT to all mice. $GFRAL^{DTR}$ mice exhibit similar feed refusal and CTA formation as $GFRAL^{WT}$ mice. Our experiments

demonstrate that neither GFRAL itself nor the neurons are necessary to induce anorexia or aversion, as illustrated by the intact illness symptoms in $GFRAL^{KO}$ and $GFRAL^{DTR}$ mice.

$GFRAL^{DTR}$ mice exhibited a greater variability in CTA formation, with some DON conditioned mice drinking more saccharine than others compared to $GFRAL^{WT}$ mice. It is possible that there is variable ablation of GFRAL neurons and very few GFRAL neurons are required to elicit aversion. In this case, the variability in saccharine consumption would be a result of differential GFRAL neuron ablation with diphtheria toxin. Further, GFRAL neurons represent just a fraction of neuronal populations within the AP and NTS. Although we have determined that GFRAL neurons are not necessary for DON's illness effects, central CaSR signaling on other neuronal populations is possible, as CaSR is widely expressed in the brain [227–229]. Additionally, CaSR is expressed in the hypothalamus which has recently been vaguely hypothesized to be implicated in regulating DON induced food refusal. A handful of studies have detected alterations in cFos and mRNA within the arcuate nucleus and POMC and AgRP neurons in response to DON, though with conflicting results [104,112,224,230,231]. This is further confounded by variability between species. As many of these studies have inconsistent data at the contribution of various gut hormones and activation of hypothalamic networks, it is possible that a combination of hormones and factors are contributing. Thus, further research in mice investigating neuronal activation and the peripheral hormone response is necessary.

3.5 Materials and methods

Animals

All rodent experiments were approved by the University of Michigan Institutional Animal Care & Use Committee at (Animal Use Protocol # PRO00007908). Animals were single housed (at minimum for 1 week prior to experimentation) in temperature controlled rooms containing a 12hr:12hr light:dark cycle and given *ad libitum* access to chow (PicoLab 5L0D) or 60% high fat diet (Research Diets Inc., D12492).

GLP-1R^{KO}, Gcg^{KO} and GFRAL^{KO} mice were generated as previously described [33,206]. WT littermates (GFRAL^{WT}, Gcg^{WT}, GFRAL^{WT}) were used as controls. To generate the GFRAL^{eGFP} mice, the LSL cassette from the ROSA26$^{eGFP\text{-}L10a}$ allele was excised by Gfral^{Cre} as previously described [23,232]. Male and female GFRAL$^{eGFP\text{-}L10a}$ mice were used for cfos immunohistochemical analysis of the area postrema. A separate cohort of male and female GfralCre$^{eGFP\text{-}L10a}$ were used for TRAP. Gfral$^{cre\text{-}eGFP\text{-}L10}$ mice were bred with mice expressing B6-iDTR, ROSA26iDTR (C57BL/6-Gt(ROSA)26Sor$^{tm1(HBEGF)}$Awai; no: 007900, The Jackson Laboratory) to generate Gfral$^{eGFP\text{-}DTR}$ (Gfral^{DTR}) mice which express diphtheria toxin receptor in GFRAL cells. Gfral$^{cre\text{-}eGFP\text{-}L10}$ mice were used as controls.

Pharmacological agents

Lyophilized deoxynivalenol (Sigma 5mg D0156) was reconstituted into 1mg/ml saline aliquots and frozen at -80deg. On the day of experiment, vomitoxin was thawed, diluted with saline to the appropriate concentration (1mg/ml or 2.5mg/ml) and filtered through a 0.22um PVDF membrane

filter (Millipore Sigma, SLGV033RS) for i.p. administration. 0.4mg/kg of mouse GDF15 (Novo Nordisk) was prepared by diluting with a MIC-1 buffer (5 mM acetate salt, 2.25% glycerol and 70ppm Tween 20 at pH 4). Mouse GDF15 or buffer was injected subcutaneously in mice daily. All $GFRAL^{DTR}$ and $GFRAL^{WT}$ mice were dosed with 200ug/kg diphtheria toxin dissolved in saline (Sigma, D0564-1MG) prior to experimentation.

Food intake test

Clean cages were provided and all food was removed to fast mice for 4-5 hours ($GFRAL^{KO/WT}$; $GFRAL^{DTR/WT}$; GLP-1R $^{KO/WT}$; Gcg $KO^{/WT}$) with full access to water. Animals were randomized for treatment and administered saline or vomitoxin (2.5 mg/kg ip) 1 hour prior to dark onset and return of pre-weighed diet. Remaining food in cage was measured at 1,2,4, and 24 hours after food return to determine food intake. The same was repeated for food intake analysis of pharmacological GDF15 except GFRALcre/ $GFRAL^{WT}$ mice were not fasted and measurements were taken at the same time every 24 hours.

Conditioned taste aversion (CTA) assay

Mice were handled and injected with saline for a minimum of 1 week prior to experimentation. On day 0, mice began habituation to removal of lixit access and replacement with two water bottles. On day 3, water bottles were removed 1 hour prior to lights off to induce thirst for 23 hours. On day 4 (conditioning day), 2 bottles containing 0.15% saccharine in water solution were given to mice for 2 hours prior to lights out. At lights out, mice received an injection of either saline or DON (2.5mg/kg, ip). Saccharine bottles were then removed and 2 water bottles were

added back to the cages immediately. On day 5, water bottles were removed for 23 hours to induce thirst. On day 6 (test day), a pre-weighed water bottle and saccharine bottle were added to the cages (0 hr; baseline) to give the mice a two-bottle choice 1 hour prior to lights out. Bottles were measured for the following 1, 2, 4, and 24 hours. Volume of water and saccharine consumed were calculated at each time point and represented as a % of total volume intake (saccharine intake/(saccharine + water intake)*100.

Body Composition

Fat and lean mass were measured using an EchoMRI (Echo Medical Systems).

IHC (DON cfos in $GFRAL^{eGFP}$ mice; $GFRAL^{DTR}$ ablation)

$GFRAL^{eGFP\text{-}L10}$ mice were injected with 2.5mg/kg vomitoxin i.p. 2 hours prior to CO_2 asphyxiation. $GFRAL^{DTR}$ and $GFRAL^{WT}$ mice were injected with GDF15 s.c. 4 hours prior to euthanization with isoflurane. Mice were then perfused with phosphate buffered saline (PBS) followed by a 10% buffered formalin solution. Brains were harvested and post fixed in a 30% sucrose solution. 30um brain slices were taken using a freezing microtome (Leica). Brain sections were then treated with 1% hydrogen peroxide/0.5% sodium hydroxide, 0.3% glycine, 0.03% sodium dodecyl sulfate, and blocked with 0.1% triton, 3% normal donkey serum in PBS (Fisher Scientific). After an overnight room temperature incubation with anti-FOS antibody, slices were washed and incubated with secondary antibody. Microscopy and analysis of images were done (Olympus BX51 microscope).

Statistical Analysis

All statistical analysis was performed in either GraphPad Prism v8.4.2 3BF and is represented as mean +/- SEM. Student's t-test, one-way, two-way or three-way ANOVA with Tukey's post-hoc tests were utilized to determine significance. Significance was defined as $p<0.05$.

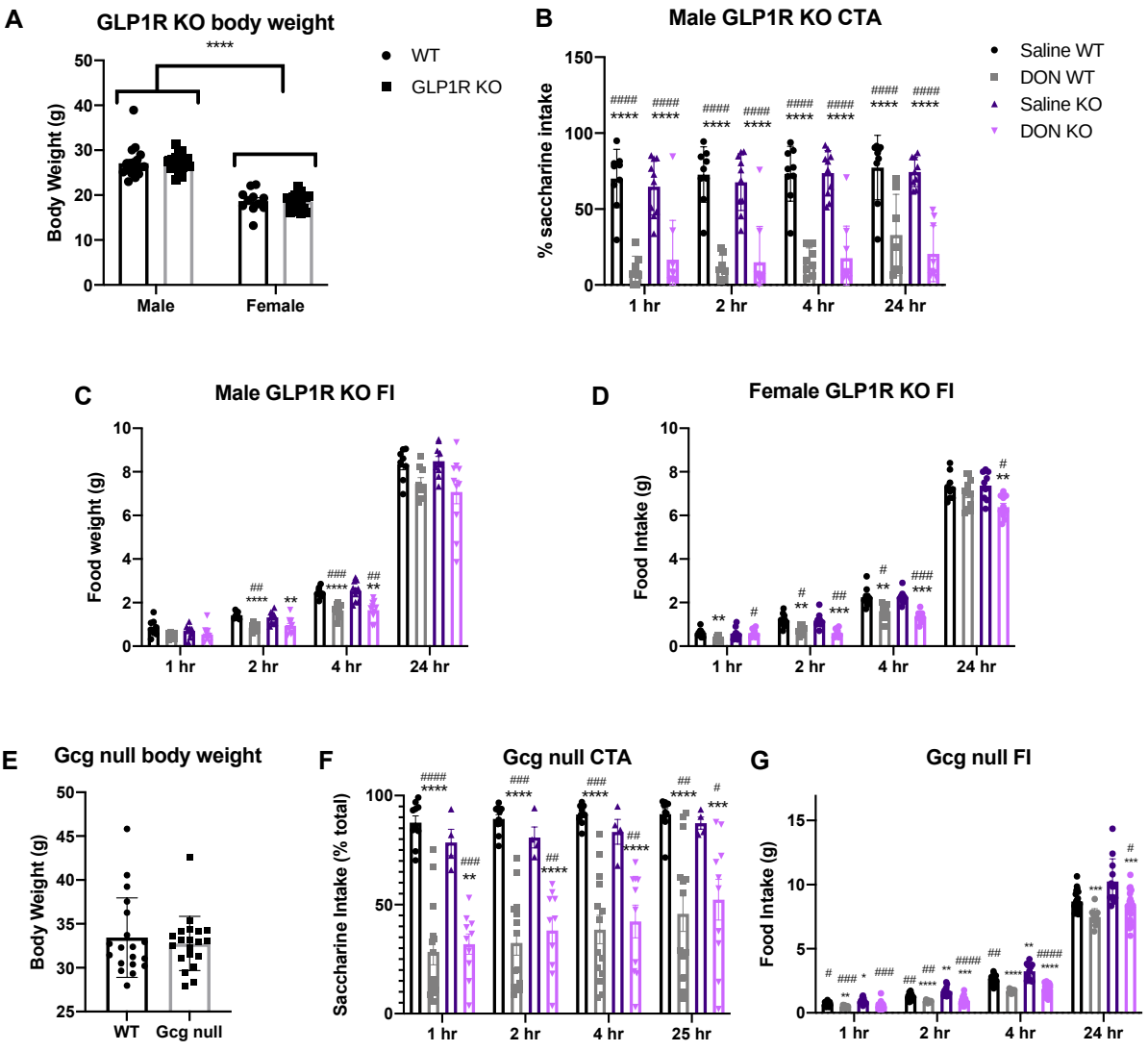

Figure 8: GLP-1 signaling in male and female mice

Body weights of male WT (n= 19), male GLP-1R KO (n=21), female WT (n=11) and female GLP-1R KO (n=21) mice prior to experimentation (A) 2-way ANOVA with Tukey's multiple comparisons; **** male vs female.

Conditioned taste aversion (CTA) assay in male WT and GLP-1R KO mice conditioned to saline or 2.5mg/kg DON (n= 8-10 per group) (B).

Food intake (FI) test in WT and GLP-1R KO male (n=8-10 per group) (C) and female (n=9-10) (D) mice fasted for 4-5 hours and injected with 2.5mg/kg DON; */ **/ ***/ **** compared to WT saline and #/ ##/ ###/ #### compared to KO saline by 2-way ANOVA with Tukey's multiple comparison test.

Body weights of WT and Gcg null male and female mice (n=19-20) (E) two-tailed students t-test; no significant differences. CTA assay in male and female WT and Gcg null mice

conditioned to saline or 2.5mg/kg DON (n=4-14 per group) (F) Food intake test in WT and Gcg null male and female mice (n= 4-14) (G) */ **/ ***/ **** compared to WT saline and #/ ##/ ###/ #### compared to KO saline by 2-way ANOVA with Tukey's multiple comparison test. All data are represented as mean +/- SEM. */#$p<0.05$; **/##$p<0.01$; ***/###$p<0.001$; ****/####$p<0.0001$.

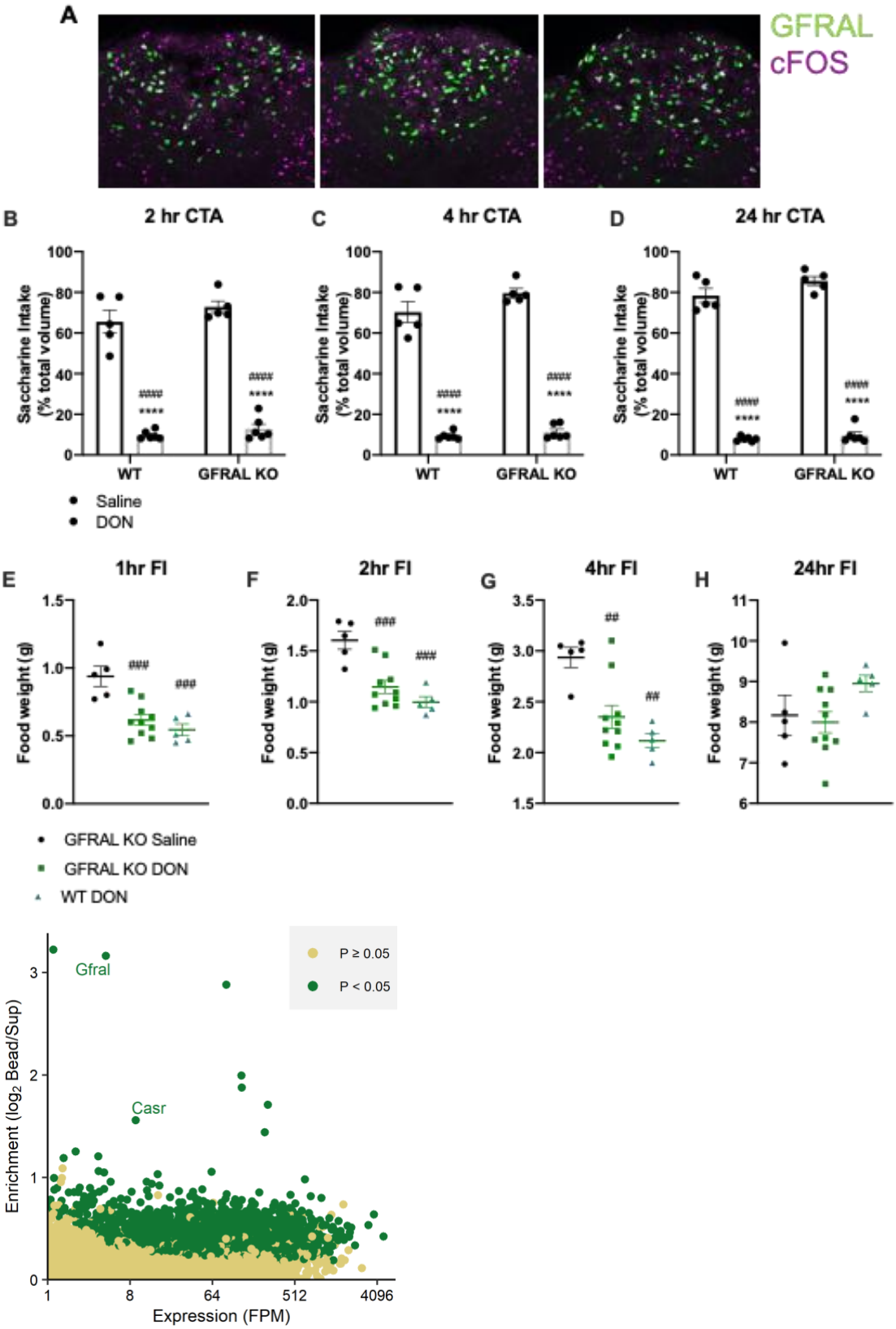
A
GFRAL
cFOS
B
2 hr CTA
C
4 hr CTA
D
24 hr CTA
Saccharine Intake (% total volume)
WT
GFRAL KO
Saline
DON
E
1hr FI
F
2hr FI
G
4hr FI
H
24hr FI
Food weight (g)
GFRAL KO Saline
GFRAL KO DON
WT DON
Gfral
Casr
P ≥ 0.05
P < 0.05
Enrichment (log2 Bead/Sup)
Expression (FPM)

Figure 9: GFRAL signaling

Immunohistochemical staining of area postrema from male and female GFRAL eGFP-L10 mice injected with 2.5mg/kg DON for cfos (n=3)(Fig1.A). Conditioned taste aversion (CTA) assay of female GFRAL KO and WT mice with ip administration of saline or 2.5mg/kg DON at 2hr (B), 4hr (C), and 24 hr (D) (n=5-6 per group). Food intake (FI) test of 5 hr fasted mice conditioned to saline or 2.5mg/kg DON at 1hr (E) 2hr (F) 4hr (G) and 24hr (H) (n=5-10). */ **/ ***/ **** compared to WT saline and #/ ##/ ###/ #### compared to GFRAL KO saline by 2-way ANOVA with Tukey's multiple comparison test. Transcripts enriched in TRAP fraction of the AP in male and female GFRAL$^{eGFP\text{-}L10}$ mice (I). Differential expression was determined by CuffDiff analysis with threshold set to P <0.05. Expression is represented as fragments per million (FPM). (n=12). All data are represented as mean +/- SEM. */#p<0.05; **/##p<0.01; ***/###p<0.001; ****/####p<0.0001.

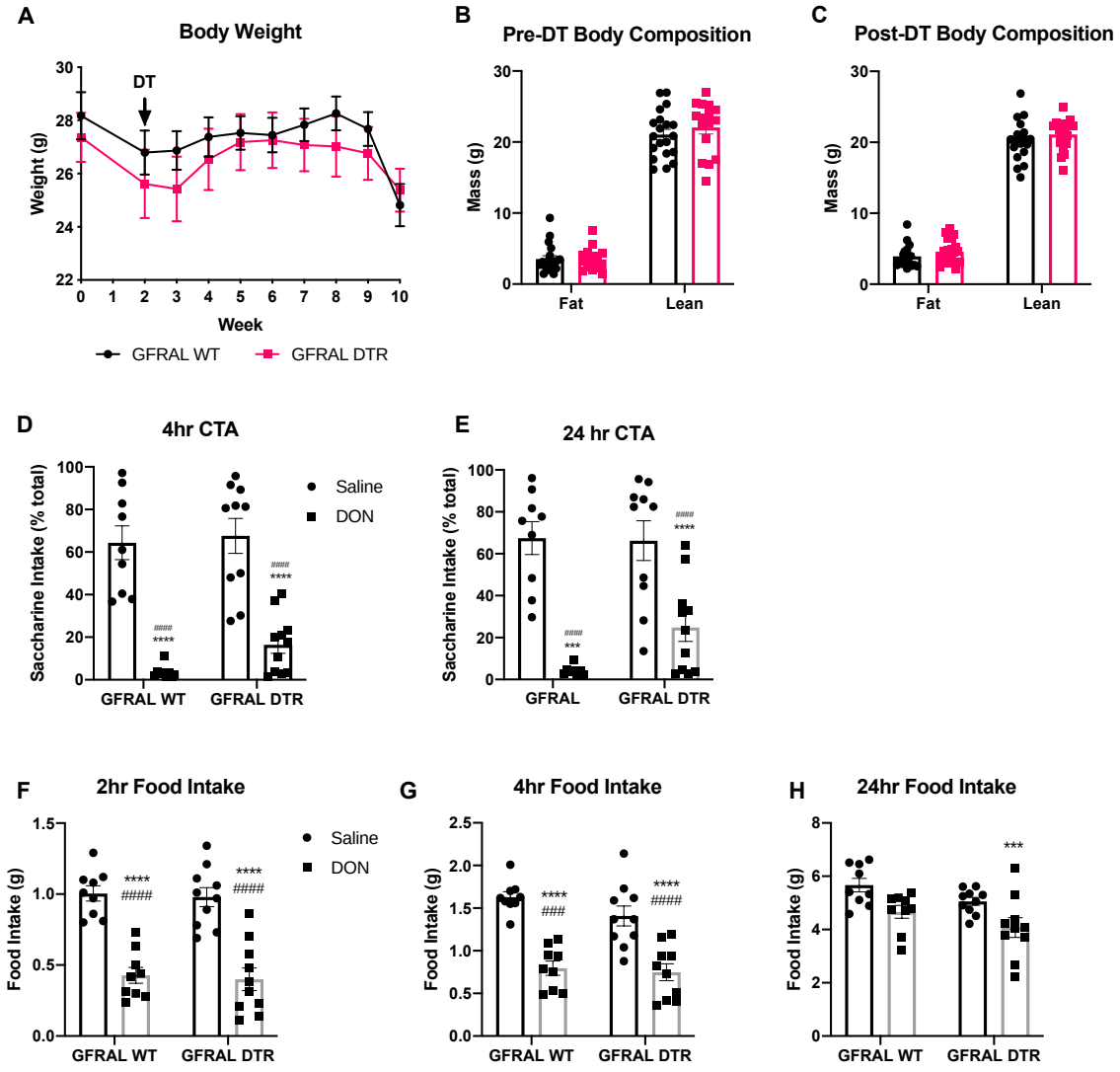

Figure 10: GFRAL neuronal ablation

Body weight 2 weeks before and 7 weeks after diphtheria toxin injection in GFRAL WT and GFRALcre mice (n=18-20 per group) (A); 2-way ANOVA with Sidak's multiple comparison test. Body composition of GFRAL WT and GFRALcre mice 2 weeks prior to diphtheria toxin administration (n=18-20 per group) (B) and 15 weeks after diphtheria toxin administration (n=18-20 per group) (C); 2-way ANOVA with Tukey's multiple comparison test. Conditioned taste aversion (CTA) assay in male GFRAL WT and GFRALcre mice conditioned to saline or 2.5mg/kg DON at 4 hours (D) and 24 hours (E) after addition of two bottle choices (n= 9-11 per group); 2-way ANOVA with Tukey's multiple comparison test. Food intake test after a 4-5 hour fast in GFRAL WT and GFRALcre mice with either saline or 2.5mg/kg DON injection at 2 hours (F) 4 hours (G) and 24 hours (H) after food return; 2-way ANOVA with Tukey's multiple comparison test. */ **/ ***/ **** compared to GFRAL WT saline and #/ ##/ ###/ #### compared to GFRALcre saline. All data are represented as mean +/- SEM. */#p<0.05; **/##p<0.01; ***/###p<0.001; ****/####p<0.0001.

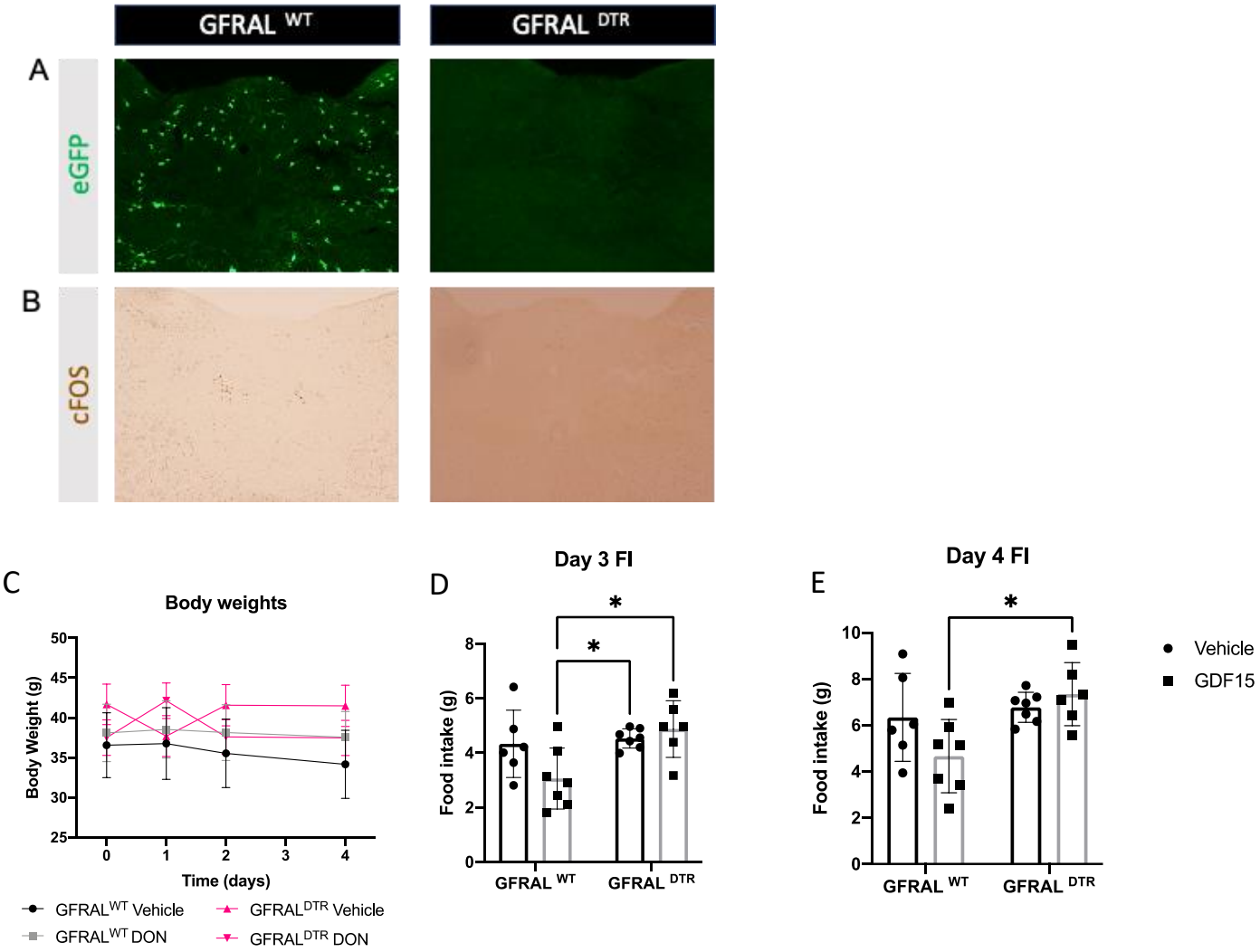

Figure 11: GFRAL DTR neuron ablation confirmation

GFRAL WT and GFRAL DTR mice 4 hours after s.c. dose of GDF15. Representative immunostaining of the AT/NTS for eGFP labeling GFRAL neurons (A) and cFOS (B). Body weights of mice dosed with s.c. vehicle or GDF15 daily on days 1, 2, and 3 (C) and cumulative food intake on day 3 (D) and day 4 (E) (n=6-7 per group); 2-way ANOVA with Tukey's post hoc test. All data are represented as mean +/- SEM; *p<0.05

[3]Chapter 4: GLP-2 Receptor Signaling Controls Circulating Bile Acid Levels but Not Glucose Homeostasis in Gcgr-/- Mice and is Dispensable for the Metabolic Benefits Ensuing after Vertical Sleeve Gastrectomy

4.1 Chapter summary

Therapeutic interventions that improve glucose homeostasis such as attenuation of glucagon receptor (Gcgr) signaling and bariatric surgery share common metabolic features conserved in mice and humans. These include increased circulating levels of bile acids (BA) and the proglucagon-derived peptides (PGDPs), GLP-1 and GLP-2. Whether BA acting through TGR5 (Gpbar1) increases PGDP levels in these scenarios has not been examined. Furthermore, although the importance of GLP-1 action has been interrogated in *Gcgr*$^{-/-}$ mice and after bariatric surgery, whether GLP-2 contributes to the metabolic benefits of these interventions is not known.

To assess whether BA acting through Gpbar1 mediates improved glucose homeostasis in *Gcgr*$^{-/-}$ mice we generated and characterized *Gcgr*$^{-/-}$:*Gpbar1*$^{-/-}$ mice. The contribution of GLP-2 receptor (GLP-2R) signaling to intestinal and metabolic adaptation arising following loss of the Gcgr was studied in *Gcgr*$^{-/-}$:*Glp2r*$^{-/-}$ mice. The role of the GLP-2R in the metabolic

[3] This chapter represents the following manuscript:

Patel, A., Yusta, B., Matthews, D., Charron, M.J., Seeley, R.J., Drucker, D.J., 2018. GLP-2 receptor signaling controls circulating bile acid levels but not glucose homeostasis in Gcgr−/− mice and is dispensable for the metabolic benefits ensuing after vertical sleeve gastrectomy. Molecular Metabolism 16: 45–54, Doi: 10.1016/j.molmet.2018.06.006.

improvements evident after bariatric surgery was studied in high fat-fed *Glp2r*$^{-/-}$ mice subjected to vertical sleeve gastrectomy (VSG).

Circulating levels of BA were markedly elevated yet similar in *Gcgr*$^{-/-}$:*Gpbar1*$^{+/+}$ vs. *Gcgr*$^{-/-}$:*Gpbar1*$^{-/-}$ mice. Loss of GLP-2R lowered levels of BA in *Gcgr*$^{-/-}$ mice. *Gcgr*$^{-/-}$:*Glp2r*$^{-/-}$ mice also exhibited shifts in the proportion of circulating BA species. Loss of *Gpbar1* did not impact body weight, intestinal mass, or glucose homeostasis in *Gcgr*$^{-/-}$ mice. In contrast, small bowel growth was attenuated in *Gcgr*$^{-/-}$:*Glp2r*$^{-/-}$ mice. The improvement in glucose tolerance, elevated circulating levels of GLP-1, and glucose-stimulated insulin levels were not different in *Gcgr*$^{-/-}$:*Glp2r*$^{+/+}$ vs. *Gcgr*$^{-/-}$:*Glp2r*$^{-/-}$ mice. Similarly, loss of the GLP-2R did not attenuate the extent of weight loss and improvement in glucose control after VSG.

These findings reveal that GLP-2R controls BA levels and relative proportions of BA species in *Gcgr*$^{-/-}$ mice. Nevertheless, the GLP-2R is not essential for i) control of body weight or glucose homeostasis in *Gcgr*$^{-/-}$ mice or ii) metabolic improvements arising after VSG in high fat-fed mice. Furthermore, despite elevations of circulating levels of BA, Gpbar1 does not mediate elevated levels of PGDPs or major metabolic phenotypes in *Gcgr*$^{-/-}$ mice. Collectively these findings refine our understanding of the relationship between Gpbar1, elevated levels of BA, PGDPs, and the GLP-2R in amelioration of metabolic derangements arising following loss of Gcgr signaling or after vertical sleeve gastrectomy.

4.2 Introduction

Although multiple organ systems contribute to control of energy balance, the complex network of enteroendocrine cells has received increasing attention as physiological regulators of metabolic homeostasis [233,234]. Notably, L cells that produce the proglucagon-derived

peptides (PGDPs) have been extensively studied, as PGDPs exert pleiotropic actions regulating appetite, gastrointestinal motility, nutrient absorption, gut epithelial integrity, gallbladder emptying, and the uptake and assimilation of nutrients in peripheral tissues [235,236]. Indeed, PGDP secretion from enteroendocrine L cells is stimulated by a range of nutrients, microbial metabolites, and bile acids (BA), through direct and indirect mechanisms [234].

Glucagon-like peptide-1 (GLP-1), the best characterized PGDP, is a 30 amino acid peptide that exerts its actions through a single well-defined G protein-coupled receptor [236]. GLP-1 is physiologically essential for glucose control and energy homeostasis, as revealed in preclinical studies using GLP-1 receptor (GLP-1R) antagonists or Glp1r-/- mice [236]. GLP-1 also attenuates the rate of gastric emptying and small bowel motility, and promotes expansion of the intestinal mucosal epithelium, actions serving to optimize the efficiency of nutrient absorption [237]. Although less well studied, the related PGDP GLP-2 also controls the absorption of nutrients through reduction of gut motility, upregulation of nutrient transport and via optimization of mucosal surface area and gut integrity [238].

A number of experimental therapeutic manipulations resulting in improvement of glucose metabolism and either resistance to weight gain or development of weight loss are characterized by simultaneous elevation of circulating BA and PGDPs. Thus, partial or complete blockade of glucagon action, achieved through genetic loss of hepatic glucagon receptor (Gcgr) expression or pharmacological antagonism of GCGR signaling, is associated with a rapid rise in circulating levels of GLP-1 and GLP-2 [239,240]. Unexpectedly, reduction of Gcgr signaling is also associated with markedly increased circulating levels of BA [241,242]. Indeed plasma levels of PGDPs and BA are increased in humans with T2D following daily or chronic administration of GCGR antagonists [240,243].

Bariatric surgery represents a second therapeutic paradigm characterized by increased levels of circulating BA, GLP-1 and GLP-2. Both vertical sleeve gastrectomy (VSG) and Roux-en-Y gastric bypass (RYGB), when performed experimentally in animals, or therapeutically in humans, lead to elevated levels of BA and PGDPs [160,244–247]. Although BA are known stimulators of L cell PGDP secretion via signaling through TGR5 (Gpbar1) [248–250], the extent if any, to which elevated levels and action of BA contribute to increased levels of circulating PGDPs i) in animals or humans with loss of GCGR action or ii) following bariatric surgery, has not been yet determined.

The finding that enhanced circulating levels of BA and PGDPs are simultaneously associated with improved glucose control in the setting of loss of GCGR signaling or metabolic surgery raises important mechanistic questions [251–253]. Notably, preclinical studies implicate a role for BA, acting through changes in the gut microbiota and via the nuclear Farnesoid X Receptor (FXR), in the improvements in glucose control and weight loss ensuing following VSG [152]. Consistent with the importance of BA in this setting, the metabolic benefits ensuing from bariatric surgery are also attenuated in Gpbar1-/- mice [254,255]. Although somewhat controversial, GLP-1 contributes to improvements in β-cell function in some [256], but not all murine studies of metabolic surgery [251,257]. It seems likely that GLP-1 improves β-cell function in humans after bariatric surgery, and in rare instances, promotes development of hyperinsulinemic hypoglycemia [252].

In contrast to the extensive literature describing the metabolic roles of GLP-1, much less is known about the effects of GLP-2 on glucose control and body weight. Notably, GLP-2 inhibits ghrelin secretion [258], enhances hepatic insulin sensitivity [259], and suppresses food intake [260], actions mirroring some of the metabolic benefits ensuing after bariatric surgery or

GCGR antagonism. Furthermore, GLP-2 enhances gut adaptation and barrier function while reducing metabolic endotoxemia [238,261], consistent with intestinal adaptation evident after VSG or RYGB [262,263]. Collectively, these observations raise the possibility that elevated levels of GLP-2, arising secondarily to or independent from increased levels of BA, may contribute to the metabolic benefits arising following i) reduction of GCGR signaling or ii) metabolic surgery. To interrogate the potential role of BA signaling through Gpbar1 and the importance of GLP-2R for the metabolic improvements in Gcgr-/- mice, we generated Gcgr-/-:Gpbar1-/- and Gcgr-/-:Glp2r-/- mice. Simultaneously, we examined the importance of GLP-2R signaling in Glp2r-/- mice following experimental VSG.

4.3 Materials and methods

Animals and vertical sleeve gastrectomy surgical procedure

Gcgr-/- mice provided by Maureen Charron [264], Tgr5-/- (Gpbar1-/-) mice [265], obtained from Schering-Plough/Merck, and Glp2r-/- mice [266], all on a C57Bl/6 background were bred at the Toronto Centre for Phenogenomics animal facility. Gcgr-/-:Gpbar1-/- and Gcgr-/-:Glp2r-/- double knockout mice were generated by crossing double heterozygous Gcgr+/-:Gpbar1+/- or Gcgr+/-:Glp2r+/- to obtain wild-type, single knockout and double knockout littermates. All experiments involving Gcgr-/-:Gpbar1-/- and Gcgr-/-:Glp2r-/- double knockout mice and their single knockout and wild-type littermates were performed in male aged 12-26 weeks, housed up to 5 per cage, with free access to food (2018 Tecklad global, Envigo Corp, Mississauga, ON, Canada) and water. VSG or sham surgeries were performed on male Glp2r-/- and wild-type littermate mice bred in-house at the University of Michigan. Four to 11 week old mice were placed on a 60% high fat diet (HFD) (D12492, Research Diets, New Brunswick, NJ, USA) were

single housed and given ad libitum access to food. After 8 weeks, surgeries were performed as previously described [267]. Briefly, while mice were anesthetized under isoflurane inhalation, an abdominal midline laparotomy was made followed by incision of the underlying abdominal muscle and exteriorization of the stomach. For VSG the lateral 80% of the stomach was excised using an ETS 35-mm staple gun (Ethicon Endo-Surgery, Cincinnati, OH, USA) leaving a tubular gastric sleeve in continuity with the esophagus proximally and the pylorus distally. The sham procedure involved the application of light pressure on the stomach with blunt forceps. Mice were fed Osmolite 1.0 Cal liquid diet (Abbott Nutrition, Lake Forest, IL, USA) from 1 day prior to surgery to 3 days following surgery before returning to 60% HFD. Glp2r-/- pair-fed animals underwent sham surgery and were restricted to eating the daily average amount of food eaten by the Glp2r-/- mice subjected to VSG. Pair-feeding continued until sacrifice. Body composition was measured using an EchoMRI (Echo Medical Systems, Houston, TX, USA) 1 week prior to surgery and 6 and 8 weeks after surgery. Body weights were measured daily for 1 week after surgery and weekly for 10 weeks thereafter. All animal experiments performed in Toronto were conducted according to protocols approved by the Animal Care and Use Subcommittee at the Toronto Centre for Phenogenomics, Mt. Sinai Hospital, and were consistent with the ARRIVE guidelines. Studies on Glp2r-/- mice done in Ann Arbor were approved by the Institutional Animal Care & Use Committee at the University of Michigan (Animal Use Protocol #PRO00005678).

Glucose tolerance tests and measurement of plasma insulin, GLP-1 and bile acids

Glucose tolerance tests in Gcgr-/-:Gpbar1-/- and Gcgr-/-:Glp2r-/- double knockout mice and their single knockout and wild-type littermates were carried out in 12- to 15-week-old mice. Fed

or overnight fasted (16-18 hours in cages with wire grid flooring) mice were administered glucose (2 mg/g body weight) via either an oral gavage or i.p. injection. Glycemic excursion curves were delineated by measuring tail blood glycemia using a Contour blood glucose meter (Bayer Inc, Mississauga, ON, Canada) at 0, 15, 30 60 and 90 min after glucose loading. Glucose tolerance tests in Glp2r-/- and wild-type littermate mice that underwent VSG or SH surgeries were performed during postoperative week 5 following a 4 h fasting after the onset of light. Baseline blood glucose was measured in tail blood using an Accu-Check glucometer (Roche Diabetes Care, Mannheim, Germany) 30 min prior to i.p. injection of 2 mg glucose/g body weight or oral gavage of 2.6 mg glucose/g body weight. Tail blood glucose was measured at 15, 30-, 45-, 60-, and 120-min following glucose administration. For plasma BA measurement, blood samples were collected from the tail vein into heparin-coated tubes (Sarstedt, Montreal, QC, Canada). For plasma insulin and GLP-1 determination, blood samples collected into heparin-coated tubes, were supplemented with 1/10 the blood volume of a solution containing 5000 KIU/ml Trasylol (Bayer Inc, Mississauga, ON, Canada), 32 mM EDTA, and 0.01 mM Diprotin A (Sigma, St. Louis, MO, USA). Plasma was separated by centrifugation at 4°C and stored at –80°C until assayed for insulin (ultrasensitive mouse insulin ELISA; Alpco Diagnostics, Salem, NH, USA) and GLP-1 (mouse/rat total GLP-1 assay kit; Mesoscale Discovery, Gaithersburg, MD, USA). GLP-1, but not GLP-2, was measured as a readout of L cell secretion since the commercially available GLP-2 assays have not been sufficiently validated to ensure accurate measurement of total or intact GLP-2 [238]. Total bile acid levels in plasma were quantified using an assay kit based in the colorimetric detection of thio-NADH generated following oxidation of the bile acids by the enzyme 3-alpha-hydroxysteroid dehydrogenase in the presence of excess NADH (Diazyme Laboratories, Poway, CA, USA).

Intestinal biometry

Following euthanasia, mice were weighed and tibial length measured with a caliper. The entire gastrointestinal tract from the stomach to the rectum was removed, cleaned of mesenteric fat and gut weight and length determined. Small intestine length was measured under tension by suspending a 1-g weight from the distal end, prior to flushing with PBS to remove luminal content, whereas colon length was measured on a horizontal ruler after flushing. The entire small bowel and colon were then blotted to remove PBS before being weighed.

RNA isolation and analysis of mRNA expression

Total RNA from mouse ileum and liver was extracted by the guanidinium thiocyanate method using TRI Reagent (Molecular Research Center Inc, Cincinnati, OH, USA). Reverse transcription was performed with 500 ng of total RNA treated with DNase I (#EN0521, Thermo-Fisher Scientific, Markham ON, Canada), using random hexamers (#58875) and SuperScript III (#18080-044) from Thermo-Fisher Scientific. The resultant cDNA was used to assess mRNA expression by real-time quantitative PCR (QuantStudio 5 System, Thermo-Fisher Scientific) with TaqMan Fast Advanced Master Mix (#4444557, Thermo-Fisher Scientific) and TaqMan Gene Expression Assays (Thermo-Fisher Scientific). The specific gene expression assays used are listed in Supplementary Table 1. Quantification of transcript levels was performed by the 2-ΔCt method using 18S rRNA or Ppia for normalization.

Quantitative profiling of bile acids from ileum and plasma

Samples of plasma and ileum (with associated luminal content) from random-fed Gcgr-/-:Glp2r-/- double knockout mice and their single knockout and wild-type littermates, were analyzed by the Michigan Regional Comprehensive Metabolomics Resource (MRC2) facility using a modified protocol as previously described [268]. Serum and ileum samples underwent a two-step solvent extraction as follows. Samples were mixed with 100% ethanol with isotope-labeled internal standards and homogenized using a probe sonication. Samples rested on ice for 10 minutes and subsequently vortexed. An aliquot of this sample was transferred to a new glass tube and centrifuged. Supernatant was transferred to a microtube. An 8:1:1 solution of methanol, chloroform, and water was mixed to the glass tube and rested for 10 min followed by centrifugation. Supernatants were collected and combined. Samples were then dried at 45°C using a vacuum centrifuge for 45min and reconstituted in 50% methanol in water solution.

LC-MS analysis: LC-MS analysis was performed on an Agilent system consisting of a 1290 UPLC module coupled with a 6490 Triple Quad (QqQ) mass spectrometer (Agilent Technologies, Santa Clara, CA) operated in MRM mode. Metabolites were separated on a 100mm x 2.1mm Acquity BEH UPLC (1.7 uM) column (Waters Corp, Milford, MA) using H2O, 0.1% Formic acid, as mobile phase A, and Acetonitrile, 0.1% Formic acid, as mobile phase B. The flow rate was 0.25 mL/min with the following gradient: linear from 5 to 25% B over 2 minutes, linear from 25 to 40% B over 14 mins, linear from 40 to 95% B over 2 minutes, followed by isocratic elution at 95% B for 5 minutes. The system was returned to starting conditions (5% B) in 0.1 min and held there for 3 minutes to allow for column re-equilibration before injecting another sample. The mass spectrometer was operated in ESI. Data were processed using MassHunter Quantitative analysis version B.07.00. Metabolites were normalized

to the nearest isotope labeled internal standard and quantitated using 2 replicated injections of 5 standards to create a linear calibration curve with accuracy better than 80% for each standard.

Bile acid data from ileum were normalized to sample weight prior to processing. Concentrations of GHDA and GUDCA in plasma and CA in ileum are not reported as they were below the detection threshold. (TαMCA+TβMCA), (CDCA+DCA) and (TUDCA+THDCA) indicate sum of concentrations of the indicated pairs of BA which could not be distinguished from each other in the analysis process. Bile acid abbreviations: αMCA (α-Muricholate), βMCA (β-Muricholate), ωMCA (ω-Muricholate), CA (Cholate), CDCA (Chenodeoxycholate), HCA (Hyocholate), DCA (Deoxycholate), UDCA (Ursodeoxycholate), HDCA (Hyodeoxycholate). Taurine (T) conjugated bile acids: TαMCA, TβMCA, TCA, THCA, TCDCA, TDCA, TUDCA, THDCA, TLCA (Taurolithocholate). Glycine (G) conjugated bile acids: GCA, GHCA, GCDCA, GDCA, GUDCA, GHDCA.

Statistical analysis

Except where indicated, results are presented as scatter plots with overlapping mean ± SD. As specified in the Figure legends, statistical significance was assessed by one-way or two-way ANOVA followed by Bonferroni's multiple comparison post hoc test and, where appropriate, by unpaired Student's t-test. Statistical significance was accepted when $p<0.05$. All statistical analyses were performed using GraphPad Prism v.7.0 (GraphPad Software, San Diego, CA, USA).

4.4 Results

As GLP-2 induces the expression of intestinal BA transporters [269], and enhances bile flow [270], we examined whether BAs, acting through Gpbar1, or GLP-2, acting through the GLP-2R, contributes to the metabolic phenotypes arising in Gcgr-/- mice with markedly increased circulating levels of BA and PGDPs [239,263]. Plasma BA levels were increased in fasted and fed Gcgr-/- mice but not significantly different in Gcgr-/-:Gpbar1-/- mice (Figure 12A). In contrast, plasma BA levels remained elevated but were significantly lower in the fed (but not the fasted) state, in Gcgr-/-:Glp2r-/- mice, relative to levels in Gcgr-/-Glp2r+/+ mice (Figure 12B). Hence GLP-2R controls fed state BA levels in Gcgr-/- mice.

We next examined the potential roles of Gpbar1 and Glp2r in the intestinal and metabolic phenotypes arising in Gcgr-/- mice. Body weight and tibial length were not different in Gcgr-/- mice with loss of Gpbar1 (Figure 13A,B) or Glp2r (Figure 13D,E). Small bowel (SB) mass and length was increased in Gcgr-/- Gpbar+/+ mice but not different in Gcgr-/-:Gpbar1-/- mice (Figure 13C), whereas large bowel (LB) weight and length were similar in Gcgr-/-:Gpbar+/+ vs. Gcgr-/-:Gpbar1-/- mice (Figure 13C). SB weight was increased in Gcgr-/-:Glp2r+/+ mice but not in Gcgr-/-:Glp2r-/- mice (Figure 13F). In contrast, increases in SB length, as well as LB weight and length were not dependent on the presence or absence of the Glp2r (Figure 13F). Hence GLP-2R mediates SB growth in Gcgr-/- mice.

Consistent with favorable metabolic phenotypes described in Gcgr-/- mice [239,264,271] fasted and fed blood glucose levels were lower and plasma GLP-1 levels were markedly elevated in Gcgr-/-:Gpbar1+/+ mice, but not different from levels observed in Gcgr-/-:Gpbar1-/- mice (Figure 13A,B). Similarly, both intraperitoneal and oral glucose tolerance was improved and plasma levels of insulin were increased after glucose challenge in Gcgr-/-:Gpbar1+/+ mice, but

no differences in these parameters were observed following elimination of Gpbar1 (Figure 14C,D).

Despite evidence linking Glp2r to control of glucose homeostasis and insulin sensitivity in mice [259,260], the presence or absence of the Glp2r did not impair the reduction in fed or fasted glycemia, or improvements in glucose tolerance and increases in plasma insulin levels detected in Gcgr-/-:Glp2r+/+ vs. Gcgr-/-:Glp2r-/- mice (Figure 14 E,G-H). Furthermore, although levels of fed BA were lower in Gcgr-/-:Glp2r-/- mice, fasted or fed plasma GLP-1 levels measured as a surrogate for the co-secreted PGDP GLP-2, were not different in Gcgr-/-:Glp2r+/+ vs. Gcgr-/-:Glp2r-/- mice (Figure 14F).

As plasma BA were lower in fed Gcgr-/-:Glp2r-/- mice (Figure 14B), we next examined the profiles of different BAs in plasma vs. the ileum from Gcgr-/-:Glp2r+/+ vs. Gcgr-/-:Glp2r-/- mice. Notably, relative proportions of circulating taurine-conjugated BAs, cholic acid and muricholic acid were increased in Gcgr-/-:Glp2r+/+ but were lower in Gcgr-/-:Glp2r-/- mice (Figure 15A,B and Supplementary Figure 1). In contrast, no appreciable differences were detected in proportions of major BA species in the ileum from Gcgr-/-:Glp2r+/+ vs. Gcgr-/-:Glp2r-/- mice (Supplementary Figures 2 and 3).

To explore the impact of changes in BA in the same mice, we analyzed the relative expression of a panel of BA-regulated genes in liver and ileum. No consistent genotype-dependent differences were detected in hepatic levels of mRNA transcripts for Abcc2, Abcc3, Slc10a1, Abcb11, Nr1h4, Nr0b2, Cyp7a1, Cyp8b1 (Figure 16A). In contrast, hepatic mRNA levels of Slc51b, encoding the membrane-associated bile acid transporter, were elevated in Gcgr-/-:Glp2r+/+ but not in Gcgr-/-:Glp2r-/- mice (Figure 16A). Moreover levels of mRNA transcripts for Abcc2, Abcc3, Slc51a, Slc51b, Nr1h4, Fabp6, and Fgf15 were not different in ileum RNA

from Gcgr-/-:Glp2r+/+ vs. Gcgr-/-:Glp2r-/- mice (Figure 16B), whereas levels of Slc10a2 were elevated in ileum from Gcgr-/-:Glp2r+/+ but not in Gcgr-/-:Glp2r-/- mice. Similarly, although levels of Slc51b and Abcb11 were elevated in liver of Gcgr-/-:Gpbar1+/+ mice and Slc10a2 was increased in ileum, no genotype-dependent differences in expression of these transcripts was detected in liver or ileum from Gcgr-/-:Gpbar1-/- mice (Supplementary Figure 4)

The results of recent studies have demonstrated that the metabolic improvements arising following VSG are attenuated in Nr1h4-/- [152] and Gpbar1-/- mice [254], in a body weight-independent manner [255]. To determine whether the presence or absence of the Glp2r modifies key metabolic outcomes following bariatric surgery, we analyzed body weight and glucose control in high fat diet-fed Glp2r+/+ vs. Glp2r-/- mice after VSG. Body weight, fat mass and lean mass were reduced to a similar extent in Glp2r+/+ vs. Glp2r-/- mice (Figure 17A,B). Similarly, fasting glucose and both oral and intraperitoneal glucose tolerance were improved after VSG, but not different in Glp2r+/+ vs. Glp2r-/- mice (Figure 17C).

4.5 Discussion

The studies reported here were initiated in part to understand the potential relationship between and importance of the simultaneous elevations in BA and PGDPs observed in animal and human studies examining the metabolic consequences of genetic or pharmacological loss of GCGR signaling [239,240,243]. As BA are known to directly enhance PGDP secretion through TGR5, encoded by Gpbar1, localized to the basolateral surface of enteroendocrine L cells [248,249] it is plausible that increased levels of PGDPs may arise in part through the sustained activation of Gpbar1 on L cells. Nevertheless, Gcgr-/-:Gpbar1-/- mice continue to exhibit improvements in glucose homeostasis and maintain increased circulating concentrations of GLP-

1 at levels comparable to those detected in Gcgr-/- mice. These observations reveal that Gpbar1 is not critical for increased PGDP secretion or the principal metabolic phenotypes arising following genetic or pharmacological reduction of glucagon action. Furthermore, despite experimental evidence that BA independently promote intestinal growth [272], the increased bowel mass evident in Gcgr-/- mice was not diminished in Gcgr-/-:Gpbar1-/- mice. It remains possible that some of the metabolic benefit ensuing from elevated BA in the context of diminished or extinguished glucagon action reflects signaling through FXR. Notably, both Gpbar1-/- and Nr1h4-/- mice exhibit independent reductions in acute nutrient-stimulated GLP-1 secretion [273]. Hence the putative independent contribution(s) of FXR to the Gcgr-/- phenotype and the actions of BAs on PGDP secretion in different experimental paradigms requires further study.

The examination of the role of GLP-2 in the phenotypes arising following loss of Gcgr signaling was prompted by observations in animals and humans that GLP-2 levels are increased following partial or complete attenuation of glucagon action [239,240,242]. Although studies of GLP-2 action are often focused on the gut mucosa where it acts to expands enterocyte mass and augment nutrient absorption [238,274], complementary evidence supports a role for central GLP-2 action in the control of energy homeostasis and insulin action. Intracerebroventricular administration of GLP-2 inhibits food intake [275] through GLP-2R signaling within a subset of proopiomelanocortin (POMC) neurons [260]. The anorectic actions of exogenous GLP-2 were abolished in Mcr4-/- mice, whereas deletion of the Glp2r within POMC neurons produced hyperphagia and weight gain [260]. Furthermore, augmentation of central GLP-2 action suppressed hepatic glucose production and enhanced insulin sensitivity, favorable metabolic phenotypes overlapping with those reported in studies of Gcgr-/- mice [264,276]. Nevertheless,

we did not detect differences in body weight, fasting glucose, or glucose tolerance in Gcgr-/-:Glp2r-/- mice, relative to findings in Gcgr-/-:Glp2r+/+ mice, alone. Hence, the GLP-2R does not contribute to the major metabolic phenotypes arising from whole body loss of glucagon action in mice. In contrast, our findings confirm the importance of GLP-2R for the intestinal mucosal adaptation, including increased small bowel weight and length, that arises in Gcgr-/- mice [277]. These findings are consistent with a similar role for GLP-2R in the gut mucosa, actions arising secondarily to stimulation of crypt cell proliferation and increased crypt and villous depth of the small bowel epithelium [266,278].

Our experiments revealed a role for the GLP-2R in the elevation of circulating BAs in Gcgr-/- mice, as BA levels were lower in fed Gcgr-/-:Glp2r-/- compared to Gcgr-/-:Glp2r+/+ mice. Moreover, the relative proportion of individual circulating BA is altered in Gcgr-/-:Glp2r-/- mice. Understanding precisely how GLP-2 controls plasma BA levels will require further analysis, however we did not detect compelling evidence for GLP-2R in control of ileal BA levels in Gcgr-/- mice. Infusion of GLP-2 in neonatal piglets maintained on parenteral nutrition increased liver bile acid content and upregulated hepatic expression of several bile export genes, as well as FXR [279]. GLP-2 also increased the expression of mRNA transcripts encoding the bile acid transport protein (Fabp6) in the distal small intestine of parenterally-fed rats [269]. Nevertheless, our previous analyses did not reveal an acute effect of GLP-2 on hepatic bile flow or ileal uptake and systemic appearance of taurocholic acid in mice [280]. Furthermore, our current studies reveal that with the exception of i) a reduction in the ileal expression of Slc10a2 (encoding the apical sodium dependent bile acid transporter), and ii) decreased hepatic expression of Slc51b (encoding a basolateral bile acid transporter), loss of the Glp2r in the context of Gcgr-/- mice had little effect on BA-regulated gene expression in the intestine or liver.

Hence the putative mechanisms linking GLP-2 action to the control of BA uptake, transport, or enterohepatic recirculation, and the corresponding reduction of circulating BA levels in Gcgr-/-:Glp2r-/- mice, require further investigation.

Metabolic surgery represents a second intervention associated with increased plasma levels of BAs and PGDPs [252]. Indeed, there is considerable interest, based on results of preclinical studies of bariatric surgery in Gpbar1-/- [254,255] and Nr1h4-/- mice [152], in understanding the contributions of BAs to the mechanisms underlying improved glucose homeostasis and weight loss following experimental or clinical metabolic surgery. Similarly, plasma GLP-1 levels are often markedly increased after RYGB and increased, although to a lesser extent, after VSG [252]. These observations have fostered a vigorous debate surrounding the putative contribution(s) of GLP-1 action to the weight loss and improved glucose control evident following metabolic surgery [251–253]. Remarkably, although circulating GLP-2 levels are also considerably elevated after metabolic surgery [281], there has been little attention directed at examining whether GLP-2 receptor signaling contributes to the metabolic improvement after RYGB or VSG.

Our current studies reveal that the GLP-2R is not essential for reduction in glycemia and weight loss, arising after VSG in high fat-fed mice. These findings are surprising given data supporting a role for the GLP-2R in control of food intake, body weight and insulin sensitivity in mice [259,260,275,282]. Nevertheless, the lack of contribution of Glp2r to weight loss and reduced glycemia after VSG in mice is consistent with related findings demonstrating that the Glp1r is not required for the metabolic improvements arising after RYGB or VSG in high fat fed mice [283–285]. Hence, the hypothesis that elevated circulating levels of PGDPs, including

GLP-2, contribute to the improvements in glucose control following glucagon receptor blockade, or metabolic surgery, is not substantiated by the current experimental evidence.

4.6 Conclusions

Our studies have a number of limitations. First, we studied BA biology and GLP-2 action in mice with germ line mutations in the Gcgr, Gpbar1, and Glp2r, and the interpretation of our data may be complicated by unanticipated compensatory adaptations arising in mice with germline gene deletions. Second, Gcgr-/- mice are relatively resistant to development of diabetes and obesity [286], hence the data generated here in non-obese Gcgr-/- mice may not be relevant to findings obtained with transient Gcgr antagonism in more obese or diabetic mice or humans. Furthermore, although plasma levels of PGDPs, including GLP-2, are elevated in mice, rats and humans after VSG [251,252,281], it is possible that GLP-2 levels may be elevated to a greater extent, and the biology of GLP-2R may be more important, in experimental models analyzing the metabolic consequences of RYGB. Surprisingly, despite multiple reports linking GLP-2 to the control of appetite, glucose homeostasis, and insulin sensitivity, our data using two different experimental models characterized by increased levels of PGDPs failed to demonstrate a key role for the GLP-2R in regulation of glucose control or body weight evident after disruption of Gcgr signaling, or following VSG. Similarly, despite the documented role for Gpbar1 for linking BA to control of PGDP secretion, plasma levels of circulating PGDPs were not different after loss of Gpbar1 in Gcgr-/- mice. Nevertheless, our findings reveal a role for the GLP-2R in a) gut adaptation b) the pathophysiological elevations of bile acids arising in fed Gcgr-/- mice and c) the relative proportions of circulating BA in Gcgr-/- mice, Our data, coupled with recent evidence linking GLP-2 to the control of gallbladder emptying [280], support the emergence of a

GLP-2-BA axis, further expanding the complex relationship between BA, enteroendocrine cells, and the actions of the glucagon-like peptides.

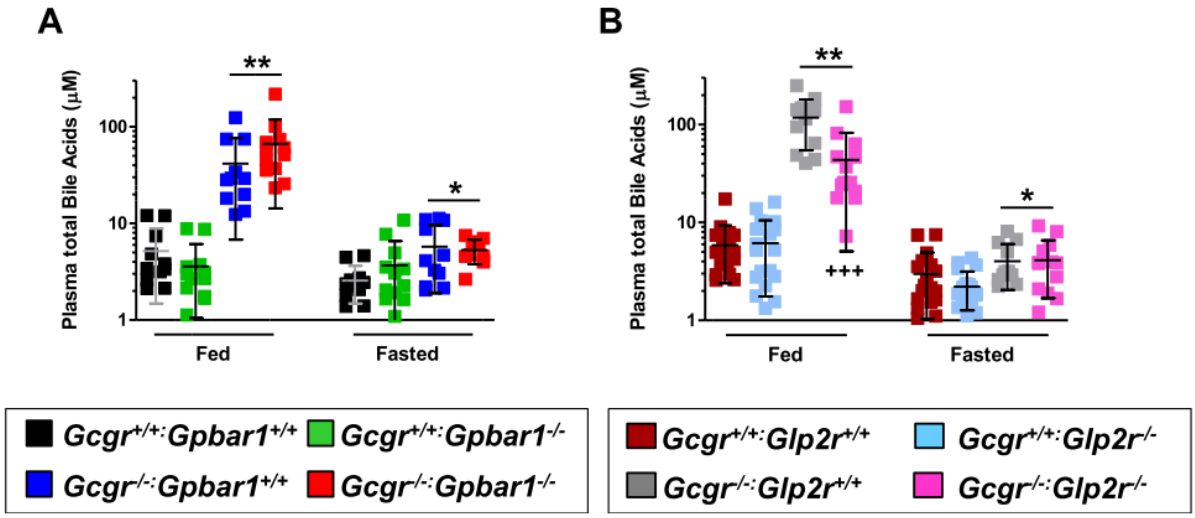

Figure 12: Plasma bile acids in Gcgr-/- and Gpbar-/- mice

Plasma total bile acid levels in Gcgr-/-:Gpbar1-/- (A) and Gcgr-/-:Glp2r-/- (B) double knockout mice and their single knockout and wild-type littermates. Shown are individual data points with overlapping mean±SD (n=11-16 mice per genotype, combined from 2 independent mouse cohorts). Panel A: *p<0.05 & **p<0.01 Gcgr-/-:Gpbar1+/+ & Gcgr-/-:Gpbar1-/- vs Gcgr+/+:Gpbar1+/+& Gcgr+/+:Gpbar1-/-. Panel B: *p<0.05 $Gcgr^{-/-}$:$Glp2r^{+/+}$ & $Gcgr^{-/-}$:$Glp2r^{-/-}$ vs $Gcgr^{+/+}$:$Glp2r^{-/-}$; **p<0.01 $Gcgr^{-/-}$:$Glp2r^{+/+}$ & $Gcgr^{-/-}$:$Glp2r^{-/-}$ vs $Gcgr^{+/+}$:$Glp2r^{+/+}$ & $Gcgr^{+/+}$:$Glp2r^{-/-}$; +++p<0.001 $Gcgr^{-/-}$:$Glp2r^{-/-}$ vs $Gcgr^{-/-}$:$Glp2r^{+/+}$. Statistical significance was assessed by one-way ANOVA followed by Bonferroni's multiple comparison post hoc test.

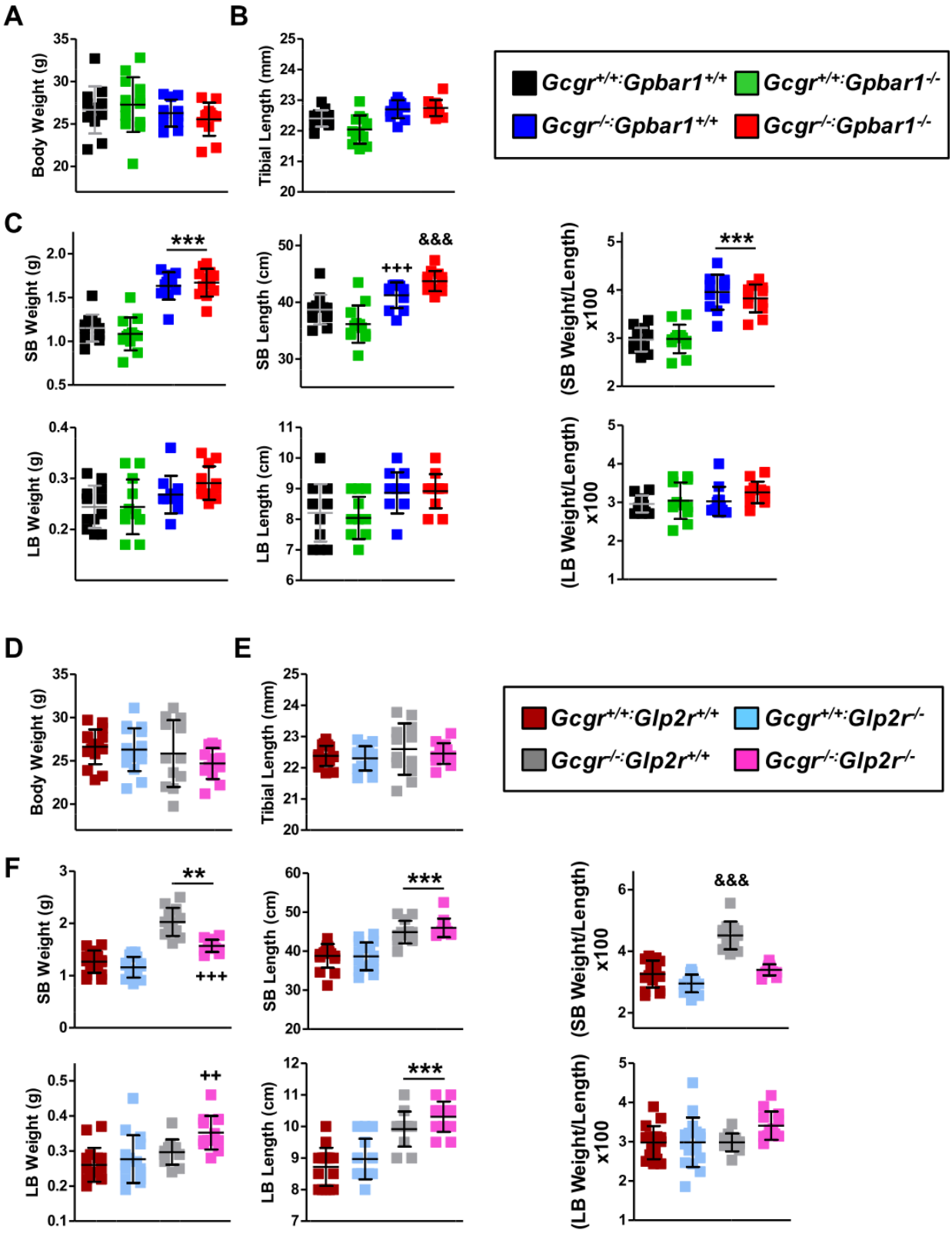
A
B
Body Weight (g)
Tibial Length (mm)
Gcgr+/+:Gpbar1+/+
Gcgr+/+:Gpbar1-/-
Gcgr-/-:Gpbar1+/+
Gcgr-/-:Gpbar1-/-
C
SB Weight (g)
SB Length (cm)
(SB Weight/Length) x100
LB Weight (g)
LB Length (cm)
(LB Weight/Length) x100
***
+++
&&&
D
E
Gcgr+/+:Glp2r+/+
Gcgr+/+:Glp2r-/-
Gcgr-/-:Glp2r+/+
Gcgr-/-:Glp2r-/-
F
**
++

Figure 13: Intestinal morphology in Gcgr-/- and Gpbar-/- mice

Body weight (A & D), tibial length (B & E) and intestinal biometry (C & F) in Gcgr-/-:Gpbar1-/- (A-C) and *Gcgr*$^{-/-}$*:Glp2r*$^{-/-}$ (D-F) double knockout mice and their single knockout and wild-type littermates. Body weight was assessed following overnight fasting 1 week before take down which was performed under random-fed conditions. Shown are individual data points with overlapping mean±SD (n=11-16 mice per genotype, combined from 2 independent mouse cohorts). SB: small bowel, LB: large bowel. Panel C: ***p<0.001 *Gcgr*$^{-/-}$*:Gpbar1*$^{+/+}$ & *Gcgr*$^{-/-}$*:Gpbar1*$^{-/-}$ vs *Gcgr*$^{+/+}$*:Gpbar1*$^{+/+}$ & *Gcgr*$^{+/+}$*:Gpbar1*$^{-/-}$; +++p<0.001 *Gcgr*$^{-/-}$*:Gpbar1*$^{+/+}$ vs *Gcgr*$^{+/+}$*:Gpbar1*$^{-/-}$; &&&p<0.001 *Gcgr*$^{-/-}$*:Gpbar1*$^{-/-}$ vs *Gcgr*$^{+/+}$*:Gpbar1*$^{+/+}$ & *Gcgr*$^{+/+}$*:Gpbar1*$^{-/-}$. Panel F: **p<0.01 & ***p<0.001 *Gcgr*$^{-/-}$*:Glp2r*$^{+/+}$ & *Gcgr*$^{-/-}$*:Glp2r*$^{-/-}$ vs *Gcgr*$^{+/+}$*:Glp2r*$^{+/+}$ & *Gcgr*$^{+/+}$*:Glp2r*$^{-/-}$; ++p<0.01 *Gcgr*$^{-/-}$*:Glp2r*$^{-/-}$ vs *Gcgr*$^{+/+}$*:Glp2r*$^{+/+}$ & *Gcgr*$^{+/+}$*:Glp2r*$^{-/-}$; +++p<0.001 *Gcgr*$^{-/-}$*:Glp2r*$^{-/-}$ vs *Gcgr*$^{-/-}$*:Glp2r*$^{+/+}$; &&&p<0.001 *Gcgr*$^{-/-}$*:Glp2r*$^{+/+}$ vs *Gcgr*$^{+/+}$*:Glp2r*$^{+/+}$, *Gcgr*$^{+/+}$*:Glp2r*$^{-/-}$ & *Gcgr*$^{-/-}$*:Glp2r*$^{-/-}$. Statistical significance was assessed by one-way ANOVA followed by Bonferroni's multiple comparison post hoc test.

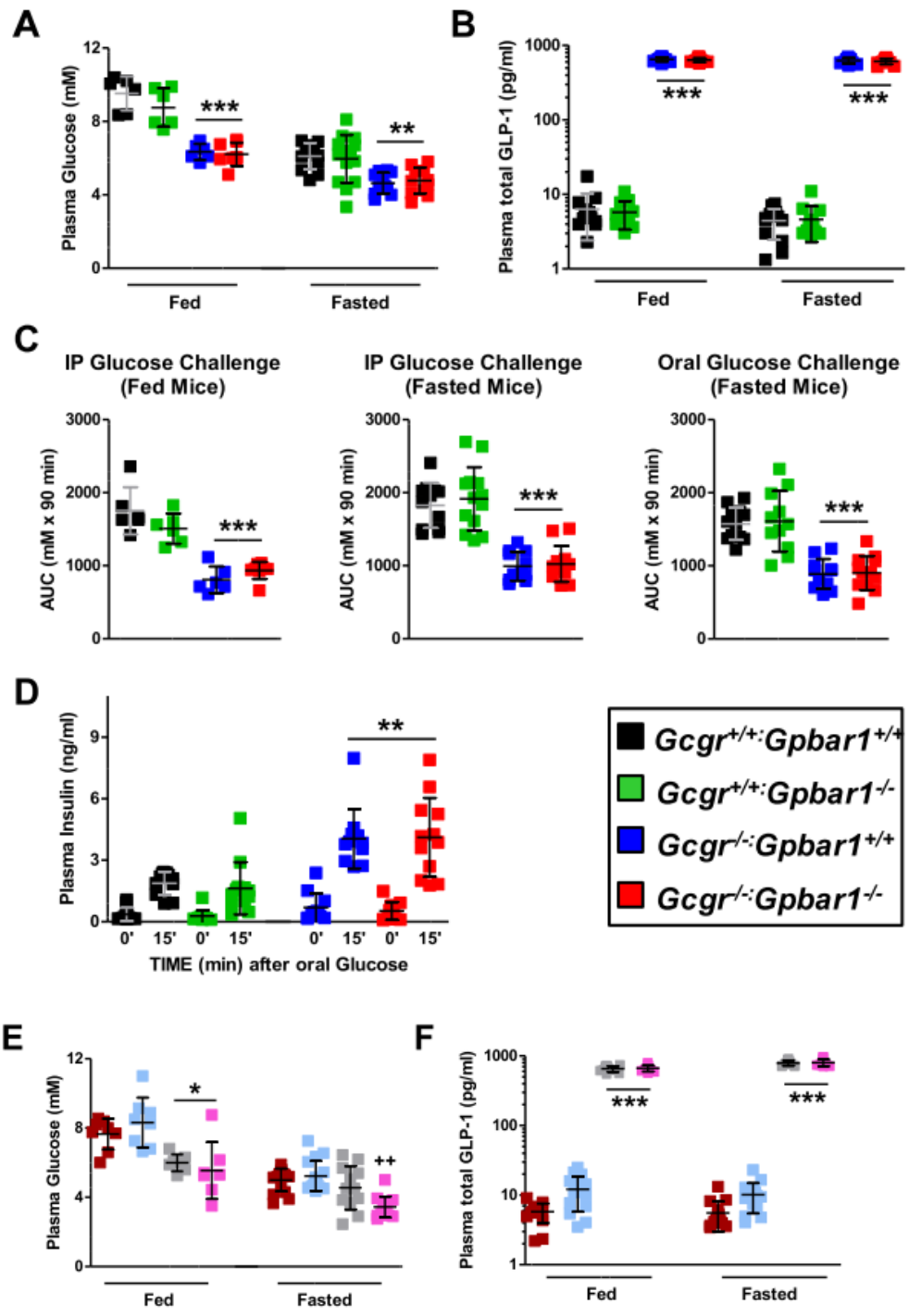
A
Plasma Glucose (mM)
12
8
4
0
***
**
Fed
Fasted
B
Plasma total GLP-1 (pg/ml)
1000
100
10
1
***
***
Fed
Fasted
C
IP Glucose Challenge (Fed Mice)
IP Glucose Challenge (Fasted Mice)
Oral Glucose Challenge (Fasted Mice)
AUC (mM x 90 min)
3000
2000
1000
0
***
***
***
D
Plasma Insulin (ng/ml)
9
6
3
0
**
0' 15' 0' 15' 0' 15' 0' 15'
TIME (min) after oral Glucose
Gcgr+/+:Gpbar1+/+
Gcgr+/+:Gpbar1-/-
Gcgr-/-:Gpbar1+/+
Gcgr-/-:Gpbar1-/-
E
Plasma Glucose (mM)
12
8
4
0
*
++
Fed
Fasted
F
Plasma total GLP-1 (pg/ml)
1000
100
10
1
***
***
Fed
Fasted

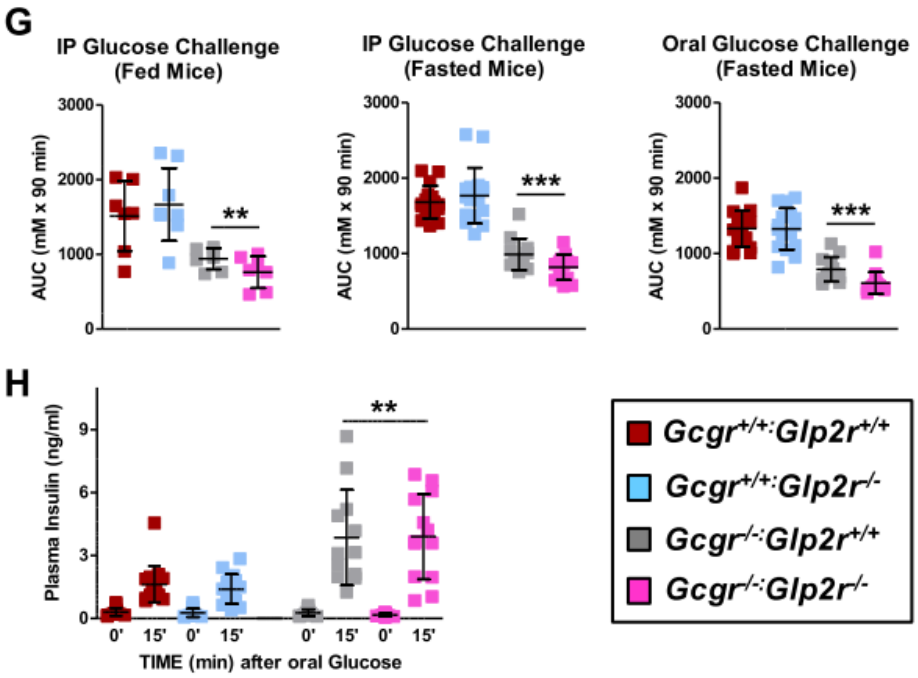

Figure 14: Glucose clearance in Gcgr-/- and Gpbar-/- and GLP2R-/- mice

Fasting and fed glycemia (A & E) and plasma total GLP-1 (B & F), area under the glycemic excursion curves (AUC) (C & G) and plasma insulin at 0 and 15 min after oral glucose challenge in *Gcgr*$^{-/-}$*:Gpbar1*$^{-/-}$ (A-D) and *Gcgr*$^{-/-}$*:Glp2r*$^{-/-}$ (E-H) double knockout mice and their single knockout and wild-type littermates. Glycemic excursion curves were delineated by measuring tail blood glycemia at 0, 15, 30 60 and 90 min after the specified glucose challenge and glucose tolerance determined by calculating the corresponding AUCs. Shown are individual data points with overlapping mean±SD (n=11-16 mice per genotype, combined from 2 independent mouse cohorts, except data from fed mice in panels A, C, E and G wherein n=6-8 per genotype). Panels A, B & C: **p<0.01 & ***p<0.001 *Gcgr*$^{-/-}$*:Gpbar1*$^{+/+}$ & *Gcgr*$^{-/-}$*:Gpbar1*$^{-/-}$ vs *Gcgr*$^{+/+}$*:Gpbar1*$^{+/+}$ & *Gcgr*$^{+/+}$*:Gpbar1*$^{-/-}$. Panels E, F, & G: *p<0.05, **p<0.01 & ***p<0.001 *Gcgr*$^{-/-}$*:Glp2r*$^{+/+}$ & *Gcgr*$^{-/-}$*:Glp2r*$^{-/-}$ vs *Gcgr*$^{+/+}$*:Glp2r*$^{+/+}$ & *Gcgr*$^{+/+}$*:Glp2r*$^{-/-}$; ++p<0.01 *Gcgr*$^{-/-}$*:Glp2r*$^{-/-}$ vs *Gcgr*$^{+/+}$*:Glp2r*$^{+/+}$, *Gcgr*$^{+/+}$*:Glp2r*$^{-/-}$ & *Gcgr*$^{-/-}$*:Glp2r*$^{+/+}$. Panels D & H: insulin levels 15 min after oral glucose were significantly higher than at 0 min (p<0.001) irrespective of the mouse genotype. Panel D: **p<0.01 *Gcgr*$^{-/-}$*:Gpbar1*$^{+/+}$ & *Gcgr*$^{-/-}$*:Gpbar1*$^{-/-}$ insulin at 15 min vs *Gcgr*$^{+/+}$*:Gpbar1*$^{+/+}$ & *Gcgr*$^{+/+}$*:Gpbar1*$^{-/-}$ insulin at 15 min. Panel H: **p<0.01 *Gcgr*$^{-/-}$*:Glp2r*$^{+/+}$ & *Gcgr*$^{-/-}$*:Glp2r*$^{-/-}$ insulin at 15 min vs *Gcgr*$^{+/+}$*:Glp2r*$^{+/+}$ & *Gcgr*$^{+/+}$*:Glp2r*$^{-/-}$ insulin at 15 min Statistical significance was assessed by one-way ANOVA followed by Bonferroni's multiple comparison post hoc test. Unpaired Student's t test was used for the comparisons insulin at 15 min vs insulin at 0 min.

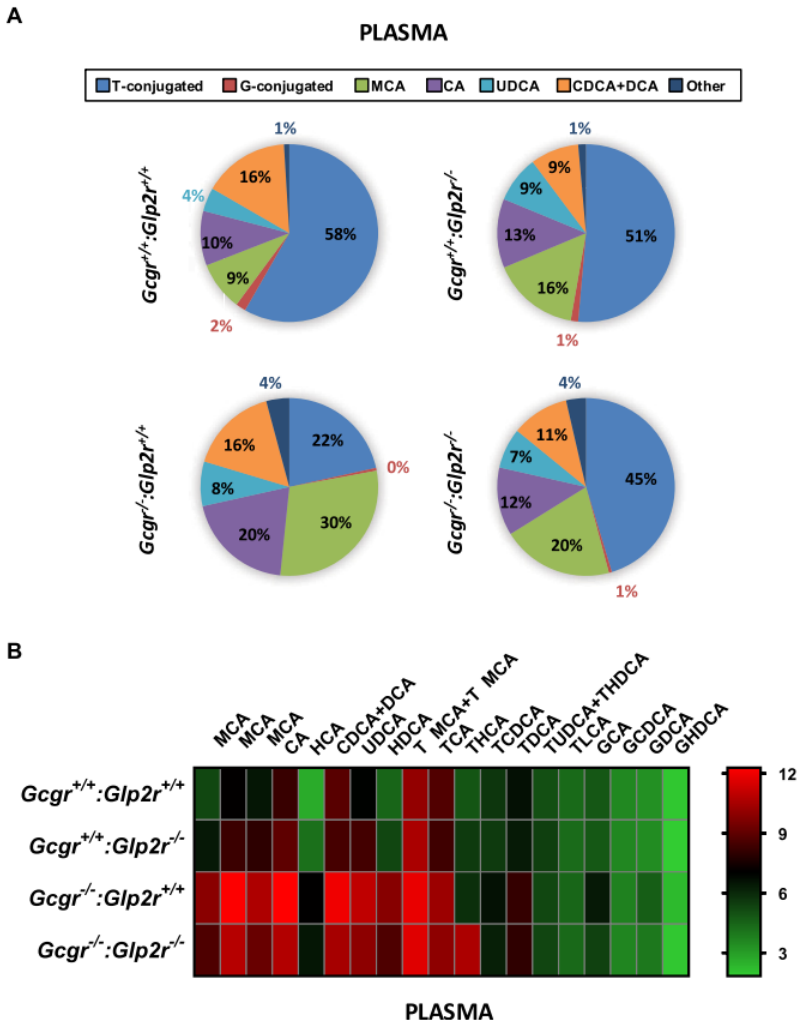

Figure 15: Plasma bile acid profiling and composition in Gcgr-/- and Glp2r-/- mice

Quantitative profiling of bile acid in plasma from random-fed *Gcgr*$^{-/-}$:*Glp2r*$^{-/-}$ double knockout mice and their single knockout and wild-type littermates. Panel A: Bile acid composition analysis representing the percentage of the major BA which contribute to the BA pool in plasma. Total average concentrations of bile acids in plasma were: *Gcgr*$^{+/+}$:*Glp2r*$^{+/+}$ = 2947.6 nM, *Gcgr*$^{+/+}$:*Glp2r*$^{-/-}$ = 4013.2 nM, *Gcgr*$^{-/-}$:*Glp2r*$^{+/+}$=24942.5 nM and *Gcgr*$^{-/-}$:*Glp2*$^{-/-}$ =13513.9 nM. Panel B: Heat map summarizing the concentrations of the different molecular species of BA quantified in plasma samples. The color code represents the log2 transformation of the corresponding mean BA concentration values. For both Panels A & B n=8 mice per genotype, combined from 2 independent mouse cohorts. T-conjugated (taurine-conjugated BA), G-conjugated (Glycine-conjugated BA), MCA (sum of αMCA, βMCA and ωMCA concentrations). Scatter plots for the BA illustrated in the heat map are presented in Supplementary Figure 1.

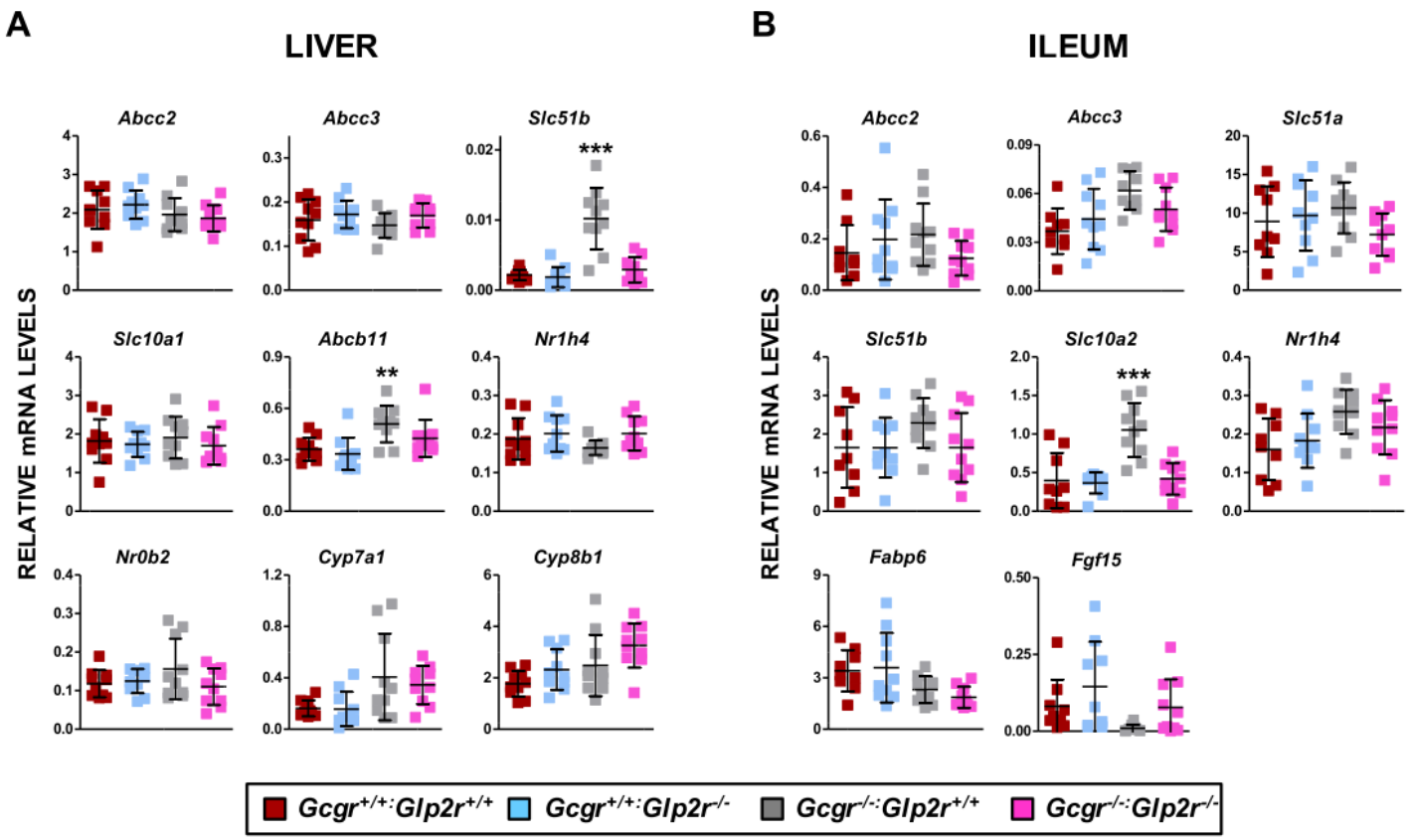

Figure 16: Bile acid metabolism in Gcgr-/- and Glp2r-/-

Expression of genes involved in bile acid metabolism in the liver (A) and ileum (B) of random-fed *Gcgr*$^{-/-}$*:Glp2r*$^{-/-}$ double knockout mice and their single knockout and wild-type littermates. mRNA levels of the indicated genes was assessed by real-time qPCR and normalized to *Ppia* and 18S rRNA levels in liver and ileum, respectively. Shown are individual data points with overlapping mean±SD (n=10 mice per genotype, combined from 2 independent mouse cohorts). Panels A & B: **p<0.01 *Gcgr*$^{-/-}$*:Glp2r*$^{+/+}$vs *Gcgr*$^{+/+}$*:Glp2r*$^{+/+}$ & *Gcgr*$^{+/+}$*:Glp2r*$^{-/-}$; ***p<0.001 *Gcgr*$^{-/-}$*:Glp2r*$^{+/+}$ vs *Gcgr*$^{+/+}$*:Glp2r*$^{+/+}$, *Gcgr*$^{+/+}$*:Glp2r*$^{-/-}$ & *Gcgr*$^{-/-}$*:Glp2r*$^{-/-}$. Statistical significance was assessed by one-way ANOVA followed by Bonferroni's multiple comparison post hoc test.

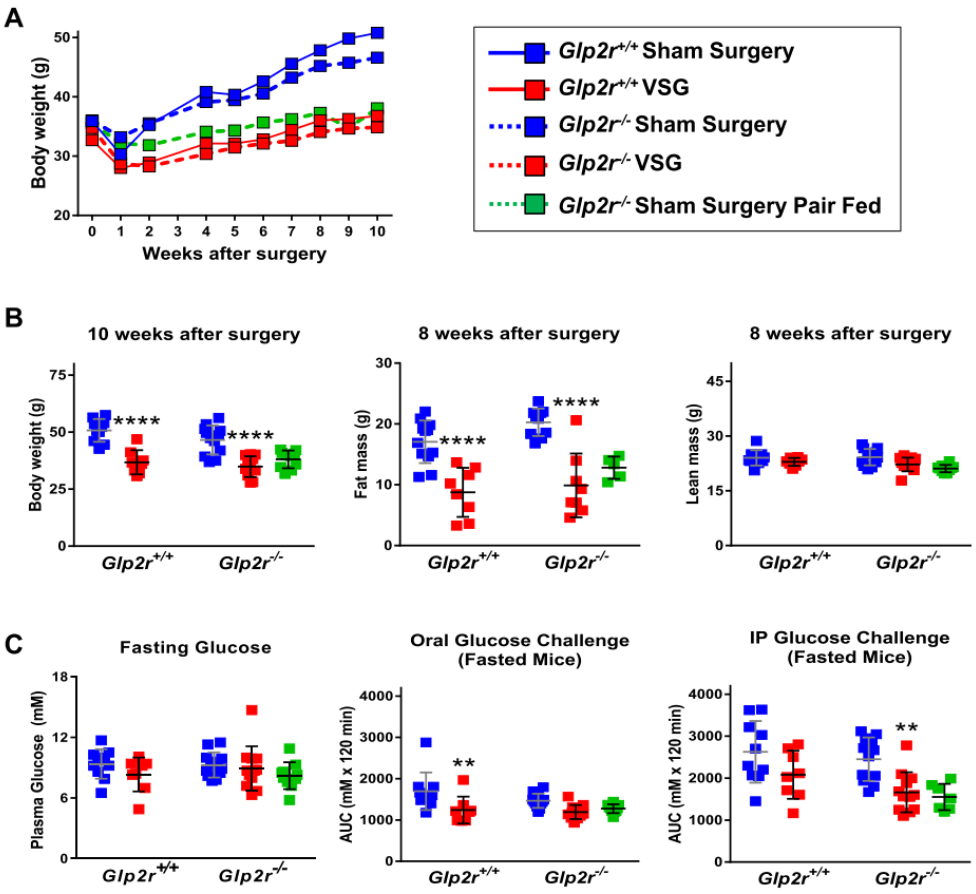

Figure 17: VSG surgery in Glp2r-/- mice

Body weight, body composition (A & B) and glucose tolerance (C) in *Glp2r* wild-type and knockout mice following vertical sleeve gastrectomy (VSG) surgery. Panel A: to facilitate body weight data visualization only means without their associated error bars are shown. The coefficients of variation of the entire data set were ≥ 5.1% and ≤ 17.7% (n=8-12 per group). Illustrated in panel B are individual data points with overlapping means ± SD (n=8-12 mice per group, except n=5 for Sham Surgery Pair Fed fat mass). Panel C: Glycemic excursion curves were delineated by measuring tail blood glycemia at 0, 15, 30, 45, 60 and 120 min after the specified glucose challenge, and glucose tolerance determined by calculating the corresponding AUCs. Shown are individual data points with overlapping mean±SD (n=8-12 mice per group). 2-way ANOVA indicated a not significant interaction term and also a not significant effect of VSG or genotype on "8 weeks after surgery lean mass" (panel B) and "fasting glucose" (panel C). In contrast, 2-way ANOVA indicated a not significant interaction term and a not significant effect of the genotype but a highly significant effect of VSG on "10 week after surgery body weight" ($F_{(1, 37)}$=56.79, p<0.0001), "8 weeks after surgery fat mass" ($F_{(1, 34)}$=56.11, p<0.0001) (panel B), "Oral Glucose Challenge AUC" ($F_{(1, 38)}$=15.84, p<0.0003) and "IP Glucose Challenge AUC" ($F_{(1, 38)}$=13.76, p<0.0007) (panel C). Panels B and C: **p<0.01 & ****p<0.0001 VSG vs Sham Surgery. The Sham Surgery Pair Fed group was not included in the statistical analysis.

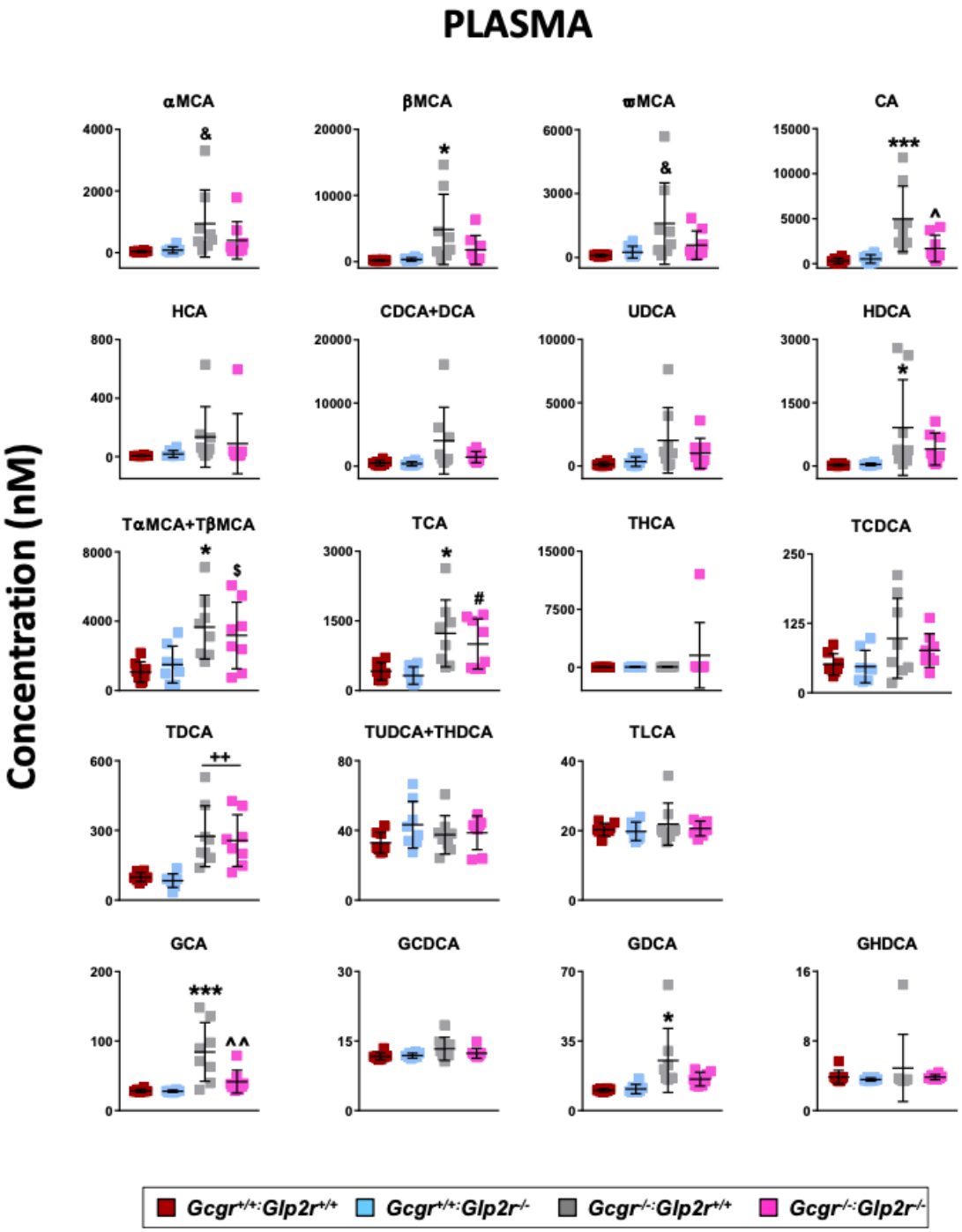

Supplementary Figure 1: Plasma bile acid concentration in Gcgr-/- and Glp2r-/- mice

Bile acid concentrations in plasma from random-fed Gcgr-/-:Glp2r-/- double knockout mice and their single knockout and wild-type littermates. Illustrated are individual data points with overlapping mean±SD (n=8 per genotype combined from 2 independent mouse cohorts). ++p<0.01 Gcgr-/-:Glp2r+/+& Gcgr-/-:Glp2r-/- vs Gcgr+/+:Glp2r+/+ & Gcgr+/+:Glp2r-/-, *p<0.05 Gcgr-/-:Glp2r+/+vs Gcgr+/+:Glp2r+/+ & Gcgr+/+:Glp2r-/-, **p<0.01 Gcgr-/-

:Glp2r+/+vs Gcgr+/+:Glp2r+/+ & Gcgr+/+:Glp2r-/-, ***p<0.001 Gcgr-/-:Glp2r+/+vs Gcgr+/+:Glp2r+/+ & Gcgr+/+:Glp2r-/-, &p<0.05 Gcgr-/-:Glp2r+/+vs Gcgr+/+:Glp2r+/+, ^p<0.05 Gcgr-/-:Glp2r-/- vs Gcgr-/-:Glp2r+/+, ^^p<0.01 Gcgr-/-:Glp2r-/- vs Gcgr-/-:Glp2r+/+, #p<0.05 Gcgr-/-:Glp2r-/- vs Gcgr+/+:Glp2r-/-, $p<0.05 Gcgr-/-:Glp2r-/- vs Gcgr+/+:Glp2r+/+. Statistical significance was assessed by two-way ANOVA followed by Bonferroni's multiple comparison post hoc test.

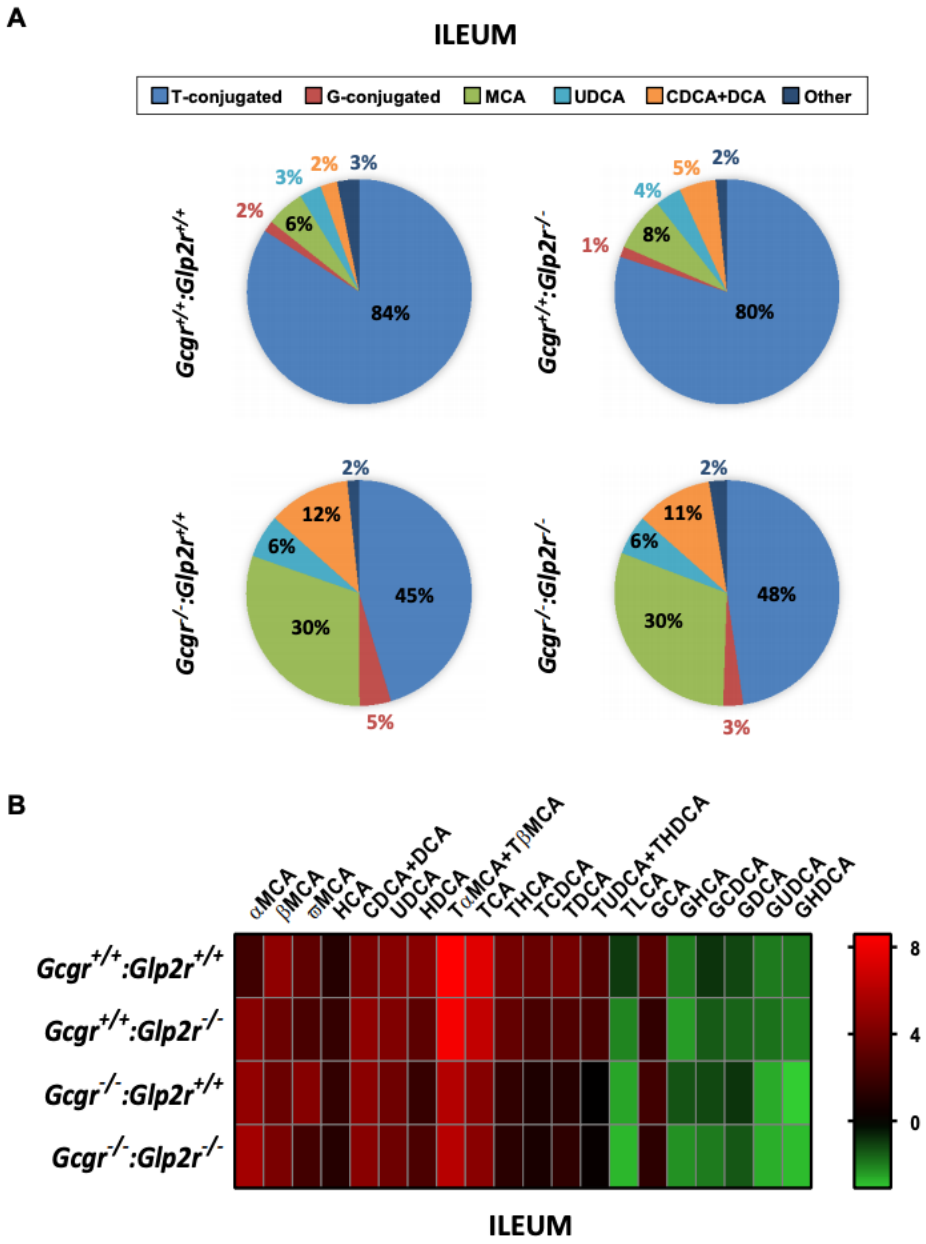

Supplementary Figure 2: Ileum bile acid composition and profiling in Gcgr-/- and Glp2r-/- mice

Quantitative profiling of bile acid in ileum from random-fed Gcgr-/-:Glp2r-/- double knockout mice and their single knockout and wild-type littermates. Panel A: Bile acid composition analysis representing the percentage of the major BA which contribute to the BA pool in ileum. Total average concentrations of bile acids in ileum were: Gcgr+/+:Glp2r+/+ = 737.3 pmol/mg,

Gcgr+/+:Glp2r-/- = 521.9 pmol/mg, Gcgr-/-:Glp2r+/+=208.3 pmol/mg and Gcgr-/-:Glp2r-/-=219.0 pmol/mg. Panel B: Heat map summarizing the concentrations of the different molecular species of BA quantified in ileum samples. The color code represents the log2 transformation of the corresponding mean BA concentration values. For both Panels A & B n=8 mice per genotype, combined from 2 independent mouse cohorts, except for αMCA, βMCA, ωMCA and GHCH wherein n=4-6 per genotype). T-conjugated (taurine-conjugated BA), G-conjugated (Glycine-conjugated BA), MCA (sum of αMCA, βMCA and ωMCA concentrations). Scatter plots for the BA illustrated in the heat map are presented in Supplementary Figure 3.

ILEUM

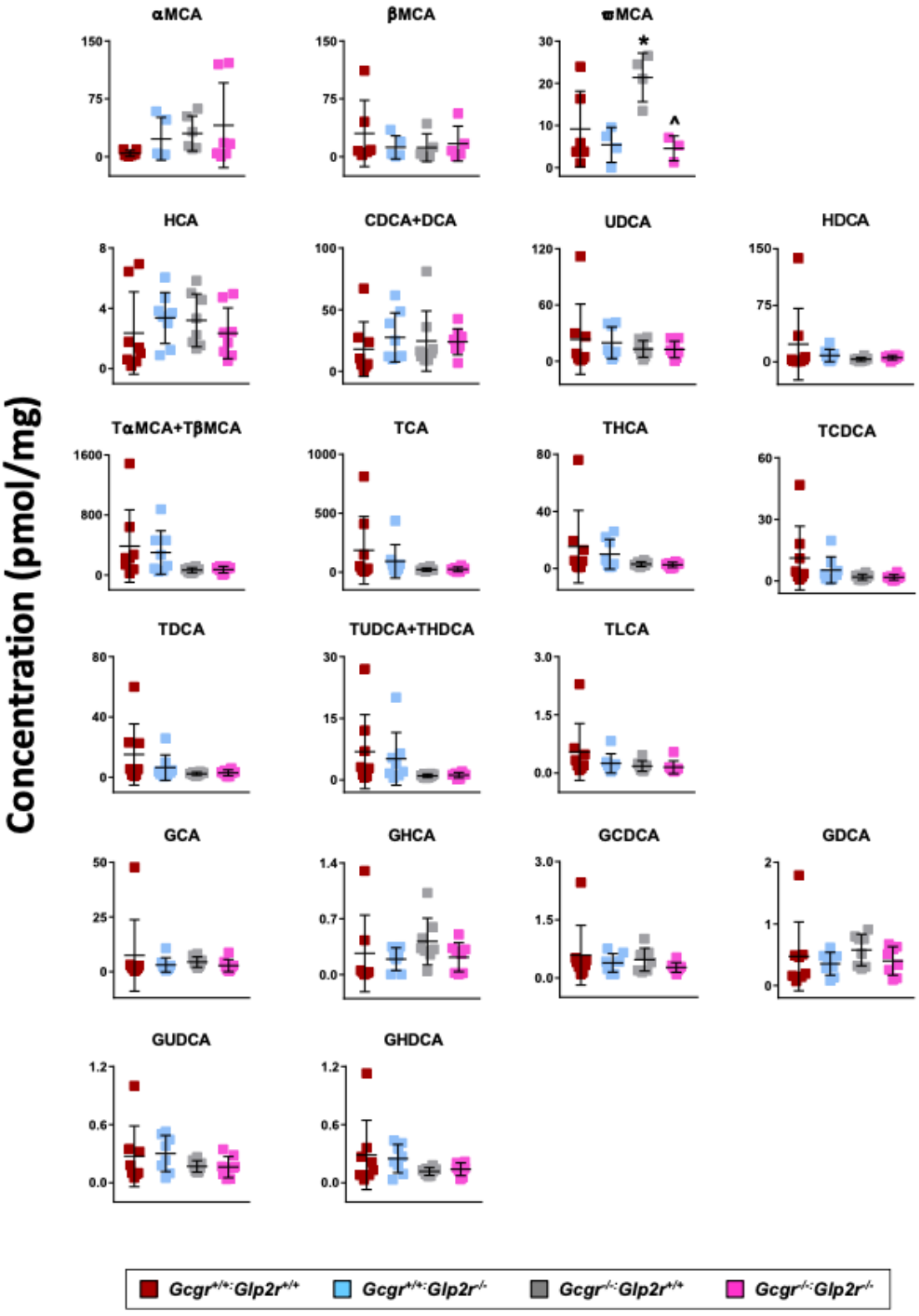
Concentration (pmol/mg)
αMCA
βMCA
ωMCA
HCA
CDCA+DCA
UDCA
HDCA
TαMCA+TβMCA
TCA
THCA
TCDCA
TDCA
TUDCA+THDCA
TLCA
GCA
GHCA
GCDCA
GDCA
GUDCA
GHDCA
Gcgr+/+:Glp2r+/+
Gcgr+/+:Glp2r-/-
Gcgr-/-:Glp2r+/+
Gcgr-/-:Glp2r-/-

Supplementary Figure 3: Ileum bile acid concentrations in Gcgr-/- and Glp2r-/- mice

Bile acid concentrations in ileum from random-fed *Gcgr*$^{-/-}$*:Glp2r*$^{-/-}$ double knockout mice and their single knockout and wild-type littermates. Illustrated are individual data points with overlapping mean±SD (n=8 per genotype combined from 2 independent mouse cohorts, except for αMCA, βMCA, ωMCA and GHCH wherein n=4-6 per genotype). *p<0.05 *Gcgr*$^{+/+}$*:Glp2r*$^{-/-}$ vs *Gcgr*$^{+/+}$*:Glp2r*$^{-/-}$, ^p<0.05 *Gcgr*$^{-/-}$*:Glp2r*$^{-/-}$ vs *Gcgr*$^{-/-}$*:Glp2r*$^{+/+}$. Statistical significance was assessed by two-way ANOVA followed by Bonferroni's multiple comparison post hoc test.

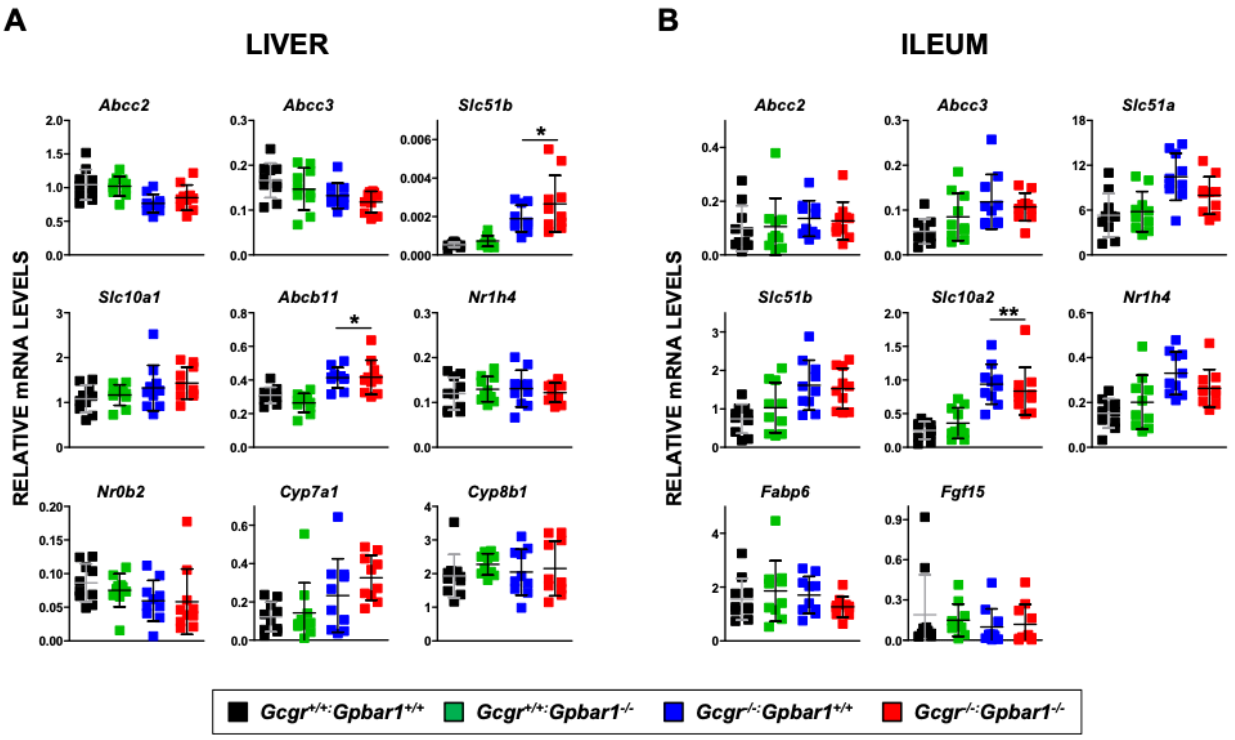

Supplementary Figure 4: Liver and Ileum bile acid metabolism in Gcgr-/- and Gpbar-/- mice

Expression of genes involved in bile acid metabolism in the liver (A) and ileum (B) of random-fed Gcgr-/-:Gpbar1-/- double knockout mice and their single knockout and wild-type littermates. mRNA levels of the indicated genes was assessed by real-time qPCR and normalized to Ppia and 18S rRNA levels in liver and ileum, respectively. Shown are individual data points with overlapping mean±SD (n=10 mice per genotype, combined from 2 independent mouse cohorts). Panels A & B: *p<0.05 & **p<0.01 Gcgr-/-:Gpbar1+/+& Gcgr-/-:Gpbar1-/- vs Gcgr+/+:Gpbar1+/+ & Gcgr+/+:Gpbar1-/-. Statistical significance was assessed by one-way ANOVA followed by Bonferroni's multiple comparison post hoc test.

Chapter 5: Conclusions

5.1 Summary

As obesity continues to rapidly spread, we face a threatening landscape worldwide. Comorbidities place a heavy burden on the quality of life and come with crippling healthcare costs. Amongst these, rates of cancer, associated with additional wasting conditions such as cachexia, have increased. Further, obesity renders individuals more susceptible to cancer and systemic infections which can be accompanied by severe anorexia and mortality. Thus, it becomes increasingly critical to investigate a variety of feeding disorders that currently have insufficient treatments. Pharmacologically regulating feeding through specific neural networks and coordinating central and peripheral responses is a promising strategy to create more accessible treatments for obesity, metabolic and feeding disorders. As there are a multitude of circulating peripheral signals, deciphering which gut mediators and downstream neural networks are important is a complex task.

This body of work is focused on intestinal and peripheral signaling to neural networks, in the context of physical stressors such as obesity and visceral illness. The multifaceted relationship between peripheral signaling molecules and hindbrain neuronal networks to mediate visceral illness in bacterial and fungal infection is explored in Chapters 2 and 3, respectively. Chapter 4 explored the effects gut peptides on weight loss surgery and bile acids.

5.2 Illness anorexia

While under normal conditions endogenous mechanisms to reduce feeding are triggered in response to excess nutrition, they are also induced in pathological states. Sickness behaviors have important purposes to the maintenance of the human species by promoting physiological adaptations and survival. Negative valence and aversive pathways ensure that toxic compounds stray away from repetitively ingesting toxic compounds. Further, anorexia limits caloric intake to promote immune tolerance mechanisms. In infections in which acute anorexia is maladaptive for host health it is hypothesized that the response is protective to transmission of the infection on a population level by reducing fecal shedding [87]. In contrast, forced feeding to counteract nutrient reduction in models of some bacterial infections show a beneficial impact on host mortality. Thus, reduction of energy intake is a common response to illness, initially induced as a protective mechanism, that can become chronic and detrimental.

Using fungal and bacterial infection models, Chapters 2 and 3 show that GDF15 is significantly induced under stress conditions but does not drive anorexia and nausea. Moderate doses of LPS infection are enough to cause a marked elevation of GDF15 levels in circulation. However, GDF15 and GFRAL KO mice display intact anorexia and nausea in response to i.p. LPS. Even at high doses of LPS administration which mimics severe sepsis, GDF15 is not a necessary signaling component as demonstrated by GDF15 KO mice. This effect is similarly true for the fungal infection by DON. Thus, the implications and functions of elevated GDF15 in response to infection remains to be determined. Whether GDF15 contributes to the pathogenicity or recovery from sepsis has been debated. In Chapter 3, we show that GDF15 KO animals do not have altered mortality in response to severe sepsis induced using a sublethal dose of LPS. Interestingly, while the function of elevated GDF15 levels remain elusive, there is potential for

GDF15 to be used as a biomarker of illness severity. A study done in 219 patients showed that serum GDF15 levels at the time of admittance to the ICU correlated with later organ dysfunction, and ultimately mortality over the course of 2 years [57].

5.3 CaSR and DON

The hindbrain represents a critical region to receive gut signals and is home to diverse sets of neuronal populations that are defined by the expression patterns of receptors or peptides. In order to separate the effects of hormone receptor signaling from the neuronal population, we can use inducible diphtheria toxin ablation or tetanus toxin silencing in combination with cell specific cre mice. Expression of diphtheria toxin receptor (DTR) onto specific cell populations allows ablation of DTR expressing neurons exclusively when exposed to diphtheria toxin. In Chapter 3, we crossed mice with cre inducible diphtheria toxin receptor expression with GFRAL cre mice to allow specific ablation of the GFRAL neuronal population. This allowed us to separate the effects of GFRAL signaling from the neurons themselves. Although key signaling regions for GDF15 (AP/NTS and PBN) are highly activated and necessary for the aversive and anorectic effects of DON, we found that GFRAL neurons are not an essential part of the illness inducing circuit. The AP is a likely target of deoxynivalenol, considering the permeable blood brain barrier and the rapid DON entry into the brain. Thus, other neuronal populations are likely required to mediate the effects of DON.

Chapter 3 demonstrates that loss of GDF15/GFRAL signaling does not contribute to feeding or nausea responses to DON. In DON induced fungal infection, a myriad of gut hormones is altered. We tested the necessity of another gut anorectic hormone (GLP-1) and found that it is similarly unnecessary in inducing nausea and food refusal. Further, intestinal

hormones such as PYY and CCK are released rapidly after DON exposure in mice. It is reasonable to hypothesize that these gut hormones contribute to the anorectic effects, as they are both well-known anorectic factors. However, previous studies have shown conflicting results. Moreover, CaSR is present in diverse intestinal cells including intestinal L cells, I cells, and gastric cells, eliciting GLP-1, PYY and CCK and inhibiting ghrelin secretion. This efflux of gut hormones may simply be a byproduct of direct CaSR signaling on enteroendocrine cells that serve a function that has yet to be determined.

Another possibility is that DON is signaling directly though the hindbrain AP /NTS cells onto a population of neurons that have yet to be characterized. CaSR expressed in the brain is widespread and has high expression in the hypothalamus, circumventricular organs and hippocampus. While CaSR has been demonstrated to play a role in neural development and plasticity, its impact on neuronal function is complex [228,229,287]. Heightened or artificial CaSR signaling in humans also leads to nausea. For example, patients experiencing hyperparathyroidism, in which pathological parathyroid hormone release is accompanied by increased calcium uptake and CaSR signaling, present with increased gastrointestinal symptoms such as nausea and loss of appetite. Hyperparathyroidism is sometimes treated with cinacalcet, a CaSR agonist used to suppress PTH levels and thereby reduce body calcium. 30% of patients treated with cinacalcet experience adverse effects of nausea and vomiting, which [288,289]. While GFRAL neurons have a high enrichment of CaSR, they likely represent a fraction of CaSR positive cells in the AP capable of binding DON. Investigating CaSR positive neural populations within the AP /NTS and projections into the PBN would further provide value to understanding the illness neural networks. Deoxynivalenol signaling thus represents a model to

study activation of CaSR positive neurons, some of which are GFRAL cells, and illness networks in the hindbrain.

Further, another hypothesis for DON induced anorexia is inflammatory signaling. Central cytokines such as IL-6 and TNFa, both of which are elevated with DON exposure, may contribute to acute anorexia [106,224,290]. Mouse liver, spleen, intestines hypothalamus and DVC all show increased inflammatory cytokine gene expression [111,290,291]. However, TNF-aR KO and IL-6R KO mice do not show a difference in DON food refusal and nausea compared to WT mice [292,293]. The significance of inflammatory signaling is further complicated by the diversity of responses. Cellular sources of cytokines, various combinations of inflammatory signaling, and severity of signaling produce differing responses, and timing all play a role in disease progression and may be crucial to our understanding of nausea and anorexia. Though there is a clear increase in inflammatory mediators, functional significance for induction of anorexia still needs to be proven.

5.4 GFRAL limitations

Historically, there have been 2 major issues that have limited GDF15/GFRAL research. One is the integrity of commercial GDF15. A common way to study GDF15 actions was to use recombinant GDF15 which is often contaminated with TGFβ [21], which can have off target effects on a variety of receptors that are expressed widely. The use of these compounds have often concluded effects of GDF15 in culture systems that do not contain GFRAL. Secondly, lack of known receptor made it difficult to hone hypotheses around GDF15 signaling. The finding that GFRAL is localized to the AP refuted previous studies using pharmacological experiments in cell cultures in which endogenous GFRAL should not be present [15] . Thus, the source and

purity of GDF15 drugs, the antagonist abilities, all must be taken into consideration when reviewing current GDF15 literature. The last several decades since GDF15 has been discovered has shown a significant increase in research around the pathway, particularly after the identification of GFRAL, research has grown exponentially resulting in several clinical trials.

5.5 Clinical applications

Due to its potent ability to reduce food intake, body weight, and adiposity in mice and non-human primates when exogenously administered, GDF15 has become a strong candidate for obesity therapy. In contrast to the classical satiety hormones that are currently more prevalent in pharmaceuticals (i.e. GLP-1 and PYY analogues), GDF-15 represents a unique factor in mediating weight as a stress induced protein. Further, GDF15/GFRAL can be manipulated in both directions to either induce or reduce feeding in pathological conditions, increasing its utility.

A common challenge to manipulating gut-brain signaling compounds is the limited half-life of endogenous hormones. For GDF15, the half-life is only a mere 3 hrs. Because weight reducing compounds require long term use to show great and sustained effects, pharmacological enhancement of longevity is required. To date, several GDF15 analogs have been made with increased stability by attaching a human serum albumin HSA or constant fragment Fc domain. Recently, Merck pharmaceuticals licensed a once daily GDF15 (NGM386) but quickly dropped the clinical trial after a phase-1 clinical trial showed no benefits on weight loss in overweight and individuals with obesity. While this was disappointing, it may simply reflect the integrity of the compound. NGM is currently testing another long-acting once weekly GDF15 variant NGM395 for weight and fat mass reduction. In contrast, there is great potential for GFRAL antagonists for

pathologies that are associated with devastating anorexia, such as cancer. Pfizer and NGM have a monoclonal antibody against GDF15 (PF-0646860) and GFRAL antagonist (NGM 120) respectively currently in phase 1 clinical trial.

An obvious potential side effect of GDF15 analogs and GFRAL agonists is gastrointestinal malaise. However, despite the capability of GDF15 in mice to elicit aversion responses, there is evidence to suggest that it may be well tolerated in clinical use. For example, GLP1R agonists that are used to improve glucose tolerance in patients with type 2 diabetes initially present with mild nausea but most often do not result in discontinuation of therapy [294]. Most patients who remain on liraglutide treatment, become tolerant to effects of nausea [295]. Additionally, considering the recent discovery that the commonly prescribed drug metformin treatment may harness GDF15 signaling to induce its effect on energy balance, GDF15 analogues and GFRAL agonists may mimic the positive tolerability and safety profile [7]. More pointed data comes from pregnant individuals who exhibit high levels of GDF15 circulating without concurrent vomiting events [74]. It is possible that nausea accompanying drugs targeting the GDF15 and GFRAL neuronal pathway may be elicited transiently, if at all. Thus the larger set of data set suggests that manipulating the GDF15 signaling pathway may be well tolerated in the long-term. However, the induction time course of adverse illness symptoms in humans remains to be clinically tested and will necessitate careful titration of dosage.

While increasing GDF15 signaling is a promising candidate for obesity, we unfortunately do not currently have much data on long term effects of exogenous administration. Infection as a spectrum is a state of immediate stress, and as such, is accompanied by a substantial GDF15 release whose function remains undetermined. Beyond cancer, systemic infection often presents with elevated GDF15 levels concurrent with anorexia, drawing into question whether GDF15

signaling is a key driver of protective or detrimental effects associated visceral illness. Levels of GDF15 are linked to mortality but it is unclear whether it contributes to that mortality. Most data on mortality thus far is correlational and is often associated with disease severity in sepsis, kidney and cardiovascular disease. Therefore, it remains to be investigated how long-term use of GDF15 will impact health, particularly in those prone to cardiovascular and kidney diseases.

Some studies have linked high levels of circulating GDF15 to tissue damage or altered tolerance mechanisms [5]. Reducing physiological tolerance or resistance responses could have direct implications of GDF15 blocking therapies in cancer patients who are susceptible to infections. Although we did not test the impact of increasing GDF15 by overexpression or administration of GDF15 protein, our results in Chapter 2 show no differences in mortality to severe sepsis in mice with or without GDF15. Whether these data translate to humans remains to be determined, but data in mice of bacterial sepsis, in combination with that of metformin and pregnancy nausea supports a promising safety profile.

Moreover, neural circuits that reduce feeding without the risk for nausea represent a highly attractive therapeutic opportunity. Many current mimetic therapeutics to reduce feeding result in some gastrointestinal malaise. Circumventing the illness response of aversion entirely while still eliciting anorexia via hindbrain neurocircuitry would be an ideal target for pharmacological interventions. Although illness is commonly cited as a dysregulated response, one that represents overactivation of the anorectic system, there is evidence to suggest that it is guided by distinct neural pathways from satiety. A key difference is the stimulation of aversion. In satiety, foods ingested during a meal induces reward for future consumption. In contrast, illness responses elicit a long-term learned aversion to ingested toxic substances.

Although the NTS is most well-known for inducing satiety and controlling meal size via nutrient induced gut-brain signaling, hindbrain neurocircuitry controlling illness induced behavior and long-term energy balance is gaining clarity. As such, distinct hindbrain neural circuits that control feeding are being identified. It has been proposed that the NTS to CGRP network represents a generalized emergency "alarm" for diverse threats. However, different threats require different behavioral responses, as in the case of differing effects of immune tolerance mechanisms. Thus, differences in circuitry distinguishing responses to toxic substances, such as viral, bacterial and fungal infections would be interesting. Additionally, it is possible that there are more subset populations of neurons in the PBN that relay diverging signals of illness vs satiety.

There is evidence to suggest that the two illness responses of anorexia and aversion do not completely overlap in NTS neuronal populations. That is, hindbrain networks that control food refusal may be separable from those that elicit aversive. Amongst the dense circuits projecting from the NTS to the PBN, there is some level of heterogeneity. The most recent and pointed data come from a study utilizing salmon calcitonin which results in the reduction feeding and elicits aversion via calcitonin receptors (CALCR). CALCR neurons within the NTS are responsible for reducing feeding without eliciting the aversive response by targeting non-CGRP cells within the PBN. The circuit represents an aversion independent anorectic network distinct from CCK NTS to CGRP PBN neurons which can elicit both anorexia and aversion [296].. Similarly, it is possible that GFRAL neurocircuitry to elicit nausea and anorexia is similarly distinct in subpopulations in the NTS and PBN.

Further, there is some evidence that suggests that NTS neurons implicated in feeding may communicate locally to neighboring cells. Activating CCK neurons within the NTS using CNO

activation of DREADDs induces cFOS in CCK neurons as well as local DBH neurons. Whether local communication within the NTS or within the PBN exists in distinct feeding circuits and whether it leads to any functional differences in anorectic and illness responses is unclear. GFRAL neurons have been shown to colocalize partially with CCK and DBH. The NTS DBH to CGRP circuit has been recently shown to induce anorexia without aversion. Similarly, there may be subpopulations of GFRAL neurons in the AP that elicit distinct effects.

5.6 Concluding remarks

The gut sends a myriad of diverse hormonal and neural signals to hindbrain circuits in order to induce specific feeding behaviors. As such, distinct hindbrain neural circuits that control feeding behaviors are still being elucidated. Further understanding of the gut-brain axis will unquestionably lead to therapeutic development for a wide swath of diseases, including obesity, cachexia, and sepsis. GDF15 and GFRAL neural circuitry represents one such mechanism with considerable potential to manipulate feeding. Deciphering hindbrain neuronal populations within the AP/NTS and PBN with greater granularity will undoubtedly further our understanding of illness associated behaviors in pathological states. It is possible that a combination of gut-brain signaling changes are required to sustain long-term changes. Thus, we can continue to use various bariatric procedures not just as clinical tools, but also as research tools to alter gut-brain signaling.

References

[1] Fairlie, W.D., Moore, A.G., Bauskin, A.R., Russell, P.K., Zhang, H.-P., Breit, S.N., 1999. MIC-1 is a novel TGF-β superfamily cytokine associated with macrophage activation. Journal of Leukocyte Biology 65(1): 2–5, Doi: 10.1002/jlb.65.1.2.

[2] Bootcov, M.R., Bauskin, A.R., Valenzuela, S.M., Moore, A.G., Bansal, M., He, X.Y., et al., 1997. MIC-1, a novel macrophage inhibitory cytokine, is a divergent member of the TGF-β superfamily. Proceedings of the National Academy of Sciences of the United States of America 94(21): 11514–9, Doi: 10.1073/pnas.94.21.11514.

[3] Hsu, J.Y., Crawley, S., Chen, M., Ayupova, D.A., Lindhout, D.A., Higbee, J., et al., 2017. Non-homeostatic body weight regulation through a brainstem-restricted receptor for GDF15. Nature 550(7675): 255–9, Doi: 10.1038/nature24042.

[4] Klein, A.B., Nicolaisen, T.S., Ørtenblad, N., Gejl, K.D., Jensen, R., Fritzen, A.M., et al., n.d. Pharmacological but not physiological GDF15 suppresses feeding and the motivation to exercise Corresponding author, Doi: 10.1101/2020.10.23.352864.

[5] Luan, H.H., Wang, A., Hilliard, B.K., Carvalho, F., Rosen, C.E., Ahasic, A.M., et al., 2019. GDF15 Is an Inflammation-Induced Central Mediator of Tissue Tolerance. Cell 178(5): 1231-1244.e11, Doi: 10.1016/j.cell.2019.07.033.

[6] Xiong, Y., Walker, K., Min, X., Hale, C., Tran, T., Komorowski, R., et al., 2017. Long-acting MIC-1/GDF15 molecules to treat obesity: Evidence from mice to monkeys. Science Translational Medicine 9(412), Doi: 10.1126/scitranslmed.aan8732.

[7] Coll, A.P., Chen, M., Taskar, P., Rimmington, D., Patel, S., Tadross, J.A., et al., 2020. GDF15 mediates the effects of metformin on body weight and energy balance. Nature 578(7795): 444–8, Doi: 10.1038/s41586-019-1911-y.

[8] Patel, S., Alvarez-Guaita, A., Melvin, A., Rimmington, D., Dattilo, A., Miedzybrodzka, E.L., et al., 2019. GDF15 Provides an Endocrine Signal of Nutritional Stress in Mice and Humans. Cell Metabolism 29(3): 707-718.e8, Doi: 10.1016/j.cmet.2018.12.016.

[9] Turco, M.Y., Gardner, L., Kay, R.G., Hamilton, R.S., Prater, M., Hollinshead, M.S., et al., 2018. Trophoblast organoids as a model for maternal–fetal interactions during human placentation. Nature 564(7735): 263–81, Doi: 10.1038/s41586-018-0753-3.

[10] Moore, A.G., Brown, D.A., Fairlie, W.D., Bauskin, A.R., Brown, P.K., Munier, M.L.C., et al., 2000. The Transforming Growth Factor-β Superfamily Cytokine Macrophage Inhibitory Cytokine-1 Is Present in High Concentrations in the Serum of Pregnant Women 1 . The Journal of Clinical Endocrinology & Metabolism 85(12): 4781–8, Doi:

10.1210/jcem.85.12.7007.

[11] Zhang, Y., Jiang, M., Nouraie, M., Roth, M.G., Tabib, T., Winters, S., et al., 2019. GDF15 is an epithelial-derived biomarker of idiopathic pulmonary fibrosis. American Journal of Physiology-Lung Cellular and Molecular Physiology 317(4): L510–21, Doi: 10.1152/ajplung.00062.2019.

[12] Johnen, H., Lin, S., Kuffner, T., Brown, D.A., Tsai, V.W.W., Bauskin, A.R., et al., 2007. Tumor-induced anorexia and weight loss are mediated by the TGF-β superfamily cytokine MIC-1. Nature Medicine 13(11): 1333–40, Doi: 10.1038/nm1677.

[13] Emmerson, P.J., Wang, F., Du, Y., Liu, Q., Pickard, R.T., Gonciarz, M.D., et al., 2017. The metabolic effects of GDF15 are mediated by the orphan receptor GFRAL. Nature Medicine 23(10): 1215–9, Doi: 10.1038/nm.4393.

[14] Yang, L., Chang, C.C., Sun, Z., Madsen, D., Zhu, H., Padkjær, S.B., et al., 2017. GFRAL is the receptor for GDF15 and is required for the anti-obesity effects of the ligand. Nature Medicine 23(10): 1158–66, Doi: 10.1038/nm.4394.

[15] Mullican, S.E., Lin-Schmidt, X., Chin, C.N., Chavez, J.A., Furman, J.L., Armstrong, A.A., et al., 2017. GFRAL is the receptor for GDF15 and the ligand promotes weight loss in mice and nonhuman primates. Nature Medicine 23(10): 1150–7, Doi: 10.1038/nm.4392.

[16] Price, C.J., Hoyda, T.D., Ferguson, A. V., 2008. The area postrema: A brain monitor and integrator of systemic autonomic state. Neuroscientist: 182–94, Doi: 10.1177/1073858407311100.

[17] Bentivoglio, M., Kristensson, K., Rottenberg, M.E., 2018. Circumventricular Organs and Parasite Neurotropism: Neglected Gates to the Brain? Frontiers in Immunology: 2877, Doi: 10.3389/fimmu.2018.02877.

[18] Tansey, M.G., Baloh, R.H., Milbrandt, J., Johnson, E.M., 2000. GFRα-mediated localization of RET to lipid rafts is required for effective downstream signaling, differentiation, and neuronal survival. Neuron 25(3): 611–23, Doi: 10.1016/S0896-6273(00)81064-8.

[19] Heger, J., Schiegnitz, E., von Waldthausen, D., Anwar, M.M., Piper, H.M., Euler, G., 2010. Growth differentiation factor 15 acts anti-apoptotic and pro-hypertrophic in adult cardiomyocytes. Journal of Cellular Physiology 224(1): n/a-n/a, Doi: 10.1002/jcp.22102.

[20] Xu, J., Kimball, T.R., Lorenz, J.N., Brown, D.A., Bauskin, A.R., Klevitsky, R., et al., 2006. GDF15/MIC-1 functions as a protective and antihypertrophic factor released from the myocardium in association with SMAD protein activation. Circulation Research 98(3): 342–50, Doi: 10.1161/01.RES.0000202804.84885.d0.

[21] Olsen, O.E., Skjærvik, A., Størdal, B.F., Sundan, A., Holien, T., 2017. TGF-β contamination of purified recombinant GDF15. PLOS ONE 12(11): e0187349, Doi: 10.1371/journal.pone.0187349.

[22] Tsai, V.W.-W., Macia, L., Feinle-Bisset, C., Manandhar, R., Astrup, A., Raben, A., et al., 2015. Serum Levels of Human MIC-1/GDF15 Vary in a Diurnal Pattern, Do Not Display

a Profile Suggestive of a Satiety Factor and Are Related to BMI. PLOS ONE 10(7): e0133362, Doi: 10.1371/journal.pone.0133362.

[23] Sabatini, P. V., Frikke-Schmidt, H., Arthurs, J., Gordian, D., Patel, A., Adams, J.M., et al., n.d. Gfral-expressing Neurons Suppress Food Intake via Aversive Pathways, Doi: 10.1101/2020.05.11.088773.

[24] Tsai, V.W.-W., Macia, L., Johnen, H., Kuffner, T., Manadhar, R., Jørgensen, S.B., et al., 2013. TGF-b Superfamily Cytokine MIC-1/GDF15 Is a Physiological Appetite and Body Weight Regulator. PLoS ONE 8(2): e55174, Doi: 10.1371/journal.pone.0055174.

[25] Macia, L., Tsai, V.W.W., Nguyen, A.D., Johnen, H., Kuffner, T., Shi, Y.C., et al., 2012. Macrophage inhibitory cytokine 1 (MIC-1/GDF15) decreases food intake, body weight and improves glucose tolerance in mice on normal & obesogenic diets. PLoS ONE 7(4), Doi: 10.1371/journal.pone.0034868.

[26] Chrysovergis, K., Wang, X., Kosak, J., Lee, S.H., Kim, J.S., Foley, J.F., et al., 2014. NAG-1/GDF-15 prevents obesity by increasing thermogenesis, lipolysis and oxidative metabolism. International Journal of Obesity 38(12): 1555–64, Doi: 10.1038/ijo.2014.27.

[27] Baek, S.J., Okazaki, R., Lee, S.H., Martinez, J., Kim, J.S., Yamaguchi, K., et al., 2006. Nonsteroidal Anti-Inflammatory Drug-Activated Gene-1 Over Expression in Transgenic Mice Suppresses Intestinal Neoplasia. Gastroenterology 131(5): 1553–60, Doi: 10.1053/j.gastro.2006.09.015.

[28] Tsai, V.W.W., Macia, L., Johnen, H., Kuffner, T., Manadhar, R., Jørgensen, S.B., et al., 2013. TGF-b Superfamily Cytokine MIC-1/GDF15 Is a Physiological Appetite and Body Weight Regulator. PLoS ONE 8(2), Doi: 10.1371/journal.pone.0055174.

[29] Tsai, V.W.W., Zhang, H.P., Manandhar, R., Schofield, P., Christ, D., Lee-Ng, K.K.M., et al., 2019. GDF15 mediates adiposity resistance through actions on GFRAL neurons in the hindbrain AP/NTS. International Journal of Obesity 43(12): 2370–80, Doi: 10.1038/s41366-019-0365-5.

[30] Tran, T., Yang, J., Gardner, J., Xiong, Y., 2018. GDF15 deficiency promotes high fat diet-induced obesity in mice. PLOS ONE 13(8): e0201584, Doi: 10.1371/journal.pone.0201584.

[31] Gerstein, H.C., Pare, G., Hess, S., Ford, R.J., Sjaarda, J., Raman, K., et al., 2017. Growth differentiation factor 15 as a novel biomarker for metformin. Diabetes Care 40(2): 280–3, Doi: 10.2337/dc16-1682.

[32] Tsai, V.W.-W., Manandhar, R., Jørgensen, S.B., Lee-Ng, K.K.M., Zhang, H.P., Marquis, C.P., et al., 2014. The anorectic actions of the TGFβ cytokine MIC-1/GDF15 require an intact brainstem area postrema and nucleus of the solitary tract. PloS One 9(6): e100370, Doi: 10.1371/journal.pone.0100370.

[33] Frikke-Schmidt, H., Hultman, K., Galaske, J.W., Jørgensen, S.B., Myers, M.G., Seeley, R.J., 2019. GDF15 acts synergistically with liraglutide but is not necessary for the weight loss induced by bariatric surgery in mice. Molecular Metabolism 21: 13–21, Doi: 10.1016/j.molmet.2019.01.003.

[34] Clemmensen, C., Mü, T.D., Woods, S.C., Berthoud, H.-R., Seeley, R.J., Tschö P, M.H., 2017. Gut-Brain Cross-Talk in Metabolic Control, Doi: 10.1016/j.cell.2017.01.025.

[35] Carter, M.E., Soden, M.E., Zweifel, L.S., Palmiter, R.D., 2013. Genetic identification of a neural circuit that suppresses appetite. Nature 503(7474): 111–4, Doi: 10.1038/nature12596.

[36] Borner, T., Arnold, M., Ruud, J., Breit, S.N., Langhans, W., Lutz, T.A., et al., 2017. Anorexia-cachexia syndrome in hepatoma tumour-bearing rats requires the area postrema but not vagal afferents and is paralleled by increased MIC-1/GDF15. Journal of Cachexia, Sarcopenia and Muscle 8(3): 417–27, Doi: 10.1002/jcsm.12169.

[37] Worth, A.A., Shoop, R., Tye, K., Feetham, C.H., D'agostino, G., Dodd, G.T., et al., 2020. The cytokine GDF15 signals through a population of brainstem cholecystokinin neurons to mediate anorectic signalling. ELife 9: 1–19, Doi: 10.7554/eLife.55164.

[38] Roman, C.W., Derkach, V.A., Palmiter, R.D., 2016. Genetically and functionally defined NTS to PBN brain circuits mediating anorexia. Nature Communications 7(1): 1–11, Doi: 10.1038/ncomms11905.

[39] Herbert, H., Moga, M.M., Saper, C.B., 1990. Connections of the parabrachial nucleus with the nucleus of the solitary tract and the medullary reticular formation in the rat. Journal of Comparative Neurology 293(4): 540–80, Doi: 10.1002/cne.902930404.

[40] Palmiter, R.D., 2018. The Parabrachial Nucleus: CGRP Neurons Function as a General Alarm. Trends in Neurosciences: 280–93, Doi: 10.1016/j.tins.2018.03.007.

[41] Essner, R.A., Smith, A.G., Jamnik, A.A., Ryba, A.R., Trutner, Z.D., Carter, M.E., 2017. AgRP neurons can increase food intake during conditions of appetite suppression and inhibit anorexigenic parabrachial neurons. Journal of Neuroscience 37(36): 8678–87, Doi: 10.1523/JNEUROSCI.0798-17.2017.

[42] Wu, Q., Clark, M.S., Palmiter, R.D., 2012. Deciphering a neuronal circuit that mediates appetite. Nature 483(7391): 594–7, Doi: 10.1038/nature10899.

[43] Campos, C.A., Bowen, A.J., Schwartz, M.W., Palmiter, R.D., 2016. Parabrachial CGRP Neurons Control Meal Termination. Cell Metabolism 23(5): 811–20, Doi: 10.1016/j.cmet.2016.04.006.

[44] Palmiter, R.D., 2018. The Parabrachial Nucleus: CGRP Neurons Function as a General Alarm, Doi: 10.1016/j.tins.2018.03.007.

[45] Alhadeff, A.L., Holland, R.A., Zheng, H., Rinaman, L., Grill, H.J., De Jonghe, B.C., 2017. Excitatory hindbrain-forebrain communication is required for cisplatin-induced anorexia and weight loss. Journal of Neuroscience 37(2): 362–70, Doi: 10.1523/JNEUROSCI.2714-16.2016.

[46] Campos, C.A., Bowen, A.J., Han, S., Wisse, B.E., Palmiter, R.D., Schwartz, M.W., 2017. Cancer-induced anorexia and malaise are mediated by CGRP neurons in the parabrachial nucleus. Nature Neuroscience 20(7): 934, Doi: 10.1038/NN.4574.

[47] Han, S., Soleiman, M., Soden, M., Zweifel, L., Palmiter, R.D., 2015. Elucidating an

Affective Pain Circuit that Creates a Threat Memory. Cell 162(2): 363–74, Doi: 10.1016/j.cell.2015.05.057.

[48] Brown, D.A., Ward, R.L., Buckhaults, P., Liu, T., Romans, K.E., Hawkins, N.J., et al., 2003. MIC-1 Serum Level and Genotype: Associations with Progress and Prognosis of Colorectal Carcinoma 1.

[49] Daniels, L.B., Clopton, P., Laughlin, G.A., Maisel, A.S., Barrett-Connor, E., 2011. Growth-differentiation factor-15 is a robust, independent predictor of 11-year mortality risk in community-dwelling older adults: The rancho bernardo study. Circulation 123(19): 2101–10, Doi: 10.1161/CIRCULATIONAHA.110.979740.

[50] Wang, T.J., Wollert, K.C., Larson, M.G., Coglianese, E., McCabe, E.L., Cheng, S., et al., 2012. Prognostic utility of novel biomarkers of cardiovascular stress: The framingham heart study. Circulation 126(13): 1596–604, Doi: 10.1161/CIRCULATIONAHA.112.129437.

[51] Hagström, E., Held, C., Stewart, R.A.H., Aylward, P.E., Budaj, A., Cannon, C.P., et al., 2017. Growth differentiation factor 15 predicts all-cause morbidity and mortality in stable coronary heart disease. Clinical Chemistry 63(1): 325–33, Doi: 10.1373/clinchem.2016.260570.

[52] Kempf, T., Eden, M., Strelau, J., Naguib, M., Willenbockel, C., Tongers, J., et al., 2006. The transforming growth factor-β superfamily member growth-differentiation factor-15 protects the heart from ischemia/reperfusion injury. Circulation Research 98(3): 351–60, Doi: 10.1161/01.RES.0000202805.73038.48.

[53] Wollert, K.C., Kempf, T., Wallentin, L., 2017. Growth differentiation factor 15 as a biomarker in cardiovascular disease. Clinical Chemistry: 140–51, Doi: 10.1373/clinchem.2016.255174.

[54] Eitel, I., Blase, P., Adams, V., Hildebrand, L., Desch, S., Schuler, G., et al., 2011. Growth-differentiation factor 15 as predictor of mortality in acute reperfused ST-elevation myocardial infarction: Insights from cardiovascular magnetic resonance. Heart 97(8): 632–40, Doi: 10.1136/hrt.2010.219543.

[55] Liu, J., Kumar, S., Dolzhenko, E., Alvarado, G.F., Guo, J., Lu, C., et al., 2017. Molecular characterization of the transition from acute to chronic kidney injury following ischemia/reperfusion. JCI Insight 2(18), Doi: 10.1172/jci.insight.94716.

[56] Wiklund, F.E., Bennet, A.M., Magnusson, P.K., Eriksson, U.K., Lindmark, F., Wu, L., et al., 2010. Macrophage inhibitory cytokine-1 (MIC-1/GDF15): a new marker of all-cause mortality. Aging Cell 9(6): 1057–64, Doi: 10.1111/j.1474-9726.2010.00629.x.

[57] Buendgens, L., Yagmur, E., Bruensing, J., Herbers, U., Baeck, C., Trautwein, C., et al., 2017. Growth Differentiation Factor-15 Is a Predictor of Mortality in Critically Ill Patients with Sepsis, Doi: 10.1155/2017/5271203.

[58] Wang, X.B., Jiang, X.R., Yu, X.Y., Wang, L., He, S., Feng, F.Y., et al., 2014. Macrophage inhibitory factor 1 acts as a potential biomarker in patients with esophageal squamous cell carcinoma and is a target for antibody-based therapy. Cancer Science

105(2): 176–85, Doi: 10.1111/cas.12331.

[59] Skipworth, R.J.E., Deans, D.A.C., Tan, B.H.L., Sangster, K., Paterson-Brown, S., Brown, D.A., et al., 2010. Plasma MIC-1 correlates with systemic inflammation but is not an independent determinant of nutritional status or survival in oesophago-gastric cancer. British Journal of Cancer 102(4): 665–72, Doi: 10.1038/sj.bjc.6605532.

[60] Koopmann, J., Buckhaults, P., Brown, D.A., Zahurak, M.L., Sato, N., Fukushima, N., et al., 2004. Serum Macrophage Inhibitory Cytokine 1 as a Marker of Pancreatic and Other Periampullary Cancers. Clinical Cancer Research 10(7): 2386–92, Doi: 10.1158/1078-0432.CCR-03-0165.

[61] Staff, A.C., Bock, A.J., Becker, C., Kempf, T., Wollert, K.C., Davidson, B., 2010. Growth differentiation factor-15 as a prognostic biomarker in ovarian cancer. Gynecologic Oncology 118(3): 237–43, Doi: 10.1016/j.ygyno.2010.05.032.

[62] Brown, D.A., Lindmark, F., Stattin, P., Bälter, K., Adami, H.O., Zheng, S.L., et al., 2009. Macrophage inhibitory cytokine 1: A new prognostic marker in prostate cancer. Clinical Cancer Research 15(21): 6658–64, Doi: 10.1158/1078-0432.CCR-08-3126.

[63] Bauskin, A.R., Brown, D.A., Kuffner, T., Johnen, H., Lou, X.W., Hunter, M., et al., 2006. Role of macrophage inhibitory cytokine-1 in tumorigenesis and diagnosis of cancer. Cancer Research: 4983–6, Doi: 10.1158/0008-5472.CAN-05-4067.

[64] Welsh, J.B., Sapinoso, L.M., Kern, S.G., Brown, D.A., Liu, T., Bauskin, A.R., et al., 2003. Large-scale delineation of secreted protein biomarkers overexpressed in cancer tissue and serum. Proceedings of the National Academy of Sciences of the United States of America 100(6): 3410–5, Doi: 10.1073/pnas.0530278100.

[65] Lerner, L., Hayes, T.G., Tao, N., Krieger, B., Feng, B., Wu, Z., et al., 2015. Plasma growth differentiation factor 15 is associated with weight loss and mortality in cancer patients. Journal of Cachexia, Sarcopenia and Muscle 6(4): 317–24, Doi: 10.1002/jcsm.12033.

[66] Baracos, V.E., Martin, L., Korc, M., Guttridge, D.C., Fearon, K.C.H., 2018. Cancer-associated cachexia. Nature Reviews Disease Primers: 1–18, Doi: 10.1038/nrdp.2017.105.

[67] Argilés, J.M., Busquets, S., Stemmler, B., López-Soriano, F.J., 2014. Cancer cachexia: Understanding the molecular basis. Nature Reviews Cancer: 754–62, Doi: 10.1038/nrc3829.

[68] Suriben, R., Chen, M., Higbee, J., Oeffinger, J., Ventura, R., Li, B., et al., 2020. Antibody-mediated inhibition of GDF15–GFRAL activity reverses cancer cachexia in mice. Nature Medicine 26(8): 1264–70, Doi: 10.1038/s41591-020-0945-x.

[69] Jones, J.E., Cadena, S.M., Gong, C., Wang, X., Chen, Z., Wang, S.X., et al., 2018. Supraphysiologic Administration of GDF11 Induces Cachexia in Part by Upregulating GDF15. Cell Reports 22(6): 1522–30, Doi: 10.1016/j.celrep.2018.01.044.

[70] Lerner, L., Tao, J., Liu, Q., Nicoletti, R., Feng, B., Krieger, B., et al., 2016. MAP3K11/GDF15 axis is a critical driver of cancer cachexia. Journal of Cachexia, Sarcopenia and Muscle 7(4): 467–82, Doi: 10.1002/jcsm.12077.

[71] Worth, A.A., Shoop, R., Tye, K., Feetham, C.H., D'agostino, G., Dodd, G.T., et al., 2020. The cytokine GDF15 signals through a population of brainstem cholecystokinin neurons to mediate anorectic signalling. ELife 9: 1–19, Doi: 10.7554/eLife.55164.

[72] Borner, T., Shaulson, E.D., Ghidewon, M.Y., Barnett, A.B., Horn, C.C., Doyle, R.P., et al., 2020. GDF15 Induces Anorexia through Nausea and Emesis. Cell Metabolism 31(2): 351-362.e5, Doi: 10.1016/j.cmet.2019.12.004.

[73] Sabatini, P. V., Frikke-Schmidt, H., Arthurs, J., Gordian, D., Patel, A., Adams, J.M., et al., 2020. Gfral-expressing Neurons Suppress Food Intake via Aversive Pathways. BioRxiv: 2020.05.11.088773, Doi: 10.1101/2020.05.11.088773.

[74] Petry, C.J., Ong, K.K., Burling, K.A., Barker, P., Goodburn, S.F., Perry, J.R.B., et al., 2018. Associations of vomiting and antiemetic use in pregnancy with levels of circulating GDF15 early in the second trimester: A nested case-control study [version 1; referees: 3 approved]. Wellcome Open Research 3(May): 1–15, Doi: 10.12688/wellcomeopenres.14818.1.

[75] Chan, R.L., Olshan, A.F., Savitz, D.A., Herring, A.H., Daniels, J.L., Peterson, H.B., et al., 2011. Maternal influences on nausea and vomiting in early pregnancy. Maternal and Child Health Journal, Doi: 10.1007/s10995-009-0548-0.

[76] S.M., F., P.W., S., 2000. Morning sickness: A mechanism for protecting mother and embryo. Quarterly Review of Biology.

[77] Verberg, M.F.G., Gillott, D.J., Al-Fardan, N., Grudzinskas, J.G., 2005. Hyperemesis gravidarum, a literature review. Human Reproduction Update, Doi: 10.1093/humupd/dmi021.

[78] Fearon, K., Strasser, F., Anker, S.D., Bosaeus, I., Bruera, E., Fainsinger, R.L., et al., 2011. Definition and classification of cancer cachexia: An international consensus. The Lancet Oncology: 489–95, Doi: 10.1016/S1470-2045(10)70218-7.

[79] Wang, A., Huen, S.C., Luan, H.H., Yu, S., Zhang, C., Gallezot, J.D., et al., 2016. Opposing Effects of Fasting Metabolism on Tissue Tolerance in Bacterial and Viral Inflammation. Cell 166(6): 1512-1525.e12, Doi: 10.1016/j.cell.2016.07.026.

[80] Murray, M.J., Murray, A.B., 1979. Anorexia of infection as a mechanism of host defense. American Journal of Clinical Nutrition 32(3): 593–6, Doi: 10.1093/ajcn/32.3.593.

[81] Ayres, J.S., Schneider, D.S., 2009. The Role of Anorexia in Resistance and Tolerance to Infections in Drosophila. PLoS Biology 7(7): e1000150, Doi: 10.1371/journal.pbio.1000150.

[82] Feingold, K.R., Grunfeld, C., Heuer, J.G., Gupta, A., Cramer, M., Zhang, T., et al., 2012. FGF21 Is Increased by Inflammatory Stimuli and Protects Leptin-Deficient ob/ob Mice from the Toxicity of Sepsis. Endocrinology 153(6): 2689–700, Doi: 10.1210/en.2011-1496.

[83] Martins, R., Carlos, A.R., Braza, F., Thompson, J.A., Bastos-Amador, P., Ramos, S., et al., 2019. Disease Tolerance as an Inherent Component of Immunity. Annual Review of Immunology 37: 405–37, Doi: 10.1146/annurev-immunol-042718-041739.

[84] Soares, M.P., Teixeira, L., Moita, L.F., 2017. Disease tolerance and immunity in host protection against infection. Nature Reviews Immunology: 83–96, Doi: 10.1038/nri.2016.136.

[85] Hart, B.L., 1988. Biological basis of the behavior of sick animals. Neuroscience and Biobehavioral Reviews 12(2): 123–37, Doi: 10.1016/S0149-7634(88)80004-6.

[86] Soares, M.P., Weiss, G., 2015. The Iron age of host–microbe interactions. EMBO Reports 16(11): 1482–500, Doi: 10.15252/embr.201540558.

[87] Rao, S., Schieber, A.M.P., O'Connor, C.P., Leblanc, M., Michel, D., Ayres, J.S., 2017. Pathogen-Mediated Inhibition of Anorexia Promotes Host Survival and Transmission. Cell 168(3): 503-516.e12, Doi: 10.1016/j.cell.2017.01.006.

[88] Ritz, B.W., Aktan, I., Nogusa, S., Gardner, E.M., 2008. Energy restriction impairs natural killer cell function and increases the severity of influenza infection in young adult male C57BL/6 mice. Journal of Nutrition 138(11): 2269–75, Doi: 10.3945/jn.108.093633.

[89] Cecconi, M., Evans, L., Levy, M., Rhodes, A., 2018. Sepsis and septic shock. The Lancet: 75–87, Doi: 10.1016/S0140-6736(18)30696-2.

[90] Wanner, S.P., Yoshida, K., Kulchitsky, V.A., Ivanov, A.I., Kanosue, K., 2013. Lipopolysaccharide-Induced Neuronal Activation in the Paraventricular and Dorsomedial Hypothalamus Depends on Ambient Temperature. PLoS ONE 8(9): 75733, Doi: 10.1371/journal.pone.0075733.

[91] Gakis, G., Mueller, M.H., Hahn, J., Glatzle, J., Grundy, D., Kreis, M.E., 2009. Neuronal activation in the nucleus of the solitary tract following jejunal lipopolysaccharide in the rat. Autonomic Neuroscience: Basic and Clinical 148(1–2): 63–8, Doi: 10.1016/j.autneu.2009.03.004.

[92] Rivest, S., Laflamme, N., 1995. Neuronal Activity and Neuropeptide Gene Transcription in the Brains of Immune-Challenged Rats. Journal of Neuroendocrinology 7(7): 501–25, Doi: 10.1111/j.1365-2826.1995.tb00788.x.

[93] Lin, H.C., Wan, F.J., Kang, B.H., Wu, C.C., Tseng, C.J., 1999. Systemic administration of lipopolysaccharide induces release of nitric oxide and glutamate and c-fos expression in the nucleus tractus solitarii of rats. Hypertension 33(5): 1218–24, Doi: 10.1161/01.HYP.33.5.1218.

[94] Ruiz, S., Vardon-Bounes, F., Merlet-Dupuy, V., Conil, J.-M., Buléon, M., Fourcade, O., et al., 2016. Sepsis modeling in mice: ligation length is a major severity factor in cecal ligation and puncture. Intensive Care Medicine Experimental 4(1): 22, Doi: 10.1186/s40635-016-0096-z.

[95] Li, M., Song, K., Huang, X., Fu, S., Zeng, Q., 2018. GDF-15 prevents LPS and D-galactosamine-induced inflammation and acute liver injury in mice. International Journal of Molecular Medicine 42(3): 1756–64, Doi: 10.3892/ijmm.2018.3747.

[96] Santos, I., Colaço, H.G., Neves-Costa, A., Seixas, E., Velho, T.R., Pedroso, D., et al., 2020. CXCL5-mediated recruitment of neutrophils into the peritoneal cavity of Gdf15-deficient mice protects against abdominal sepsis. Proceedings of the National Academy of

Sciences of the United States of America 117(22), Doi: 10.1073/pnas.1918508117.

[97] Kent, S., Rodriguez, F., Kelley, K.W., Dantzer, R., 1994. Reduction in food and water intake induced by microinjection of interleukin-1β in the ventromedial hypothalamus of the rat. Physiology and Behavior 56(5): 1031–6, Doi: 10.1016/0031-9384(94)90339-5.

[98] Gautron, L., Layé, S., 2010. Neurobiology of inflammation-associated anorexia. Frontiers in Neuroscience 3: 3–59, Doi: 10.3389/neuro.23.003.2009.

[99] Marvel, F.A., Chen, C.C., Badr, N., Gaykema, R.P.A., Goehler, L.E., 2004. Reversible inactivation of the dorsal vagal complex blocks lipopolysaccharide-induced social withdrawal and c-Fos expression in central autonomic nuclei. Brain, Behavior, and Immunity 18(2): 123–34, Doi: 10.1016/j.bbi.2003.09.004.

[100] Liu, Y., Huang, Y., Liu, T., Wu, H., Cui, H., Gautron, L., 2016. Lipopolysacharide rapidly and completely suppresses AgRP neuron-mediated food intake in male mice. Endocrinology 157(6): 2380–92, Doi: 10.1210/en.2015-2081.

[101] Langhans, W., 2020. Signals generating anorexia during acute illness, Doi: 10.1017/S0029665107005587.

[102] Liew, W.P.P., Mohd-Redzwan, S., 2018. Mycotoxin: Its impact on gut health and microbiota. Frontiers in Cellular and Infection Microbiology: 60, Doi: 10.3389/fcimb.2018.00060.

[103] Pitt, J.I., David Miller, J., 2017. A Concise History of Mycotoxin Research. Journal of Agricultural and Food Chemistry 65(33): 7021–33, Doi: 10.1021/acs.jafc.6b04494.

[104] Girardet, C., Bonnet, M.S., Jdir, R., Sadoud, M., Thirion, S., Tardivel, C., et al., 2011. The Food-Contaminant Deoxynivalenol Modifies Eating by Targeting Anorexigenic Neurocircuitry. PLoS ONE 6(10): e26134, Doi: 10.1371/journal.pone.0026134.

[105] Zhou, H.R., Pestka, J.J., 2015. Deoxynivalenol (vomitoxin)-induced cholecystokinin and glucagon-like peptide-1 release in the STC-1 enteroendocrine cell model is mediated by calcium- sensing receptor and transient receptor potential ankyrin-1 channel. Toxicological Sciences 145(2): 407–17, Doi: 10.1093/toxsci/kfv061.

[106] Wu, W., Zhou, H.R., He, K., Pan, X., Sugita-Konishi, Y., Watanabe, M., et al., 2014. Role of cholecystokinin in anorexia induction following oral exposure to the 8-ketotrichothecenes deoxynivalenol, 15-acetyldeoxynivalenol, 3-acetyldeoxynivalenol, Fusarenon X, and nivalenol. Toxicological Sciences 138(2): 278–89, Doi: 10.1093/toxsci/kft335.

[107] Jia, H., Wu, W. Da., Lu, X., Zhang, J., He, C.H., Zhang, H. Bin., 2017. Role of glucagon-like peptide-1 and gastric inhibitory peptide in anorexia induction following oral exposure to the trichothecene mycotoxin deoxynivalenol (vomitoxin). Toxicological Sciences 159(1): 16–24, Doi: 10.1093/toxsci/kfx112.

[108] Wu, W., Sheng, K., Xu, X., Zhang, H., Zhou, G., 2018. Potential roles for glucagon-like peptide-17–36 amide and cholecystokinin in anorectic response to the trichothecene mycotoxin T-2 toxin. Ecotoxicology and Environmental Safety 153(February): 181–7, Doi: 10.1016/j.ecoenv.2018.02.003.

[109] Flannery, B.M., Clark, E.S., Pestka, J.J., 2012. Anorexia induction by the trichothecene deoxynivalenol (vomitoxin) is mediated by the release of the gut satiety hormone peptide YY. Toxicological Sciences 130(2): 289–97, Doi: 10.1093/toxsci/kfs255.

[110] Bettge, K., Kahle, M., Abd El Aziz, M.S., Meier, J.J., Nauck, M.A., 2017. Occurrence of nausea, vomiting and diarrhoea reported as adverse events in clinical trials studying glucagon-like peptide-1 receptor agonists: A systematic analysis of published clinical trials. Diabetes, Obesity and Metabolism 19(3): 336–47, Doi: 10.1111/dom.12824.

[111] Girardet, C., Bonnet, M.S., Jdir, R., Sadoud, M., Thirion, S., Tardivel, C., et al., 2011. Central inflammation and sickness-like behavior induced by the food contaminant deoxynivalenol: A PGE2-independent mechanism. Toxicological Sciences 124(1): 179–91, Doi: 10.1093/toxsci/kfr219.

[112] Phanie Gaigé, S., Bonnet, M.S., Tardivel, C., Pinton, P., Rôme Trouslard, J., Jean, A., et al., n.d. c-Fos immunoreactivity in the pig brain following deoxynivalenol intoxication: Focus on NUCB2/nesfatin-1 expressing neurons, Doi: 10.1016/j.neuro.2012.10.020.

[113] Prelusky, D.B., Hartin, K.E., Trenholm, H.L., 1990. Distribution of deoxynivalenol in cerebral spinal fluid following administration to swine and sheep. Journal of Environmental Science and Health, Part B 25(3): 395–413, Doi: 10.1080/03601239009372697.

[114] Pestka, J.J., Islam, Z., Amuzie, C.J., 2008. Immunochemical assessment of deoxynivalenol tissue distribution following oral exposure in the mouse. Toxicology Letters 178(2): 83–7, Doi: 10.1016/j.toxlet.2008.02.005.

[115] WHO., n.d. Obesity and overweight. https://www.who.int/news-room/fact-sheets/detail/obesity-and-overweight. [accessed December 2, 2020].

[116] Blüher, M., n.d. Obesity: global epidemiology and pathogenesis, Doi: 10.1038/s41574-019-0176-8.

[117] Swinburn, B.A., Sacks, G., Hall, K.D., McPherson, K., Finegood, D.T., Moodie, M.L., et al., 2011. The global obesity pandemic: Shaped by global drivers and local environments. The Lancet: 804–14, Doi: 10.1016/S0140-6736(11)60813-1.

[118] Cawley, J., Meyerhoefer, C., 2012. The medical care costs of obesity: An instrumental variables approach. Journal of Health Economics 31(1): 219–30, Doi: 10.1016/j.jhealeco.2011.10.003.

[119] Fothergill, E., Guo, J., Howard, L., Kerns, J.C., Knuth, N.D., Brychta, R., et al., 2016. Persistent metabolic adaptation 6 years after ???The Biggest Loser??? competition. Obesity 24(8): 1612–9, Doi: 10.1002/oby.21538.

[120] Stefater, M.A., Wilson-Pérez, H.E., Chambers, A.P., Sandoval, D.A., Seeley, R.J., 2012. All bariatric surgeries are not created equal: insights from mechanistic comparisons. Endocrine Reviews 33(4): 595–622, Doi: 10.1210/er.2011-1044.

[121] Schauer, P.R., Kashyap, S.R., Wolski, K., Brethauer, S.A., Kirwan, J.P., Pothier, C.E., et al., 2012. Bariatric Surgery versus Intensive Medical Therapy in Obese Patients with Diabetes. New England Journal of Medicine 366(17): 1567–76, Doi:

10.1056/nejmoa1200225.

[122] Sjöström, L., 2013. Review of the key results from the Swedish Obese Subjects (SOS) trial - a prospective controlled intervention study of bariatric surgery. Journal of Internal Medicine: 219–34, Doi: 10.1111/joim.12012.

[123] 2018. Type 2 Diabetes and Metabolic Surgery | ASMBS. ASMBS. https://asmbs.org/resources/type-2-diabetes-and-metabolic-surgery-fact-sheet. [accessed November 6, 2020].

[124] Courcoulas, A.P., Belle, S.H., Neiberg, R.H., Pierson, S.K., Eagleton, J.K., Kalarchian, M.A., et al., 2015. Three-year outcomes of bariatric surgery vs lifestyle intervention for type 2 diabetes mellitus treatment a randomized clinical trial. JAMA Surgery 150(10): 931–40, Doi: 10.1001/jamasurg.2015.1534.

[125] Sjöström, L., Narbro, K., Sjöström, C.D., Karason, K., Larsson, B., Wedel, H., et al., 2007. Effects of Bariatric Surgery on Mortality in Swedish Obese Subjects. New England Journal of Medicine 357(8): 741–52, Doi: 10.1056/nejmoa066254.

[126] Adams, T.D., Gress, R.E., Smith, S.C., Halverson, R.C., Simper, S.C., Rosamond, W.D., et al., 2007. Long-Term Mortality after Gastric Bypass Surgery. New England Journal of Medicine 357(8): 753–61, Doi: 10.1056/nejmoa066603.

[127] Grayson, B.E., Schneider, K.M., Woods, S.C., Seeley, R.J., n.d. Improved Rodent Maternal Metabolism But Reduced Intrauterine Growth After Vertical Sleeve Gastrectomy, Doi: 10.1126/scitranslmed.3006505.

[128] Stefater, M.A., Pérez-Tilve, D., Chambers, A.P., Wilson-Pérez, H.E., Sandoval, D.A., Berger, J., et al., 2010. Sleeve gastrectomy induces loss of weight and fat mass in obese rats, but does not affect leptin sensitivity. Gastroenterology 138(7): 2426–36, 2436.e1-3, Doi: 10.1053/j.gastro.2010.02.059.

[129] 2018. Metabolic and Bariatric Surgery Fact Sheet | ASMBS. Asmbs. https://asmbs.org/resources/metabolic-and-bariatric-surgery. [accessed November 6, 2020].

[130] Phillips, B.T., Shikora, S.A., 2018. The history of metabolic and bariatric surgery: Development of standards for patient safety and efficacy. Metabolism: Clinical and Experimental: 97–107, Doi: 10.1016/j.metabol.2017.12.010.

[131] Campbell, J.E., Drucker, D.J., 2013. Pharmacology, physiology, and mechanisms of incretin hormone action. Cell Metabolism: 819–37, Doi: 10.1016/j.cmet.2013.04.008.

[132] Cavin, J.B., Couvelard, A., Lebtahi, R., Ducroc, R., Arapis, K., Voitellier, E., et al., 2016. Differences in Alimentary Glucose Absorption and Intestinal Disposal of Blood Glucose after Roux-en-Y Gastric Bypass vs Sleeve Gastrectomy. Gastroenterology 150(2): 454-464.e9, Doi: 10.1053/j.gastro.2015.10.009.

[133] Laferrère, B., Teixeira, J., McGinty, J., Tran, H., Egger, J.R., Colarusso, A., et al., 2008. Effect of Weight Loss by Gastric Bypass Surgery Versus Hypocaloric Diet on Glucose and Incretin Levels in Patients with Type 2 Diabetes. The Journal of Clinical Endocrinology & Metabolism 93(7): 2479–85, Doi: 10.1210/jc.2007-2851.

[134] Secher, A., Jelsing, J., Baquero, A.F., Hecksher-Sørensen, J., Cowley, M.A., Dalbøge, L.S., et al., 2014. The arcuate nucleus mediates GLP-1 receptor agonist liraglutide-dependent weight loss. Journal of Clinical Investigation 124(10): 4473–88, Doi: 10.1172/JCI75276.

[135] Wilson-Pérez, H.E., Chambers, A.P., Ryan, K.K., Li, B., Sandoval, D.A., Stoffers, D., et al., 2013. Vertical sleeve gastrectomy is effective in two genetic mouse models of glucagon-like Peptide 1 receptor deficiency. Diabetes 62(7): 2380–5, Doi: 10.2337/db12-1498.

[136] Bjerknes, M., Cheng, H., 2001. Modulation of specific intestinal epithelial progenitors by enteric neurons. Proceedings of the National Academy of Sciences of the United States of America 98(22): 12497–502, Doi: 10.1073/pnas.211278098.

[137] McDonagh, S.C., Lee, J., Izzo, A., Brubaker, P.L., 2007. Role of glial cell-line derived neurotropic factor family receptor α2 in the actions of the glucagon-like peptides on the murine intestine. American Journal of Physiology-Gastrointestinal and Liver Physiology 293(2): G461–8, Doi: 10.1152/ajpgi.00424.2006.

[138] Tappenden, K.A., Edelman, J., Joelsson, B., 2013. Teduglutide enhances structural adaptation of the small intestinal mucosa in patients with short bowel syndrome. Journal of Clinical Gastroenterology 47(7): 602–7, Doi: 10.1097/MCG.0b013e3182828f57.

[139] Jeppesen, P.B., 2013. Teduglutide for the treatment of short bowel syndrome. Drugs of Today 49(10): 599–614, Doi: 10.1358/dot.2013.49.10.2017025.

[140] Le Roux, C.W., Borg, C., Wallis, K., Vincent, R.P., Bueter, M., Goodlad, R., et al., 2010. Gut hypertrophy after gastric bypass is associated with increased glucagon-like peptide 2 and intestinal crypt cell proliferation. Annals of Surgery 252(1): 50–6, Doi: 10.1097/SLA.0b013e3181d3d21f.

[141] Meek, C.L., Lewis, H.B., Reimann, F., Gribble, F.M., Park, A.J., 2016. The effect of bariatric surgery on gastrointestinal and pancreatic peptide hormones. Peptides: 28–37, Doi: 10.1016/j.peptides.2015.08.013.

[142] Lovshin, J., Estall, J., Yusta, B., Brown, T.J., Drucker, D.J., 2001. Glucagon-like Peptide (GLP)-2 Action in the Murine Central Nervous System is Enhanced by Elimination of GLP-1 Receptor Signaling. Journal of Biological Chemistry 276(24): 21489–99, Doi: 10.1074/jbc.M009382200.

[143] Li, J. V., Ashrafian, H., Bueter, M., Kinross, J., Sands, C., le Roux, C.W., et al., 2011. Metabolic surgery profoundly influences gut microbial-host metabolic cross-talk. Gut 60(9): 1214–23, Doi: 10.1136/gut.2010.234708.

[144] Zhang, H., DiBaise, J.K., Zuccolo, a., Kudrna, D., Braidotti, M., Yu, Y., et al., 2009. Human gut microbiota in obesity and after gastric bypass. Proc Natl Acad Sci U S A 106(7): 2365–70, Doi: 10.1073/pnas.0812600106.

[145] Liou, A.P., Paziuk, M., Luevano, J.-M., Machineni, S., Turnbaugh, P.J., Kaplan, L.M., 2013. Conserved shifts in the gut microbiota due to gastric bypass reduce host weight and adiposity. Science Translational Medicine 5(178): 178ra41, Doi:

10.1126/scitranslmed.3005687.

[146] Vrieze, A., Van Nood, E., Holleman, F., Salojärvi, J., Kootte, R.S., Bartelsman, J.F.W.M., et al., 2012. Transfer of intestinal microbiota from lean donors increases insulin sensitivity in individuals with metabolic syndrome. Gastroenterology 143(4): 913-6.e7, Doi: 10.1053/j.gastro.2012.06.031.

[147] Hemarajata, P., Versalovic, J., 2013. Effects of probiotics on gut microbiota: mechanisms of intestinal immunomodulation and neuromodulation. Therapeutic Advances in Gastroenterology 6(1): 39–51, Doi: 10.1177/1756283X12459294.

[148] Gribble, F.M., Reimann, F., 2019. Function and mechanisms of enteroendocrine cells and gut hormones in metabolism. Nature Reviews Endocrinology: 226–37, Doi: 10.1038/s41574-019-0168-8.

[149] Chiu, C.-C., Ching, Y.-H., Wang, Y.-C., Liu, J.-Y., Li, Y.-P., Huang, Y.-T., et al., 2014. Monocolonization of germ-free mice with Bacteroides fragilis protects against dextran sulfate sodium-induced acute colitis. BioMed Research International 2014: 675786, Doi: 10.1155/2014/675786.

[150] Frank, D.N., St Amand, A.L., Feldman, R.A., Boedeker, E.C., Harpaz, N., Pace, N.R., 2007. Molecular-phylogenetic characterization of microbial community imbalances in human inflammatory bowel diseases. Proceedings of the National Academy of Sciences of the United States of America 104(34): 13780–5, Doi: 10.1073/pnas.0706625104.

[151] Qin, J., Li, R., Raes, J., Arumugam, M., Burgdorf, K.S., Manichanh, C., et al., 2010. A human gut microbial gene catalogue established by metagenomic sequencing : Article : Nature. Nature 464(7285): 59–65, Doi: 10.1038/nature08821.

[152] Ryan, K.K., Tremaroli, V., Clemmensen, C., Kovatcheva-Datchary, P., Myronovych, A., Karns, R., et al., 2014. FXR is a molecular target for the effects of vertical sleeve gastrectomy. Nature 509(7499): 183–8, Doi: 10.1038/nature13135.

[153] Kohli, R., Setchell, K.D.R., Kirby, M., Myronovych, A., Ryan, K.K., Ibrahim, S.H., et al., 2013. A surgical model in male obese rats uncovers protective effects of bile acids post-bariatric surgery. Endocrinology 154(7): 2341–51, Doi: 10.1210/en.2012-2069.

[154] Kerr, T.A., Saeki, S., Schneider, M., Schaefer, K., Berdy, S., Redder, T., et al., 2002. Loss of Nuclear Receptor SHP Impairs but Does Not Eliminate Negative Feedback Regulation of Bile Acid Synthesis. Developmental Cell 2(6): 713–20, Doi: 10.1016/S1534-5807(02)00154-5.

[155] Sayin, S.I., Wahlström, A., Felin, J., Jäntti, S., Marschall, H.-U., Bamberg, K., et al., 2013. Gut microbiota regulates bile acid metabolism by reducing the levels of tauro-beta-muricholic acid, a naturally occurring FXR antagonist. Cell Metabolism 17(2): 225–35, Doi: 10.1016/j.cmet.2013.01.003.

[156] Fu, L., John, L.M., Adams, S.H., Yu, X.X., Tomlinson, E., Renz, M., et al., 2004. Fibroblast growth factor 19 increases metabolic rate and reverses dietary and leptin-deficient diabetes. Endocrinology 145(6): 2594–603, Doi: 10.1210/en.2003-1671.

[157] Ryan, K.K., Kohli, R., Gutierrez-Aguilar, R., Gaitonde, S.G., Woods, S.C., Seeley, R.J.,

2013. Fibroblast growth factor-19 action in the brain reduces food intake and body weight and improves glucose tolerance in male rats. Endocrinology 154(1): 9–15, Doi: 10.1210/en.2012-1891.

[158] Jansen, P.L.M., Van Werven, J., Aarts, E., Berends, F., Janssen, I., Stoker, J., et al., 2011. Alterations of hormonally active fibroblast growth factors after Roux-en-Y gastric bypass surgery. Digestive Diseases 29(1): 48–51, Doi: 10.1159/000324128.

[159] Seeley, R.J., Chambers, A.P., Sandoval, D.A., 2015. The Role of Gut Adaptation in the Potent Effects of Multiple Bariatric Surgeries on Obesity and Diabetes. Cell Metabolism: 1–10, Doi: 10.1016/j.cmet.2015.01.001.

[160] Patti, M.-E., Houten, S.M., Bianco, A.C., Bernier, R., Larsen, P.R., Holst, J.J., et al., 2009. Serum bile acids are higher in humans with prior gastric bypass: potential contribution to improved glucose and lipid metabolism. Obesity (Silver Spring, Md.) 17(9): 1671–7, Doi: 10.1038/oby.2009.102.

[161] Cortez, L.M., Campeau, J., Norman, G., Kalayil, M., Van der Merwe, J., McKenzie, D., et al., 2015. Bile Acids Reduce Prion Conversion, Reduce Neuronal Loss, and Prolong Male Survival in Models of Prion Disease. Journal of Virology 89(15): 7660–72, Doi: 10.1128/JVI.01165-15.

[162] Nunes, A.F., Amaral, J.D., Lo, A.C., Fonseca, M.B., Viana, R.J.S., Callaerts-Vegh, Z., et al., 2012. TUDCA, a bile acid, attenuates amyloid precursor protein processing and amyloid-β deposition in APP/PS1 mice. Molecular Neurobiology 45(3): 440–54, Doi: 10.1007/s12035-012-8256-y.

[163] Keene, C.D., Rodrigues, C.M.P., Eich, T., Chhabra, M.S., Steer, C.J., Low, W.C., 2002. Tauroursodeoxycholic acid, a bile acid, is neuroprotective in a transgenic animal model of Huntington's disease. Proceedings of the National Academy of Sciences of the United States of America 99(16): 10671–6, Doi: 10.1073/pnas.162362299.

[164] Lockhart, S.M., Saudek, V., O'Rahilly, S., 2020. GDF15: A Hormone Conveying Somatic Distress to the Brain. Endocrine Reviews 41(4): 610, Doi: 10.1210/endrev/bnaa007.

[165] Zhang, Y., Proenca, R., Maffei, M., Barone, M., Leopold, L., Friedman, J.M., 1994. Positional cloning of the mouse obese gene and its human homologue. Nature 372(6505): 425–32, Doi: 10.1038/372425a0.

[166] Allison, M.B., Patterson, C.M., Krashes, M.J., Lowell, B.B., Myers, M.G., Olson, D.P., 2015. TRAP-seq defines markers for novel populations of hypothalamic and brainstem LepRb neurons. Molecular Metabolism 4(4): 299–309, Doi: 10.1016/j.molmet.2015.01.012.

[167] Clément, K., Vaisse, C., Lahlou, N., Cabrol, S., Pelloux, V., Cassuto, D., et al., 1998. A mutation in the human leptin receptor gene causes obesity and pituitary dysfunction. Nature 392(6674): 398–401, Doi: 10.1038/32911.

[168] Considine, R. V., Sinha, M.K., Heiman, M.L., Kriauciunas, A., Stephens, T.W., Nyce, M.R., et al., 1996. Serum Immunoreactive-Leptin Concentrations in Normal-Weight and Obese Humans. New England Journal of Medicine 334(5): 292–5, Doi:

10.1056/nejm199602013340503.

[169] Xiong, Y., Walker, K., Min, X., Hale, C., Tran, T., Komorowski, R., et al., 2017. Long-acting MIC-1/GDF15 molecules to treat obesity: Evidence from mice to monkeys. Science Translational Medicine 9(412), Doi: 10.1126/scitranslmed.aan8732.

[170] Pan, W.W., Myers, M.G., 2018. Leptin and the maintenance of elevated body weight. Nature Reviews Neuroscience: 95–105, Doi: 10.1038/nrn.2017.168.

[171] Ahlma, R.S., Prabakaran, D., Mantzoros, C., Qu, D., Lowell, B., Maratos-Flier, E., et al., 1996. Role of leptin in the neuroendocrine response to fasting. Nature 382(6588): 250–2, Doi: 10.1038/382250a0.

[172] Boden, G., Chen, X., Mozzoli, M., Ryan, I., 1996. Effect of fasting on serum leptin in normal human subjects. The Journal of Clinical Endocrinology & Metabolism 81(9): 3419–23, Doi: 10.1210/jcem.81.9.8784108.

[173] Borner, T., Wald, H.S., Ghidewon, M.Y., Zhang, B., Wu, Z., Jonghe, B.C. De., et al., 2020. GDF15 Induces an Aversive Visceral Malaise State that Drives Anorexia and Weight Loss. Cell Reports 31(3), Doi: 10.1016/J.CELREP.2020.107543.

[174] Thiele, T.E., Van Dijk, G., Campfield, L.A., Smith, F.J., Burn, P., Woods, S.C., et al., 1997. Central infusion of GLP-1, but not leptin, produces conditioned taste aversions in rats. American Journal of Physiology - Regulatory Integrative and Comparative Physiology 272(2 41-2), Doi: 10.1152/ajpregu.1997.272.2.r726.

[175] Lajer, M., Jorsal, A., Tarnow, L., Parving, H.H., Rossing, P., 2010. Plasma growth differentiation factor-15 independently predicts all-cause and cardiovascular mortality as well as deterioration of kidney function in type 1 diabetic patients with nephropathy. Diabetes Care 33(7): 1567–72, Doi: 10.2337/dc09-2174.

[176] Kempf, T., von Haehling, S., Peter, T., Allhoff, T., Cicoira, M., Doehner, W., et al., 2007. Prognostic Utility of Growth Differentiation Factor-15 in Patients With Chronic Heart Failure. Journal of the American College of Cardiology 50(11): 1054–60, Doi: 10.1016/j.jacc.2007.04.091.

[177] Pressoir, M., Desné, S., Berchery, D., Rossignol, G., Poiree, B., Meslier, M., et al., 2010. Prevalence, risk factors and clinical implications of malnutrition in french comprehensive cancer centres. British Journal of Cancer 102(6): 966–71, Doi: 10.1038/sj.bjc.6605578.

[178] Weingarten, S., Senn, M., Langhans, W., 1993. Does a learned taste aversion contribute to the anorectic effect of bacterial lipopolysaccharide? Physiology and Behavior 54(5): 961–6, Doi: 10.1016/0031-9384(93)90309-4.

[179] Chen, J.Y., Campos, C.A., Jarvie, B.C., Palmiter, R.D., 2018. Parabrachial CGRP Neurons Establish and Sustain Aversive Taste Memories. Neuron 100(4): 891-899.e5, Doi: 10.1016/j.neuron.2018.09.032.

[180] Paues, J., Engblom, D., Mackerlova, L., Ericsson-Dahlstrand, A., Blomqvist, A., 2001. Feeding-related immune responsive brain stem neurons: Association with CGRP. NeuroReport 12(11): 2399–403, Doi: 10.1097/00001756-200108080-00023.

[181] Romanovsky, A.A., Steiner, A.A., Matsumura, K., 2006. Cells that trigger fever. Cell Cycle: 2195–7, Doi: 10.4161/cc.5.19.3321.

[182] Romanovsky, A.A., Kulchitsky, V.A., Simons, C.T., Sugimoto, N., 1998. Methodology of fever research: Why are polyphasic fevers often thought to be biphasic? American Journal of Physiology - Regulatory Integrative and Comparative Physiology 275(1 44-1), Doi: 10.1152/ajpregu.1998.275.1.r332.

[183] Romanovsky, A.A., Almeida, M.C., Aronoff, D.M., Ivanov, A.I., Konsman, J.P., Steiner, A.A., et al., 2005. Fever and hypothermia in systemic inflammation: Recent discoveries and revisions. Frontiers in Bioscience: 2193–216, Doi: 10.2741/1690.

[184] Garami, A., Steiner, A.A., Romanovsky, A.A., 2018. Fever and hypothermia in systemic inflammation. Handbook of Clinical Neurology, vol. 157. Elsevier B.V. p. 565–97.

[185] Steiner, A.A., Chakravarty, S., Robbins, J.R., Dragic, A.S., Pan, J., Herkenham, M., et al., 2005. Thermoregulatory responses of rats to conventional preparations of lipopolysaccharide are caused by lipopolysaccharide per se - not by lipoprotein contaminants. American Journal of Physiology - Regulatory Integrative and Comparative Physiology 289(2 58-2), Doi: 10.1152/ajpregu.00223.2005.

[186] Almeida, M.C., Steiner, A.A., Branco, L.G.S., Romanovsky, A.A., 2006. Cold-seeking behavior as a thermoregulatory strategy in systemic inflammation. European Journal of Neuroscience 23(12): 3359–67, Doi: 10.1111/j.1460-9568.2006.04854.x.

[187] Rudaya, A.Y., Steiner, A.A., Robbins, J.R., Dragic, A.S., Romanovsky, A.A., 2005. Thermoregulatory responses to lipopolysaccharide in the mouse: dependence on the dose and ambient temperature. American Journal of Physiology-Regulatory, Integrative and Comparative Physiology 289(5): R1244–52, Doi: 10.1152/ajpregu.00370.2005.

[188] Steiner, A.A., Romanovsky, A.A., 2007. Leptin: At the crossroads of energy balance and systemic inflammation. Progress in Lipid Research: 89–107, Doi: 10.1016/j.plipres.2006.11.001.

[189] Kushimoto, S., Gando, S., Saitoh, D., Mayumi, T., Ogura, H., Fujishima, S., et al., 2013. The impact of body temperature abnormalities on the disease severity and outcome in patients with severe sepsis: An analysis from a multicenter, prospective survey of severe sepsis. Critical Care 17(6): R271, Doi: 10.1186/cc13106.

[190] Rumbus, Z., Matics, R., Hegyi, P., Zsiboras, C., Szabo, I., Illes, A., et al., 2017. Fever is associated with reduced, hypothermia with increased mortality in septic patients: A meta-analysis of clinical trials. PLoS ONE 12(1), Doi: 10.1371/journal.pone.0170152.

[191] Rittig, N., Bach, E., Thomsen, H.H., Johannsen, M., Jørgensen, J.O., Richelsen, B., et al., 2016. Amino acid supplementation is anabolic during the acute phase of endotoxin-induced inflammation: A human randomized crossover trial. Clinical Nutrition 35(2): 322–30, Doi: 10.1016/j.clnu.2015.03.021.

[192] Caraballo, C., Jaimes, F., 2019. Organ Dysfunction in Sepsis: An Ominous Trajectory From Infection To Death. The Yale Journal of Biology and Medicine 92(4): 629–40.

[193] Cohen, J., 2002. The immunopathogenesis of sepsis. Nature: 885–91, Doi:

10.1038/nature01326.

[194] Nilsson, A., Wilhelms, D.B., Mirrasekhian, E., Jaarola, M., Blomqvist, A., Engblom, D., 2017. Inflammation-induced anorexia and fever are elicited by distinct prostaglandin dependent mechanisms, whereas conditioned taste aversion is prostaglandin independent. Brain, Behavior, and Immunity 61: 236–43, Doi: 10.1016/j.bbi.2016.12.007.

[195] De Jager, S.C.A., Bermúdez, B., Bot, I., Koenen, R.R., Bot, M., Kavelaars, A., et al., 2011. Growth differentiation factor 15 deficiency protects against atherosclerosis by attenuating CCR2-mediated macrophage chemotaxis. Journal of Experimental Medicine 208(2): 217–25, Doi: 10.1084/jem.20100370.

[196] Kempf, T., Zarbock, A., Widera, C., Butz, S., Stadtmann, A., Rossaint, J., et al., 2011. GDF-15 is an inhibitor of leukocyte integrin activation required for survival after myocardial infarction in mice. Nature Medicine 17(5): 581–8, Doi: 10.1038/nm.2354.

[197] Abulizi, P., Loganathan, N., Zhao, D., Mele, T., Zhang, Y., Zwiep, T., et al., 2017. Growth Differentiation Factor-15 Deficiency Augments Inflammatory Response and Exacerbates Septic Heart and Renal Injury Induced by Lipopolysaccharide /631/80/82/23 /631/326/421 /13/31 /13/2 /13 /38 /64 /64/60 article. Scientific Reports 7(1), Doi: 10.1038/s41598-017-00902-5.

[198] Kim, J.M., Kosak, J.P., Kim, J.K., Kissling, G., Germolec, D.R., Zeldin, D.C., et al., 2013. NAG-1/GDF15 Transgenic Mouse Has Less White Adipose Tissue and a Reduced Inflammatory Response. Mediators of Inflammation 2013, Doi: 10.1155/2013/641851.

[199] Ratnam, N.M., Peterson, J.M., Talbert, E.E., Ladner, K.J., Rajasekera, P. V., Schmidt, C.R., et al., 2017. NF-κB regulates GDF-15 to suppress macrophage surveillance during early tumor development. Journal of Clinical Investigation, vol. 127. American Society for Clinical Investigation p. 3796–809.

[200] Hassanpour Golakani, M., Mohammad, M.G., Li, H., Gamble, J., Breit, S.N., Ruitenberg, M.J., et al., 2019. MIC-1/GDF15 Overexpression Is Associated with Increased Functional Recovery in Traumatic Spinal Cord Injury. Journal of Neurotrauma 36(24): 3410–21, Doi: 10.1089/neu.2019.6421.

[201] Wanner, S.P., Almeida, M.C., Shimansky, Y.P., Oliveira, D.L., Eales, J.R., Coimbra, C.C., et al., 2017. Cold-Induced Thermogenesis and Inflammation-Associated Cold-Seeking Behavior Are Represented by Different Dorsomedial Hypothalamic Sites: A Three-Dimensional Functional Topography Study in Conscious Rats. The Journal of Neuroscience : The Official Journal of the Society for Neuroscience 37(29): 6956–71, Doi: 10.1523/JNEUROSCI.0100-17.2017.

[202] Saper, C.B., Romanovsky, A.A., Scammell, T.E., 2012. Neural circuitry engaged by prostaglandins during the sickness syndrome. Nature Neuroscience: 1088–95, Doi: 10.1038/nn.3159.

[203] Langhans, W., Hrupka, B., 1999. Interleukins and tumor necrosis factor as inhibitors of food intake. Neuropeptides 33(5): 415–24, Doi: 10.1054/npep.1999.0048.

[204] Wilhelms, D.B., Kirilov, M., Mirrasekhian, E., Eskilsson, A., Rtegren Kugelberg, U.O.¨.,

Klar, C., et al., 2014. Deletion of Prostaglandin E 2 Synthesizing Enzymes in Brain Endothelial Cells Attenuates Inflammatory Fever, Doi: 10.1523/JNEUROSCI.1838-14.2014.

[205] Fritz, M., Klawonn, A.M., Nilsson, A., Singh, A.K., Zajdel, J., Wilhelms, D.B., et al., 2016. Prostaglandin-dependent modulation of dopaminergic neurotransmission elicits inflammation-induced aversion in mice. Journal of Clinical Investigation 126(2): 695–705, Doi: 10.1172/JCI83844.

[206] Chambers, A.P., Sorrell, J.E., Haller, A., Roelofs, K., Hutch, C.R., Kim, K.S., et al., 2017. The Role of Pancreatic Preproglucagon in Glucose Homeostasis in Mice. Cell Metabolism 25(4): 927-934.e3, Doi: 10.1016/j.cmet.2017.02.008.

[207] Allison, M.B., Patterson, C.M., Krashes, M.J., Lowell, B.B., Myers, M.G., Olson, D.P., 2015. TRAP-seq defines markers for novel populations of hypothalamic and brainstem LepRb neurons. Molecular Metabolism 4(4): 299–309, Doi: 10.1016/j.molmet.2015.01.012.

[208] Yoshizawa, T., Morooka, N., 1973. Deoxynivalenol and its monoacetate: New mycotoxins from fusarium roseum and moldy barley. Agricultural and Biological Chemistry: 2933–4, Doi: 10.1080/00021369.1973.10861103.

[209] Vesonder, R.F., Ciegler, A., Jensen', A.H., 1973. Isolation of the Emetic Principle from Fusarium-Infected Corn. vol. 26.

[210] Forsyth, D.M., Yoshizawa, T., Morooka, N., Tuite, J., 1977. Emetic and refusal activity of deoxynivalenol to swine. Applied and Environmental Microbiology 34(5): 547–52, Doi: 10.1128/aem.34.5.547-552.1977.

[211] Abbas, H.K., Mirocha, C.J., Tuite, J., 1986. Natural occurrence of deoxynivalenol, 15-acetyl-deoxynivalenol, and zearalenone in refusal factor corn stored since 1972. Applied and Environmental Microbiology 51(4): 841–3, Doi: 10.1128/aem.51.4.841-843.1986.

[212] Pestka, J.J., 2010. Deoxynivalenol: mechanisms of action, human exposure, and toxicological relevance. Arch Toxicol 84: 663–79, Doi: 10.1007/s00204-010-0579-8.

[213] Forsell, J.H., Witt, M.F., Tai, J.H., Jensen, R., Pestka, J.J., 1986. Effects of 8-week exposure of the B6C3F1 mouse to dietary deoxynivalenol (vomitoxin) and zearalenone. Food and Chemical Toxicology 24(3): 213–9, Doi: 10.1016/0278-6915(86)90231-0.

[214] Iverson, F., Armstrong, C., Nera, E., Truelove, J., Fernie, S., Scott, P., et al., 1996. Chronic feeding study of deoxynivalenol in B6C3F1 male and female mice. Teratogenesis, Carcinogenesis, and Mutagenesis 15(6): 283–306, Doi: 10.1002/(sici)1520-6866(1996)15:6<283::aid-tcm5>3.0.co;2-e.

[215] Arnold, D., 1986. A short-term feeding study with deoxynivalenol (vomitoxin) using rats. Fundamental and Applied Toxicology 6(4): 691–6, Doi: 10.1016/0272-0590(86)90182-x.

[216] Bergsjø, B., Matre, T., Nafstad, I., 1992. Effects of Diets with Graded Levels of Deoxynivalenol on Performance in Growing Pigs. Journal of Veterinary Medicine Series A 39(1–10): 752–8, Doi: 10.1111/j.1439-0442.1992.tb00240.x.

[217] Terciolo, C., Maresca, M., Pinton, P., Oswald, I.P., 2018. Review article: Role of satiety hormones in anorexia induction by Trichothecene mycotoxins. Food and Chemical Toxicology 121: 701–14, Doi: 10.1016/j.fct.2018.09.034.

[218] Wu, W., Zhou, H.-R., Bursian, S.J., Pan, X., Link, J.E., || F.B., et al., 2014. Comparison of Anorectic and Emetic Potencies of Deoxynivalenol (Vomitoxin) to the Plant Metabolite Deoxynivalenol-3-Glucoside and Synthetic Deoxynivalenol Derivatives EN139528 and EN139544. TOXICOLOGICAL SCIENCES: 167–81, Doi: 10.1093/toxsci/kfu166.

[219] Ossenkopp, K.P., Hirst, M., Rapley, W.A., 1994. Deoxynivalenol (vomitoxin)-induced conditioned taste aversions in rats are mediated by the chemosensitive area postrema. Pharmacology, Biochemistry and Behavior 47(2): 363–7, Doi: 10.1016/0091-3057(94)90024-8.

[220] Clark, D.E., Wellman, P.J., Harvey, R.B., Lerma, M.S., 1987. Effects of vomitoxin (deoxynivalenol) on conditioned saccharin aversion and food consumption in adult rats. Pharmacology, Biochemistry and Behavior 27(2): 247–52, Doi: 10.1016/0091-3057(87)90566-1.

[221] Lachey, J.L., D'Alessio, D.A., Rinaman, L., Elmquist, J.K., Drucker, D.J., Seeley, R.J., 2005. The role of central glucagon-like peptide-1 in mediating the effects of visceral illness: Differential effects in rats and mice. Endocrinology 146(1): 458–62, Doi: 10.1210/en.2004-0419.

[222] Wu, W., Zhou, H.-R., Pestka, J.J., 2017. Potential roles for calcium-sensing receptor (CaSR) and transient receptor potential ankyrin-1 (TRPA1) in murine anorectic response to deoxynivalenol (vomitoxin). Archives of Toxicology 91(1): 495–507, Doi: 10.1007/s00204-016-1687-x.

[223] Wu, W., Zhou, H.R., Bursian, S.J., Link, J.E., Pestka, J.J., 2017. Calcium-sensing receptor and transient receptor ankyrin-1 mediate emesis induction by deoxynivalenol (vomitoxin). Toxicological Sciences 155(1): 32–42, Doi: 10.1093/toxsci/kfw191.

[224] Tominaga, M., Momonaka, Y., Yokose, C., Tadaishi, M., Shimizu, M., Yamane, T., et al., 2016. Anorexic action of deoxynivalenol in hypothalamus and intestine, Doi: 10.1016/j.toxicon.2016.04.036.

[225] Wu, W., Bates, M.A., Bursian, S.J., Flannery, B., Zhou, H.R., Link, J.E., et al., 2013. Peptide YY3-36 and 5-hydroxytryptamine mediate emesis induction by trichothecene deoxynivalenol (vomitoxin). Toxicological Sciences 133(1): 186–95, Doi: 10.1093/toxsci/kft033.

[226] Seeley, R.J., Moran, T.H., 2002. Principles for interpreting interactions among the multiple systems that influence food intake. American Journal of Physiology - Regulatory Integrative and Comparative Physiology, Doi: 10.1152/ajpregu.00021.2002.

[227] Ruat, M., Molliver, M.E., Snowman, A.M., Snyder, S.H., 1995. Calcium sensing receptor: Molecular cloning in rat and localization to nerve terminals. Proceedings of the National Academy of Sciences of the United States of America 92(8): 3161–5, Doi: 10.1073/pnas.92.8.3161.

[228] Yano, S., Brown, E.M., Chattopadhyay, N., 2004. Calcium-sensing receptor in the brain. Cell Calcium 35: 257–64, Doi: 10.1016/j.ceca.2003.10.008.

[229] Hannan, F.M., Kallay, E., Chang, W., Brandi, M.L., Thakker, R. V., 2018. The calcium-sensing receptor in physiology and in calcitropic and noncalcitropic diseases. Nature Reviews Endocrinology: 33–51, Doi: 10.1038/s41574-018-0115-0.

[230] Flannery, B.M., Clark, E.S., Pestka, J.J., 2012. Anorexia induction by the trichothecene deoxynivalenol (vomitoxin) is mediated by the release of the gut satiety hormone peptide YY. Toxicological Sciences 130(2): 289–97, Doi: 10.1093/toxsci/kfs255.

[231] Kobayashi-Hattori, K., Amuzie, C.J., Flannery, B.M., Pestka, J.J., 2011. Body composition and hormonal effects following exposure to mycotoxin deoxynivalenol in the high-fat diet-induced obese mouse. Molecular Nutrition and Food Research 55(7): 1070–8, Doi: 10.1002/mnfr.201000640.

[232] Krashes, M.J., Shah, B.P., Madara, J.C., Olson, D.P., Strochlic, D.E., Garfield, A.S., et al., 2014. An excitatory paraventricular nucleus to AgRP neuron circuit that drives hunger. Nature 507(7491): 238–42, Doi: 10.1038/nature12956.

[233] Drucker, D.J., 2016. Evolving Concepts and Translational Relevance of Enteroendocrine Cell Biology. The Journal of Clinical Endocrinology & Metabolism 101(3): 778–86, Doi: 10.1210/jc.2015-3449.

[234] Gribble, F.M., Reimann, F., 2016. Enteroendocrine Cells: Chemosensors in the Intestinal Epithelium. Annual Review of Physiology: 277–99, Doi: 10.1146/annurev-physiol-021115-105439.

[235] Sandoval, D. a., D'Alessio, D. a., 2015. Physiology of Proglucagon Peptides: Role of Glucagon and GLP-1 in Health and Disease. Physiological Reviews 95(2): 513–48, Doi: 10.1152/physrev.00013.2014.

[236] Drucker, D.J., Habener, J.F., Holst, J.J., 2017. Discovery, characterization, and clinical development of the glucagon-like peptides. Journal of Clinical Investigation: 4217–27, Doi: 10.1172/JCI97233.

[237] Drucker, D.J., n.d. Cell Metabolism Review Mechanisms of Action and Therapeutic Application of Glucagon-like Peptide-1, Doi: 10.1016/j.cmet.2018.03.001.

[238] Drucker, D.J., Yusta, B., 2014. Physiology and pharmacology of the enteroendocrine hormone glucagon-like peptide-2. Annual Review of Physiology 76: 561–83, Doi: 10.1146/annurev-physiol-021113-170317.

[239] Ali, S., Lamont, B.J., Charron, M.J., Drucker, D.J., 2011. Dual elimination of the glucagon and GLP-1 receptors in mice reveals plasticity in the incretin axis. Journal of Clinical Investigation 121(5): 1917–29, Doi: 10.1172/JCI43615.

[240] Kostic, A., King, T.A., Yang, F., Chan, K.C., Yancopoulos, G.D., Gromada, J., et al., 2018. A first-in-human pharmacodynamic and pharmacokinetic study of a fully human anti-glucagon receptor monoclonal antibody in normal healthy volunteers. Diabetes, Obesity and Metabolism 20(2): 283–91, Doi: 10.1111/dom.13075.

[241] Yang, J., MacDougall, M.L., McDowell, M.T., Xi, L., Wei, R., Zavadoski, W.J., et al., 2011. Polyomic profiling reveals significant hepatic metabolic alterations in glucagon-receptor (GCGR) knockout mice: implications on anti-glucagon therapies for diabetes. BMC Genomics 12(1), Doi: 10.1186/1471-2164-12-281.

[242] Longuet, C., Robledo, A.M., Dean, E.D., Dai, C., Ali, S., McGuinness, I., et al., 2013. Liver-specific disruption of the murine glucagon receptor produces α-cell hyperplasia evidence for a circulating α-Cell Growth Factor. Diabetes 62(4): 1196–205, Doi: 10.2337/db11-1605.

[243] Guan, H.P., Yang, X., Lu, K., Wang, S.P., Castro-Perez, J.M., Previs, S., et al., 2015. Glucagon receptor antagonism induces increased cholesterol absorption. Journal of Lipid Research 56(11): 2183–95, Doi: 10.1194/jlr.M060897.

[244] Borg, C.M., Roux, C.W.L., Ghatei, M.A., Bloom, S.R., Patel, A.G., 2007. Biliopancreatic diversion in rats is associated with intestinal hypertrophy and with increased GLP-1, GLP-2 and PYY levels. Obesity Surgery 17(9): 1193–8, Doi: 10.1007/s11695-007-9211-2.

[245] Taqi, E., Wallace, L.E., de Heuvel, E., Chelikani, P.K., Zheng, H., Berthoud, H.R., et al., 2010. The influence of nutrients, biliary-pancreatic secretions, and systemic trophic hormones on intestinal adaptation in a Roux-en-Y bypass model. Journal of Pediatric Surgery 45(5): 987–95, Doi: 10.1016/j.jpedsurg.2010.02.036.

[246] Romero, F., Nicolau, J., Flores, L., Casamitjana, R., Ibarzabal, A., Lacy, A., et al., 2012. Comparable early changes in gastrointestinal hormones after Sleeve gastrectomy and Roux-en-Y gastric bypass surgery for morbidly obese type 2 diabetic subjects. Surgical Endoscopy: 2231–9, Doi: 10.1007/s00464-012-2166-y.

[247] Cazzo, E., Pareja, J.C., Chaim, E.A., Geloneze, B., Barreto, M.R.L., Magro, D.O., 2017. GLP-1 and GLP-2 Levels are Correlated with Satiety Regulation After Roux-en-Y Gastric Bypass: Results of an Exploratory Prospective Study. Obesity Surgery 27(3): 703–8, Doi: 10.1007/s11695-016-2345-3.

[248] Thomas, C., Gioiello, A., Noriega, L., Strehle, A., Oury, J., Rizzo, G., et al., 2009. TGR5-Mediated Bile Acid Sensing Controls Glucose Homeostasis. Cell Metabolism 10(3): 167–77, Doi: 10.1016/j.cmet.2009.08.001.

[249] Brighton, C.A., Rievaj, J., Kuhre, R.E., Glass, L.L., Schoonjans, K., Holst, J.J., et al., 2015. Bile acids trigger GLP-1 release predominantly by accessing basolaterally located G protein-coupled bile acid receptors. Endocrinology 156(11): 3961–70, Doi: 10.1210/en.2015-1321.

[250] Nielsen, S., Svane, M.S., Kuhre, R.E., Clausen, T.R., Kristiansen, V.B., Rehfeld, J.F., et al., 2017. Chenodeoxycholic acid stimulates glucagon-like peptide-1 secretion in patients after Roux-en-Y gastric bypass. Physiological Reports 5(3), Doi: 10.14814/phy2.13140.

[251] Hutch, C.R., Sandoval, D., 2017. The role of GLP-1 in the metabolic success of bariatric surgery. Endocrinology: 4139–51, Doi: 10.1210/en.2017-00564.

[252] Madsbad, S., Dirksen, C., Holst, J.J., 2014. Mechanisms of changes in glucose metabolism and bodyweight after bariatric surgery. The Lancet Diabetes and

Endocrinology: 152–64, Doi: 10.1016/S2213-8587(13)70218-3.

[253] Mulla, C.M., Middelbeek, R.J.W., Patti, M.E., 2018. Mechanisms of weight loss and improved metabolism following bariatric surgery. Annals of the New York Academy of Sciences: 53–64, Doi: 10.1111/nyas.13409.

[254] Ding, L., Sousa, K.M., Jin, L., Dong, B., Kim, B.W., Ramirez, R., et al., 2016. Vertical sleeve gastrectomy activates GPBAR-1/TGR5 to sustain weight loss, improve fatty liver, and remit insulin resistance in mice. Hepatology 64(3): 760–73, Doi: 10.1002/hep.28689.

[255] McGavigan, A.K., Garibay, D., Henseler, Z.M., Chen, J., Bettaieb, A., Haj, F.G., et al., 2015. TGR5 contributes to glucoregulatory improvements after vertical sleeve gastrectomy in mice. Gut: gutjnl-2015-309871, Doi: 10.1136/gutjnl-2015-309871.

[256] Garibay, D., Mcgavigan, A.K., Lee, S.A., Ficorilli, J. V., Cox, A.L., Michael, M.D., et al., 2016. β-Cell glucagon-like peptide-1 receptor contributes to improved glucose tolerance after vertical sleeve gastrectomy. Endocrinology 157(9): 3405–9, Doi: 10.1210/en.2016-1302.

[257] Wilson-Pérez, H.E., Chambers, A.P., Ryan, K.K., Li, B., Sandoval, D.A., Stoffers, D., et al., 2013. Vertical sleeve gastrectomy is effective in two genetic mouse models of glucagon-like peptide 1 receptor deficiency. Diabetes 62(7): 2380–5, Doi: 10.2337/db12-1498.

[258] Banasch, M., Bulut, K., Hagemann, D., Schrader, H., Holst, J.J., Schmidt, W.E., et al., 2006. Glucagon-like peptide 2 inhibits ghrelin secretion in humans. Regulatory Peptides 137(3): 173–8, Doi: 10.1016/j.regpep.2006.07.009.

[259] Shi, X., Zhou, F., Li, X., Chang, B., Li, D., Wang, Y., et al., 2013. Central GLP-2 enhances hepatic insulin sensitivity via activating PI3K signaling in POMC neurons. Cell Metabolism 18(1): 86–98, Doi: 10.1016/j.cmet.2013.06.014.

[260] Guan, X., Shi, X., Li, X., Chang, B., Wang, Y., Li, D., et al., 2012. GLP-2 receptor in POMC neurons suppresses feeding behavior and gastric motility. American Journal of Physiology - Endocrinology and Metabolism 303(7), Doi: 10.1152/ajpendo.00245.2012.

[261] Cani, P.D., Possemiers, S., Van de Wiele, T., Guiot, Y., Everard, A., Rottier, O., et al., 2009. Changes in gut microbiota control inflammation in obese mice through a mechanism involving GLP-2-driven improvement of gut permeability. Gut 58(8): 1091–103, Doi: 10.1136/gut.2008.165886.

[262] Monte, S. V., Caruana, J.A., Ghanim, H., Sia, C.L., Korzeniewski, K., Schentag, J.J., et al., 2012. Reduction in endotoxemia, oxidative and inflammatory stress, and insulin resistance after Roux-en-Y gastric bypass surgery in patients with morbid obesity and type 2 diabetes mellitus. Surgery 151(4): 587–93, Doi: 10.1016/j.surg.2011.09.038.

[263] Kelly, A.S., Ryder, J.R., Marlatt, K.L., Rudser, K.D., Jenkins, T., Inge, T.H., 2016. Changes in inflammation, oxidative stress and adipokines following bariatric surgery among adolescents with severe obesity. International Journal of Obesity 40(2): 275–80, Doi: 10.1038/ijo.2015.174.

[264] Gelling, R.W., Du, X.Q., Dichmann, D.S., Rømer, J., Huang, H., Cui, L., et al., 2003.

Lower blood glucose, hyperglucagonemia, and pancreatic α cell hyperplasia in glucagon receptor knockout mice. Proceedings of the National Academy of Sciences of the United States of America 100(3): 1438–43, Doi: 10.1073/pnas.0237106100.

[265] Vassileva, G., Golovko, A., Markowitz, L., Abbondanzo, S.J., Zeng, M., Yang, S., et al., 2006. Targeted deletion of Gpbar1 protects mice from cholesterol gallstone formation. Biochemical Journal 398(3): 423–30, Doi: 10.1042/BJ20060537.

[266] Lee, S.J., Lee, J., Li, K.K., Holland, D., Maughan, H., Guttman, D.S., et al., 2012. Disruption of the murine Glp2r impairs paneth cell function and increases susceptibility to small bowel enteritis. Endocrinology 153(3): 1141–51, Doi: 10.1210/en.2011-1954.

[267] Chambers, A.P., Kirchner, H., Wilson-Perez, H.E., Willency, J.A., Hale, J.E., Gaylinn, B.D., et al., 2013. The effects of vertical sleeve gastrectomy in rodents are ghrelin independent. Gastroenterology 144(1): 50-52.e5, Doi: 10.1053/j.gastro.2012.09.009.

[268] Griffiths, W.J., Sjövall, J., 2010. Bile acids: Analysis in biological fluids and tissues. Journal of Lipid Research: 23–41, Doi: 10.1194/jlr.R001941-JLR200.

[269] Kitchen, P.A., Goodlad, R.A., FitzGerald, A.J., Mandir, N., Ghatei, M.A., Bloom, S.R., et al., 2005. Intestinal growth in parenterally-fed rats induced by the combined effects of glucagon-like peptide 2 and epidermal growth factor. Journal of Parenteral and Enteral Nutrition 29(4): 248–54, Doi: 10.1177/0148607105029004248.

[270] Lim, D.W., Wales, P.W., Josephson, J.K., Nation, P.N., Wizzard, P.R., Sergi, C.M., et al., 2016. Glucagon-Like Peptide 2 Improves Cholestasis in Parenteral Nutrition-Associated Liver Disease. Journal of Parenteral and Enteral Nutrition 40(1): 14–21, Doi: 10.1177/0148607114551968.

[271] Conarello, S.L., Jiang, G., Mu, J., Li, Z., Woods, J., Zycband, E., et al., 2007. Glucagon receptor knockout mice are resistant to diet-induced obesity and streptozotocin-mediated beta cell loss and hyperglycaemia. Diabetologia 50(1): 142–50, Doi: 10.1007/s00125-006-0481-3.

[272] Dossa, A.Y., Escobar, O., Golden, J., Frey, M.R., Ford, H.R., Gayer, C.P., 2016. Bile acids regulate intestinal cell proliferation by modulating EGFR and FXR signaling. American Journal of Physiology - Gastrointestinal and Liver Physiology 310(2): G81–92, Doi: 10.1152/ajpgi.00065.2015.

[273] Pathak, P., Liu, H., Boehme, S., Xie, C., Krausz, K.W., Gonzalez, F., et al., 2017. Farnesoid X receptor induces Takeda G-protein receptor 5 cross-talk to regulate bile acid synthesis and hepatic metabolism. Journal of Biological Chemistry 292(26): 11055–69, Doi: 10.1074/jbc.M117.784322.

[274] Drucker, D.J., Ehrlich, P., Asa, S.L., Brubaker, P.L., 1996. Induction of intestinal epithelial proliferation by glucagon-like peptide 2. Proceedings of the National Academy of Sciences of the United States of America 93(15): 7911–6, Doi: 10.1073/pnas.93.15.7911.

[275] Tang-Christensen, M., Larsen, P.J., Thulesen, J., Rømer, J., Vrang, N., 2000. The proglucagon-derived peptide, glucagon-like peptide-2, is a neurotransmitter involved in

the regulation of food intake. Nature Medicine 6(7): 802–7, Doi: 10.1038/77535.

[276] Sørensen, H., Winzell, M.S., Brand, C.L., Fosgerau, K., Gelling, R.W., Nishimura, E., et al., 2006. Glucagon receptor knockout mice display increased insulin sensitivity and impaired β-cell function. Diabetes 55(12): 3463–9, Doi: 10.2337/db06-0307.

[277] Koehler, J.A., Baggio, L.L., Yusta, B., Longuet, C., Rowland, K.J., Cao, X., et al., 2015. GLP-1R agonists promote normal and neoplastic intestinal growth through mechanisms requiring Fgf7. Cell Metabolism 21(3): 379–91, Doi: 10.1016/j.cmet.2015.02.005.

[278] Wismann, P., Barkholt, P., Secher, T., Vrang, N., Hansen, H.B., Jeppesen, P.B., et al., 2017. The endogenous preproglucagon system is not essential for gut growth homeostasis in mice. Molecular Metabolism 6(7): 681–92, Doi: 10.1016/j.molmet.2017.04.007.

[279] Lim, D.W., Wales, P.W., Mi, S.I., Yap, J.Y.K., Curtis, J.M., Mager, D.R., et al., 2016. Glucagon-Like Peptide-2 Alters Bile Acid Metabolism in Parenteral Nutrition-Associated Liver Disease. Journal of Parenteral and Enteral Nutrition 40(1): 22–35, Doi: 10.1177/0148607115595596.

[280] Yusta, B., Matthews, D., Flock, G.B., Ussher, J.R., Lavoie, B., Mawe, G.M., et al., 2017. Glucagon-like peptide-2 promotes gallbladder refilling via a TGR5-independent, GLP-2R-dependent pathway. Molecular Metabolism, Doi: 10.1016/j.molmet.2017.03.006.

[281] Cazzo, E., Gestic, M.A., Utrini, M.P., Chaim, F.D.M., Geloneze, B., Pareja, J.C., et al., 2016. GLP-2: A POORLY UNDERSTOOD MEDIATOR ENROLLED IN VARIOUS BARIATRIC/METABOLIC SURGERY-RELATED PATHOPHYSIOLOGIC MECHANISMS. Arquivos Brasileiros de Cirurgia Digestiva : ABCD = Brazilian Archives of Digestive Surgery: 272–5, Doi: 10.1590/0102-6720201600040014.

[282] Baldassano, S., Rappa, F., Amato, A., Cappello, F., Mulè, F., 2015. GLP-2 as Beneficial Factor in the Glucose Homeostasis in Mice Fed a High Fat Diet. Journal of Cellular Physiology 230(12): 3029–36, Doi: 10.1002/jcp.25039.

[283] Wilson-Pérez, H.E., Chambers, A.P., Ryan, K.K., Li, B., Sandoval, D.A., Stoffers, D., et al., 2013. Vertical sleeve gastrectomy is effective in two genetic mouse models of glucagon-like peptide 1 receptor deficiency. Diabetes 62(7): 2380–5, Doi: 10.2337/db12-1498.

[284] Ye, J., Hao, Z., Mumphrey, M.B., Leigh Townsend, R., Patterson, L.M., Stylopoulos, N., et al., 2014. GLP-1 receptor signaling is not required for reduced body weight after RYGB in rodents. American Journal of Physiology - Regulatory Integrative and Comparative Physiology 306(5), Doi: 10.1152/ajpregu.00491.2013.

[285] Mokadem, M., Zechner, J.F., Margolskee, R.F., Drucker, D.J., Aguirre, V., 2014. Effects of Roux-en-Y gastric bypass on energy and glucose homeostasis are preserved in two mouse models of functional glucagon-like peptide-1 deficiency. Molecular Metabolism 3(2): 191–201, Doi: 10.1016/j.molmet.2013.11.010.

[286] Campbell, J.E., Drucker, D.J., 2015. Islet α cells and glucagon-critical regulators of energy homeostasis. Nature Reviews Endocrinology: 329–38, Doi: 10.1038/nrendo.2015.51.

[287] Giudice, M. Lo., Mihalik, B., Dinnyés, A., Kobolák, J., 2019. The nervous system relevance of the calcium sensing receptor in health and disease. Molecules, Doi: 10.3390/molecules24142546.

[288] Block, G.A., Bushinsky, D.A., Cheng, S., Cunningham, J., Dehmel, B., Drueke, T.B., et al., 2017. Effect of etelcalcetide vs cinacalcet on serum parathyroid hormone in patients receiving hemodialysis with secondary hyperparathyroidism: A randomized clinical trial. JAMA - Journal of the American Medical Association 317(2): 156–64, Doi: 10.1001/jama.2016.19468.

[289] Filopanti, M., Corbetta, S., Barbieri, A.M., Spada, A., 2013. Pharmacology of the calcium sensing receptor. Clinical Cases in Mineral and Bone Metabolism: 162–5, Doi: 10.11138/ccmbm/2013.10.3.162.

[290] Amuzie, C.J., Harkema, J.R., Pestka, J.J., 2008. Tissue distribution and proinflammatory cytokine induction by the trichothecene deoxynivalenol in the mouse: Comparison of nasal vs. oral exposure. Toxicology 248(1): 39–44, Doi: 10.1016/j.tox.2008.03.005.

[291] Zhou, H.R., Yan, D., Pestka, J.J., 1997. Differential cytokine mRNA expression in mice after oval exposure to the trichothecene vomitoxin (Deoxynivalenol): Dose response and time course. Toxicology and Applied Pharmacology 144(2): 294–305, Doi: 10.1006/taap.1997.8132.

[292] Pestka, J.J., Zhou, H.R., 2002. Effects of tumor necrosis factor type 1 and 2 receptor deficiencies on anorexia, growth and IgA dysregulation in mice exposed to the trichothecene vomitoxin. Food and Chemical Toxicology 40(11): 1623–31, Doi: 10.1016/S0278-6915(02)00153-9.

[293] Pestka, J.J., Zhou, H.R., 2000. Interleukin-6-deficient mice refractory to IgA dysregulation but not anorexia induction by vomitoxin (Deoxynivalenol) ingestion. Food and Chemical Toxicology 38(7): 565–75, Doi: 10.1016/S0278-6915(00)00041-7.

[294] Filippatos, T.D., Panagiotopoulou, T. V., Elisaf, M.S., 2014. Adverse Effects of GLP-1 Receptor Agonists. The Review of Diabetic Studies : RDS: 202–30, Doi: 10.1900/RDS.2014.11.202.

[295] Garber, A., Henry, R.R., Ratner, R., Hale, P., Chang, C.T., Bode, B., 2011. Liraglutide, a once-daily human glucagon-like peptide 1 analogue, provides sustained improvements in glycaemic control and weight for 2 years as monotherapy compared with glimepiride in patients with type 2 diabetes. Diabetes, Obesity and Metabolism 13(4): 348–56, Doi: 10.1111/j.1463-1326.2010.01356.x.

[296] Cheng, W., Gonzalez, I., Pan, W., Tsang, A.H., Adams, J., Ndoka, E., et al., 2020. Calcitonin Receptor Neurons in the Mouse Nucleus Tractus Solitarius Control Energy Balance via the Non-aversive Suppression of Feeding. Cell Metabolism 31(2): 301-312.e5, Doi: 10.1016/j.cmet.2019.12.012.